

Effects of Adsorbate Properties on Heel Buildup on Activated Carbon Fiber Cloth during Electrothermal Regeneration

by

Monisha Alam

A thesis submitted in partial fulfillment of the requirements for the degree of

Master of Science

in

Environmental Engineering

Department of Civil and Environmental Engineering

University of Alberta

© Monisha Alam, 2017

ABSTRACT

Automotive painting booths are a major source of volatile organic compounds' (VOCs) in the automotive manufacturing sector. Adsorption on activated carbon (AC) has been widely used as a low cost and energy efficient VOC control method. A major challenge associated with the cyclic adsorption/desorption of VOCs on AC is the unwanted accumulation of adsorbates known as irreversible adsorption or heel formation, which leads to significant decrease in adsorbent capacity and lifetime. The objective of this study is to identify the effects of adsorbate properties such as boiling point, kinetic diameter and thermal stability on heel buildup and adsorption capacity loss of AC. For this purpose, five cycle adsorption/desorption tests were completed using activated carbon fiber cloth (ACFC) as adsorbent and nine different alkylbenzenes (toluene, ethylbenzene, p-xylene, m-xylene, o-xylene, isopropylbenzene, 1,2,4 trimethylbenzene (TMB), 1,3,5 TMB and neopentylbenzene) with different physical and chemical properties were used as adsorbates. The ACFCs loaded with various adsorbates were electrothermally regenerated at 400°C, with a heating rate of 70°C/ min and N₂ purge flow of 0.1 standard liter per minute (SLPM). The obtained results indicate that heel formation was mainly affected by the thermal stability of the adsorbates, whereas the adsorption capacity loss was affected by heel formation and the kinetic diameter of the adsorbates. The principal mechanism of heel formation was found to be the thermal decomposition of the adsorbates due to high temperature desorption, while the adsorbates' boiling points (or vapour pressure) and kinetic diameters controlled their exposure to high temperature during desorption. The conversion rates of the adsorbates in pyrolysis have been used as an indication of their thermal stability, and an increase in conversion rate from less than 1% to more than 90% increased heel formation from 8.9% to 17.2%, showing that lower thermal stability of adsorbates causes higher decomposition

and therefore higher heel. Bulkier compounds caused higher adsorption capacity loss exhibiting an increase in capacity loss from 25.2% to 80.0% when kinetic diameter of adsorbate molecules increased from 5.9 Å to > 7.5 Å. The results of this work will help understand how different adsorbates in industrial air streams will affect heel formation on AC. This will help to take proper measures and optimize regeneration conditions to control heel formation and extend the lifetime of adsorbents.

I dedicate this thesis to my beloved family. A special gratitude to my loving parents, Anju and Jahangir, that this success would not be possible without their endless love, invaluable support and encouragement for me in pursuing higher education.

I would also like to dedicate this work to my lovely husband, Hasan, for providing me with continuous support and encouragement and also for helping me in every aspect to achieve this success

ACKNOWLEDGMENTS

First and foremost, I would like to express my deepest gratitude to my supervisor, Dr. Zaher Hashisho, for his supervision, guidance and generous support throughout my course work and research. I highly appreciate his invaluable comments and continuous feedback throughout my MSc research. This work could not be accomplished without his profound knowledge, expertise and guidance.

I would like to acknowledge the financial support from Ford Motor Company, and the Natural Sciences and Engineering Research Council (NSERC) of Canada. I also acknowledge the financial support from Queen Elizabeth II Graduate Scholarship - Master's Level, Prairie Mines & Royalty Ltd Graduate Scholarship in Environmental Engineering and Westmoreland Coal Company Graduate Scholarship in Environmental Engineering.

I would also like to thank my colleagues in Air Quality Characterization Lab, especially Saeid Niknaddaf and Masoud Jahandar Lashaki for their availability, suggestions and assistance in my experiments.

I extend my appreciation to the technicians in the Department of Civil and Environmental Engineering for their help and support.

TABLE OF CONTENTS

CHAPTER 1. INTRODUCTION	1
1.1 Background	1
1.2 VOC Emission Sources and Control Regulations.....	2
1.3 VOC Mitigation Techniques	3
1.4 VOC Adsorption on Activated Carbon	7
1.5 Problem Statement	7
1.6 Objectives.....	8
1.7 Thesis Outline	9
CHAPTER 2. LITERATURE REVIEW	10
2.1 Adsorption.....	10
2.1.1 Types of Adsorption	11
2.1.2 Adsorption Capacity and Isotherms	11
2.2 Adsorbent Types and Properties	13
2.2.1 Non-carbonaceous adsorbates	14
2.2.2 Carbonaceous Adsorbents	15
2.3 Activated Carbon.....	16
2.3.1 Types of AC.....	18
2.3.2 Activated Carbon Fiber Cloth.....	21
2.4 Desorption/Regeneration.....	23
2.4.1 Methods of Regeneration.....	24
2.4.2 Factors Affecting Desorption Behaviour of Activated Carbon	28
2.5 Irreversible Adsorption	29
2.5.1 Mechanisms of Irreversible Adsorption	29
2.5.2 Effects of Adsorption Conditions on Irreversible Adsorption.....	31

2.5.3 Effects of Regeneration Conditions on Irreversible Adsorption	32
2.5.4 Effects of Adsorbent Properties on Irreversible Adsorption	34
2.5.5 Effects of Adsorbate Properties on Irreversible Adsorption	35
CHAPTER 3. MATERIALS AND METHODS	36
3.1 Materials.....	36
3.1.1 Adsorbent.....	36
3.1.2 Adsorbates	36
3.2 Methods.....	39
3.2.1 Adsorption and Regeneration Experiments	39
3.2.2 Characterization Tests	43
CHAPTER 4. RESULTS AND DISCUSSIONS.....	45
4.1 Breakthrough Curves.....	45
4.2 Cumulative Heel Buildup on ACFC Samples during 5-Cycle Adsorption and Regeneration Experiments.....	48
4.3 Thermo-Gravimetric Analysis.....	50
4.4 Desorption Profile and Applied Power during Regeneration Cycles.....	54
4.5 Micropore Surface Analysis.....	60
CHAPTER 5. CONCLUSIONS AND RECOMMENDATIONS	63
5.1 Conclusions.....	63
5.2 Recommendations	65
REFERENCES	66
APPENDICES	83
Appendix A: Environment Canada VOC concentration limit for automotive refinishing products.....	83
Appendix B: Detail of 5 cycle adsorption/desorption tests of toluene on ACFC	84
Appendix C: Detail of 5 cycle adsorption/desorption tests of p-xylene on ACFC.....	86

Appendix D: Detail of 5 cycle adsorption/desorption tests of m-xylene on ACFC.....	88
Appendix E: Detail of 5 cycle adsorption/desorption tests of o-xylene on ACFC	90
Appendix F: Detail of 5 cycle adsorption/desorption tests of 1,2,4 TMB on ACFC	92
Appendix G: Detail of 5 cycle adsorption/desorption tests of 1,3,5 TMB on ACFC	94
Appendix H: Detail of 5 cycle adsorption/desorption tests of ethylbenzene on ACFC.....	96
Appendix I: Detail of 5 cycle adsorption/desorption tests of isopropylbenzene on ACFC	98
Appendix J: Detail of 5 cycle adsorption/desorption tests of neopentylbenzene on ACFC ...	100

LIST OF TABLES

Table 1-1. VOC removal techniques and their advantages and disadvantages (Cooper and Alley 2011, Khan and Kr. Ghoshal 2000, Parmar and Rao 2009)	5
Table 2-1. Comparison between TSR and ESR for regeneration of activated carbon	27
Table 3-1. Properties of the tested adsorbates	38
Table 4-1. Reduction in 1% breakthrough time, cumulative heel and capacity loss of ACFC for 5 cycle adsorption/desorption of different adsorbates (Values are reported as mean \pm standard deviation of two experimental runs)	47
Table 4-2. Exposure of residual adsorbates to 400°C, 1 st cycle and 5 cycle cumulative heel, 5 cycle capacity loss and 5 cycle average power applied during regeneration of ACFCs loaded with different adsorbates. (Values are reported as mean \pm standard deviation of two experimental runs)	59
Table 4-3. BET surface area, pore volume and micropore volume of heat treated and regenerated ACFCs loaded with different adsorbates	60

LIST OF FIGURES

Figure 2-1. Pore size distribution of some commonly used adsorbents (Knaebel 2016)	14
Figure 2-2. Schematic of Different types of pores in AC (Wu 2004).....	17
Figure 2-3. Different forms of activated carbon (a) powdered (b) granular (c) beaded (d) pelleted	19
Figure 2-4. ACFC from macro to micro scale	23
Figure 2-5. Classification of methods used for regenerating activated carbon adsorbents	25
Figure 3-1. Schematic of the experimental setup of the adsorption/regeneration experiments....	41
Figure 3-2. ACFC cartridge used for adsorption/regeneration experiments.....	41
Figure 4-1. Breakthrough curves for adsorption of (a) toluene, (b) p-xylene, (c) m-xylene, (d) o-xylene, (e) 1,2,4 TMB, (f) 1,3,5 TMB, (g) ethylbenzene, (h) isopropylbenzene and (i) neopentylbenzene.....	46
Figure 4-2. Cumulative heel on ACFC samples loaded with different alkylbenzene adsorbates. Values in parentheses indicate thermal conversion rates (as % weight) from literature	48
Figure 4-3. TGA results of heat treated and regenerated ACFCs loaded with different adsorbates	51
Figure 4-4. DTG results of heat treated and regenerated ACFCs loaded with different adsorbates	51
Figure 4-5. Positions and dehydrogenation tendency of α and β -hydrogen in alkylbenzenes [modified from.....	53
Figure 4-6. Desorption profiles for the 1 st regeneration cycle of ACFC loaded with different adsorbates.....	55
Figure 4-7. Desorption profiles for the initial 30 min of the 1 st regeneration cycle of ACFC loaded with different adsorbates	56

LIST OF ACRONYMS

AC	Activated Carbon
ACFC	Activated Carbon Fiber Cloth
ACC	Activated Carbon Cloth
BAC	Beaded Activated Carbon
BET	Brunauer-Emmett-Teller
CEPA	Canadian Environmental Protection Act
CFCs	Chlorofluorocarbons
COP	Critical Oxidation Potential
DAC	Data Acquisition and Control
DFT	Density Functional Theory
DO	Dissolved Oxygen
DTG	Derivative Thermo-Gravimetric
EAC	Extruded Activated Carbon
EPA	Environmental Protection Agency
ESA	Electrothermal Swing Adsorption
ESR	Electrothermal Swing Regeneration
FID	Flame Ionization Detector
GAC	Granular Activated Carbon
IUPAC	International Union of Pure and Applied Chemistry
PAC	Powdered Activated Carbon
PPB	Parts Per Billion
PPMV	Parts Per Million (Volume fractions)
PSA	Pressure Swing Adsorption
PSR	Pressure Swing Regeneration
PSD	Pore Size Distribution
QSDFT	Quenched Solid Density Functional Theory
SFG	Surface Functional Groups
SLPM	Standard Liter per Minute
TGA	Thermo-Gravimetric Analysis

USEPA
VOC

United States Environmental Protection Agency
Volatile Organic Compound

CHAPTER 1. INTRODUCTION

1.1 Background

Volatile organic compounds (VOCs) refer to a complex group of hydrocarbons with relatively low boiling point ($<260^{\circ}\text{C}$) and higher vapour pressure, including aromatic and aliphatic hydrocarbons, ketones, esters, alcohols, and glycol ethers (Kennes and Veiga 2013, Khan and Kr. Ghoshal 2000, Kim 2011). Definition of VOCs varies among different regulatory systems based on their health and environmental impacts. The United States Environmental Protection Agency (USEPA) defines VOCs as “any compound of carbon, excluding carbon monoxide, carbon dioxide, carbonic acid, metallic carbides or carbonates, and ammonium carbonate, which participates in atmospheric photochemical reactions” (US Environmental Protection Agency 2016). According to Environment and Climate Change Canada, VOCs are defined as “organic compounds containing one or more carbon atoms that have high vapour pressures and therefore evaporate readily to the atmosphere” (Environment and Climate Change Canada 2015). In the Environment and Climate Change Canada definition of VOCs under Schedule 1 (item 65) of the Canadian Environmental Protection Act, 1999 (CEPA 1999), compounds such as methane, ethane and the chlorofluorocarbons (CFCs) are excluded because of their low photochemical reactivity. Most of the VOCs are toxic and have severe health and environmental hazards. The health effects of VOCs exposure include eye, nose, and throat irritations, headaches, nausea, dizziness etc. (Fiedler *et al.* 2005). Moreover, even at very low concentration, the VOCs cause damage to lungs, liver, nervous system and may even cause cancer and memory loss (Kampa and Castanas 2008, Khan and Kr. Ghoshal 2000, Pariselli *et al.* 2009). In presence of sunlight and in combination with NO_x , VOCs undergo photochemical

oxidation, producing a photochemical smog that pollutes the environment by affecting plants' growth and decay and it also adversely affect human and animal lives (Karatum and Deshusses 2016, Khan and Kr. Ghoshal 2000). Several halogenated VOCs are potential greenhouse gases and depletes the stratospheric ozone layer (Robinson *et al.* 2007) and also helps in formation of tropospheric or ground level ozone (Atkinson 2000). Therefore, it is highly important to restrict the VOC emission for protecting our health and environment.

1.2 VOC Emission Sources and Control Regulations

VOC sources are classified as biogenic (natural) and anthropogenic (human-made). Biogenic sources include woods, crops, oceans, and volcanic eruptions whereas industrial activities involving paints, varnishes, chemical cleaners, solvents, lubricants, and liquid fuel are the major anthropogenic sources of VOCs (Bari *et al.* 2016, Zhao *et al.* 2014). In 2014, VOC emission in Canada were 2157 kilotonnes (kt), showing an increase of 13 kt (1%) from 2013 levels, among which, the oil gas industry, paints and solvents processing industry and agricultural sector (livestock and fertilizer) were the biggest contributors of the national emissions of VOC (34%, 15%, and 12% respectively) (Environment and Climate Change Canada 2016). In North America, about 6.58 kg of VOC is used as paint solvents per vehicle in typical car manufacturing plants (Kim 2011). Due to concerns about the health and environmental impacts of VOC, many regulatory agencies issued regulations to control VOC emissions to the atmosphere. Under Title I of the US Clean Air Act Amendment of 1990, VOC emissions reduction is imposed if the VOC emission leads to an ozone concentration that exceeds the current national ambient air quality standard for ozone of 0.12 ppm (USEPA 1991). In Europe, organic vapour emission limit is 35 grams total organic compounds (TOC) per cubic meter gasoline loaded (35 g TOC/m³), according to the recently passed European Community

stage. Environment Canada is also working to reduce VOC emissions, particularly resulting from the use of solvents and solvent based products. On July 8, 2009, the VOC Concentration Limits for Automotive Refinishing Products Regulations were published and it established concentration limits for VOCs in 14 categories of automotive refinishing products. The VOC concentration limits apply to all automotive refinishing products such as primers, paints, coatings, surface cleaners etc. The VOC concentration limits in Canada applied to different categories of automotive refinishing products are listed in Appendix A (Environment and Climate Change Canada 2015). Therefore, the increasingly strict regulations on VOC emissions warrant continuous research to develop effective technologies to limit emissions of VOC pollutants.

1.3 VOC Mitigation Techniques

Several treatment technologies exist to control the emission of VOCs (Khan and Kr. Ghoshal 2000, Kim 2011). Selection of a treatment technique depends on different parameters such as the type, source, concentration and flow rate of the pollutant, presence of compounds other than VOCs, reusability of captured compounds, regulatory limits etc. (Berenjian *et al.* 2012). Moreover, the process safety, location, cost, and operative possibility of the selected technique should also be considered (Cooper and Alley 2011). VOC control techniques are classified into two main categories: (i) process and equipment modification (VOCs emissions are controlled by modifying the process, equipment or raw material) and (ii) add-on-control techniques (additional control method is applied) (Parmar and Rao 2009). In spite of being more effective and efficient, the applicability of the first type is limited since it is hard to do process modification in most cases. Therefore, the add-on-control techniques are more applicable, and are divided into two groups, destructive and non-destructive methods. Destructive methods are

preferred when VOC recovery is not technically or economically feasible, whereas non-destructive methods allow VOC recovery and reuse (Berenjian *et al.* 2012). A summary of the conventional add-on-control techniques for VOC abatement and their main merits and demerits are provided in Table 1.1. The limitation of secondary waste generation is associated with most of the conventional methods, including biomass formation in biological processes, production of greenhouse gases in oxidative methods, condensate in condensation, and spent adsorbent in adsorption (Parmar and Rao 2009). Besides these conventional techniques, in recent times, some novel VOC abatement technologies have emerged, which include VOC treatment with spark-generated carbon aerosol particles, mesoporous chromium oxide and silica fiber matrix, negative air ions treatment, electrical discharge treatment, electron beam bombardment, and ultraviolet (UV) photo-oxidation by heterogeneous photocatalyst particles (Parmar and Rao 2009). Though a few of these newer methods have shown high removal efficiencies for industrial applications, many of them are still being explored in bench-scale level, involve delicate operation and require very high operating and maintenance cost (Parmar and Rao 2009). Because of the advantages of adsorption process over other VOC mitigation techniques discussed in Table 1.1, adsorption has been widely used as an energy efficient and inexpensive method for low concentration (< 10,000 ppm) VOCs removal from both gaseous and aqueous streams (Fletcher *et al.* 2006). Therefore, adsorption was chosen as the VOC removal method in this research.

Table 1-1. VOC removal techniques and their advantages and disadvantages (Cooper and Alley 2011, Khan and Kr. Ghoshal 2000, Parmar and Rao 2009)

Method type	Process description	Advantages	Limitations
Destructive			
Oxidation	Oxidizers (afterburners, incinerators) combust and convert VOCs to CO ₂ and H ₂ O, thermal oxidizers rely on high temperature (700 – 800°C) and direct flame to ignite VOCs, catalytic oxidizer facilitates oxidation at low temperature (340 – 590°C) through a noble metal surface	Simple operation, 95-99% removal efficiency, energy recovery upto 85%, can treat variable gas concentrations and multi component streams	NO _x Formation, explosion potential, high fuel consumption, greenhouse gas emission, high cost
Biofiltration	VOC laden air passed through porous filter media (wood, compost, peat, soil etc.) supporting microorganisms, VOCs are adsorbed from air phase to water/bio-film phase and decomposed by bioreaction	Low energy consumption, operating cost, no chemical needed, non-hazardous, eco-friendly	Low removal efficiency (60-95%), generates biomass, slow process, depends on microbial growth and culture and biodegradability of contaminants, chlorinated VOCs are poisonous for microorganisms
Non-destructive			
Condensation	VOC laden gases are cooled in heat exchangers below the stream dew point to condense	VOC recovery, removal efficiency 70-85%, good for high boiling point VOCs (above 33°C)	Generates wastewater stream, extensive cooling required for low concentration gas stream, inert gas blanketing required if inlet gas falls below the upper explosive limit (UEL) to eliminate explosion hazards
Absorption	Soluble VOCs are transferred to liquid phase by liquid solvents in absorber towers	High removal efficiency (95-98%), handles a wide range of VOC concentrations (500-5,000 ppm)	Generates wastewater stream, columns are clogged by particles in gas stream, liquid absorbents transfer to exit gas stream, creating another pollution concern
Adsorption	VOCs are adsorbed on	High removal efficiency	Low efficiency for high

Method type	Process description	Advantages	Limitations
	solid adsorbents like activated carbon, zeolites, polymers etc.	(90-98%), treats low concentration VOCs, efficiently handles fluctuations in inlet gas flow rates and VOC concentrations, low operation cost, not much limited to VOCs properties (biodegradability, boiling point etc.), low operation and maintenance cost	humidity (>50% R.H), fire risk for VOCs with high heat of adsorption
Membrane Separation	Preferential transport of VOCs through a non-porous gas separation membrane under pressure differences	High removal efficiency (90-99%), can treat high VOC concentration gas economically	Requirement of vacuum pump, refrigeration equipment etc. increase capital and operating cost

1.4 VOC Adsorption on Activated Carbon

Among different adsorbent, activated carbon (AC) is one of the most widely used adsorbent in both air and water treatment due to its high surface area, high adsorption capacity and low cost (Fletcher *et al.* 2006, Hashisho *et al.* 2008). Moreover, AC can be regenerated, its physical and chemical properties can be tailored, it has good thermal stability in absence of oxygen, and can withstand acidic or basic conditions (Dabrowski *et al.* 2005). AC is available in several physical forms such as granular, powdered, beads, fibers and monoliths. Activated carbon fiber cloth (ACFC) has recently gained more attention because of some novel properties such as ash-free and high microporous structure where the internal micropores are connected to its external surface area, diminishing the mass and heat transfer limitations (Ramos *et al.* 2010). ACFC is more compact due to its continuous fibers, which provides it with higher electrical conductivity than other forms of AC, making it a suitable candidate for electrothermal swing adsorption (ESA). ESA is an efficient regeneration technique due to its fast heating rate, less purge gas consumption and minimal requirement to separate condensate water. (Niknaddaf *et al.* 2016). Therefore, in this research, ACFC is chosen as the VOC adsorbent and electrothermal desorption by resistive heating has been selected as the regeneration method for ACFC.

1.5 Problem Statement

One major challenge during cyclic adsorption/desorption of VOCs on AC is the irreversible adsorption, causing unwanted adsorbate accumulation (aka heel formation) on the adsorbent, which significantly decreases the adsorption capacity and lifetime of the adsorbents (Lashaki *et al.* 2012b, Niknaddaf *et al.* 2016). Irreversible adsorption increases the operation and maintenance costs of adsorption system by requiring frequent replacement of the adsorbent to

maintain a sufficient adsorption capacity. Previous studies have shown that heel formation on activated carbon is affected by several factors including the properties of the adsorbents and adsorbates, as well as the regeneration conditions (Lashaki *et al.* 2012b, Niknaddaf *et al.* 2016, Wang *et al.* 2012).

1.6 Objectives

The goal of this research is to investigate the effects of the properties of VOC adsorbates on heel buildup during electrothermal desorption. The main objective of this research is to investigate the effects of different adsorbate properties (kinetic diameter, boiling point, thermal stability) on heel formation on ACFC during cyclic adsorption and electrothermal desorption of alkylbenzenes on ACFC. ACFC was used in this study as the adsorbent because it has very high microporosity which can highlight the heel formation, since heel formation occurs mainly in the micropores. Besides, because of its electric resistivity, ACFC can be efficiently regenerated by electrothermal regeneration. The adsorbates chosen in this research were based on their presence in paint solvents and their potential for heel formation. Adsorbates with benzene rings in their structure, larger kinetic diameter and higher boiling points are expected to result in higher heel formation. In addition, adsorbates with lower thermal stability may be prone for thermal decomposition during desorption from ACFC at high temperature. Therefore, nine alkylbenzenes with different kinetic diameters, boiling points and thermal stability were selected as adsorbates in this research.

A better understanding of the factors contributing to the irreversible adsorption is important in identifying ways to decrease heel buildup and increase the adsorbents' lifetime. Although there is some information on how adsorbate properties contribute to heel formation on

beaded activated carbon (BAC), there is not enough information on how ACFC is affected by irreversible adsorption during electrothermal desorption. Results of this research include information on the potential of different VOC adsorbates to form heel on ACFC during subsequent adsorption/desorption. Therefore, based on these results, related industry can design an effective VOC abatement system depending on the VOC constituents of the polluted gas stream, which can effectively minimize irreversible adsorption on the adsorbent. This is expected to reduce the cost for disposal and replacement of the adsorbent. Moreover, this research can also help in bridging some of the knowledge gaps in the adsorption/desorption of VOC from polluted gas streams onto ACFC.

1.7 Thesis Outline

This thesis consists of three chapters that will contribute to fulfill the goal of the research. Chapter 1 provides an introduction about the topic including background, objective and importance of the research. A detail literature review on adsorption process, different types of adsorbents and adsorbates, regeneration process, different regeneration techniques, and factors affecting irreversible adsorption is included in Chapter 2. Chapter 3 includes description of the materials and methods used. Chapter 4 presents the experimental results and corresponding discussions, and Chapter 5 provides the major conclusions obtained from this study and future recommendations.

CHAPTER 2. LITERATURE REVIEW

2.1 Adsorption

Adsorption is a process in which atoms, ions or molecules of a gas, liquid or dissolved solid get attached onto a surface (Bansal and Goyal 2005, Slejko 1985). Adsorption is a surface-based phenomenon, and occurs mainly as a result of surface energy. The adsorbing surface providing the adsorption sites is called adsorbent, whereas the substance that gets attached to the surface is named as adsorbate (Slejko 1985). The nature of forces enhancing the adsorption depends on the species involved. Adsorption of gaseous species on a solid or liquid medium causes a decrease in the free energy of the system and the system entropy, therefore, adsorption is always an exothermic process (Radecki and American Institute of Chemical Engineers 1999, Zhou 2007). The reverse process of adsorption is known as desorption, when the adsorbates come out or rebound back from the adsorbent surface and pores.

Adsorption process exists in many natural, physical, biological and chemical system (Suffet and McGuire 1980). In addition, adsorption also has wide industrial applications, both in liquid and gas-phase. Its liquid-phase applications include removal of organic compounds from water or organic solutions, colored impurities from organics, moisture dissolved in gasoline, pollutants in wastewater treatment processes etc. (Dou *et al.* 2015, Gupta and Verma 2002, Slejko 1985). Examples of gas-phase applications of adsorption are removal of water vapor from air and other gases, sulfur compounds from natural gas, recovery of solvent vapors from air-gas mixture, VOC removal from polluted gas streams, etc. (Lapkin *et al.* 2004, Ramos *et al.* 2010, Ratnasamy *et al.* 2012, Zheng *et al.* 2013)

2.1.1 Types of Adsorption

The type of adsorption between adsorbent and adsorbate depends on several factors such as the surface reactivity, properties of adsorbent and adsorbates, and also the adsorption temperature (Slejko 1985). Based on the type of forces participating in the process, adsorption is mainly classified into two types: physical adsorption or physisorption and chemical adsorption or chemisorption (Ramos *et al.* 2010, Slejko 1985). In physisorption, adsorbates are attached to adsorbent surface through weak interaction forces (e.g. van der Waals forces) between the adsorbent and adsorbate. In contrary, chemisorption involves strong interaction forces (usually covalent bonds) and the sharing of electron between adsorbent and adsorbates leads to formation of chemical reactions (Bansal and Goyal 2005, Do 1998). The heat of adsorption for physisorption is from 10 to 20 KJ/mole, whereas in chemisorption it ranges between 40 to 400 KJ/mole (Bansal and Goyal 2005). Physisorption may occur at a faster rate at low temperature, since no activation energy is required, but chemisorption need activation energy to take place, therefore rate of chemisorption is temperature dependent (Do 1998). Besides, physisorption has a multimolecular thickness of adsorbed phase, whereas in chemisorption, the thickness is monomolecular (Bansal and Goyal 2005, Slejko 1985).

2.1.2 Adsorption Capacity and Isotherms

Adsorption capacity refers to the amount of adsorbate that can be adsorbed onto the surface of an adsorbent before the adsorbent gets saturated (Zhou 2007). Adsorption capacity depends on the equilibrium relationship between adsorbent and adsorbate (Bansal and Goyal 2005). At the beginning of adsorption process, the rate of adsorption is high due to the higher exposure of solid surface towards a liquid or gaseous adsorbate. The more the surface become covered with adsorbate molecules, the availability of bare surface decreases, therefore the rate of adsorption

decreases and the rate of desorption, which is the rate at which adsorbates rebound back from adsorbent surface, increases. With time, a stage is obtained when adsorption and desorption rates are equal and both the adsorbent and adsorbate are in equilibrium, and this equilibrium condition depends on the system pressure and temperature (Do 1998, Keller and Staudt 2005). If the temperature is kept constant then the equilibrium only depends on the equilibrium pressure, it is known as adsorption isotherms.

Adsorption isotherms are most widely used to represent the equilibrium condition, hence the adsorption capacity of an adsorbent. Adsorption isotherms can help determine the adsorbent's surface area, pore volume and pore size distribution, heat of adsorption and the relative adsorbability of different adsorbates on a particular adsorbent (Bansal and Goyal 2005, Foo and Hameed 2010, Tzabar and ter Brake, H. J. M. 2016). Some of the most important and commonly used adsorption isotherms models include the Langmuir, Freundlich, Dubinin-Radushkevich and Brunauer-Emmett-Teller (BET) isotherm models. The first two isotherms are important particularly for chemisorption, though they are useful in physisorption as well. The BET and Dubinin-Radushkevich equations are mostly used for analyzing gas physisorption on solid adsorbent such as activated carbon (Brunauer *et al.* 1938). Brunauer-Emmett-Teller (BET) adsorption isotherm model is a theoretical model and refers to multi-layer adsorption on gas-solid systems with relative pressures between 0.05 and 0.35 (Brunauer *et al.* 1938). BET model assumes no interaction between each adsorption layer and Langmuir model can be applied to each layer (Brunauer *et al.* 1938, Rouquerol 2014).

2.2 Adsorbent Types and Properties

Adsorption largely depends on the type and properties of the adsorbents. Several types of adsorbents are used for VOCs adsorption and the process is affected by the adsorbents' physical properties (e.g. surface area, pore size distribution) and chemical properties (e.g. surface functional groups, polarity etc.) (Bhatnagar 2013, Rouquerol 2014, Strazhesko and Barouch 1973). Adsorbents are mainly porous materials with high surface area, and available in many forms including spherical pellets, rods, moldings, or monoliths (Bhatnagar 2013). Adsorbents can be microporous, mesoporous, macroporous or combination of all, depending on their uses. According to the classification of The International Union of Pure and Applied Chemistry (IUPAC), the diameter of micropores are less than 2 nm, whereas the mesopores' diameter ranges between 2 to 50 nm, and macropores have diameter more than 50 nm (Che and Védrine 2012, Rouquerol 2014, Zhou 2007). Micropores and mesopores primarily contribute to the gas phase adsorption, by improving adsorption kinetics (Che and Védrine 2012). Besides, adsorbents' surface functional groups such as oxygen, nitrogen, sulphur and other acidic and basic functional groups also influence their adsorptive behavior (Riccardi *et al.* 2014, Zhang *et al.* 2016). The most common industrial adsorbents used for gaseous adsorbates mainly fall into two categories: non-carbonaceous (silica gel, activated alumina, zeolites and polymers) and carbonaceous adsorbents (activated carbon, graphite, carbon molecular sieves etc.) (Rouquerol 2014, Strazhesko and Barouch 1973), and are described in the following paragraph. Figure 2-1 shows the pore size distribution (PSD) of some common adsorbents used in industrial scale. It shows that zeolites have very well defined PSD, whereas AC has a wide range of PSD.

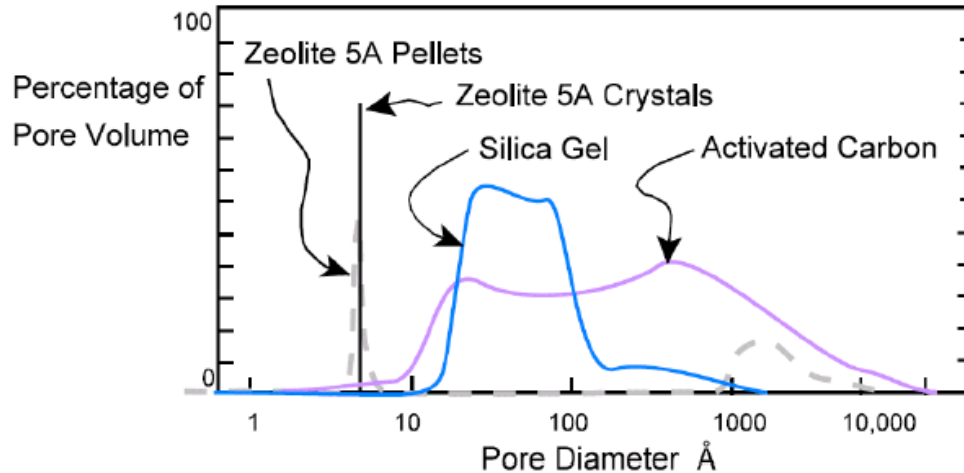


Figure 2-1. Pore size distribution of some commonly used adsorbents (Knaebel 2016)

2.2.1 Non-carbonaceous adsorbents

These adsorbates typically are hydrophilic and polar in nature such as silica gel, activated alumina, zeolites and polymeric adsorbents.

Silica gel is the amorphous form of SiO_2 , and is chemically inert and non-toxic. Its properties such as wide pore size distribution and thermal stability (usually stable at $< 400^\circ\text{C}$) makes it a good adsorbent for air drying process and hydrocarbon adsorption from natural gas (Canada 2004, Dou *et al.* 2015).

Zeolites refer to a big group of natural or synthetic aluminum silicates, usually hydrated and have crystalline structure (Davis 2002). Because of the novel properties like precise pore size distributions, zeolites can selectively adsorb and separate gas molecules, and therefore zeolites are widely used as molecular sieves (Flanigen *et al.* 1971). Zeolites have been successfully used as adsorbent in processes involving air drying and air separation, CO_4 and CO_2 separation from natural gas, CO removal from reforming gas, catalytic cracking etc. (Flanigen *et al.* 1971, Kesraoui-Ouki *et al.* 1994). Hydrophobic zeolites are primarily used for VOC

capturing, and because of their good thermal stability and less flammability than other types of adsorbents (such as AC) (Chung-Hwei Su *et al.* 2009).

Polymeric adsorbents have been emerging as an effective adsorbent due to their surface area, mechanical strength, adjustable surface chemistry and pore size distribution, and feasible regeneration under low temperature (Davankov and Tsyurupa 2011). Several applications of polymeric adsorbents include adsorption of organic pollutants, namely phenolic compounds, organic acids, aromatic and polyaromatic hydrocarbons, alkanes and their derivatives (Deosarkar and Pangarkar 2004, Pan *et al.* 2009). Additional improvements like surface modification or functionalization improved polymers' performance towards adsorption of highly water-soluble compounds and heavy metal ions, chlorinated pesticides and other poisonous compounds from waste effluents and water supplies, therefore polymers are being used as highly efficient adsorbents in water treatment and other pollution control applications (Garcia 1991, Hradil 2008, Kunin 1977, Riccardi *et al.* 2014).

2.2.2 Carbonaceous Adsorbents

Carbon is a potential element of the periodic table for adsorption, since it can establish bonds with almost any element, thus resulting in a wide spectrum of compounds. Carbon based adsorbents are generally hydrophobic and non-polar in nature (Juan Carratalá-Abril *et al.* 2009). The oldest and most widely used carbonaceous adsorbent is the activated carbon (AC), a processed form of carbon with high porosity and surface area and amorphous solid structure consisting of microcrystallites with a graphite lattice (Bansal and Goyal 2005, Kwiatkowski 2012). In recent time, a new generation of carbon structures built at the nanoscale (e.g. nanofibers, nanotubes, fullerenes, graphene, graphene nanoribbons, nanodiamonds, etc.) have

also gained attraction due to their relatively large surface area, and novel electronic and chemical properties, that can provide enhanced adsorption (Tascón 2012).

2.3 Activated Carbon

Activated carbon is the most significant carbonaceous adsorbent, due to its highly developed wide range of porosity, large surface area (500 to 3000 m²/g), tailored physical (e.g. pore size distribution and surface area) and chemical properties (e.g. surface groups), high surface reactivity, and therefore ability to economically remove very low concentration pollutants (Bansal and Goyal 2005, Kwiatkowski 2012, Rouquerol 2014). AC has proved to be a versatile adsorbent, since it performs successfully in both liquid-phase and gas-phase adsorption (Dabrowski *et al.* 2005, Juan Carratalá-Abril *et al.* 2009). The total number of pores, their shape and size determine the adsorption capacity and adsorption rate of AC. A schematic of different types of pores in AC is shown in Figure 2-2. The macropores act as transport pathways, through which the adsorbate molecules travel to the mesopores, from where they finally enter the micropores. The micropores usually constitute the largest proportion of the internal surface of the AC and contribute most to the total pore volume (Kwiatkowski 2012). Most of the gaseous adsorption occurs in the micropores, where the attractive forces are enhanced and the pores are filled at low relative pressures. Thus, the total pore and micropore volume and the pore size distribution determine the adsorption capacity.

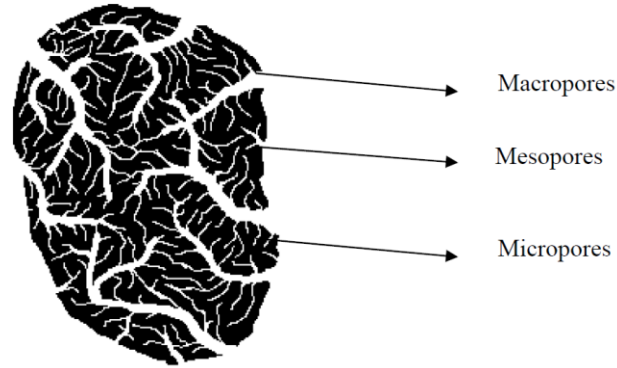


Figure 2-2. Schematic of Different types of pores in AC (Wu 2004)

AC is manufactured from materials with high carbon content such as coal (bituminous, subbituminous, and lignite), peat, wood, saw dust, bamboo, or coconut shells, petroleum coke, sub bituminous polymer etc. (Ahmad and Idris 2014, Ahmadpour and Do 1997, Ramos *et al.* 2010, Salvador *et al.* 2015). AC can also be prepared from many organic wastes like agricultural waste, biomass materials, sewage sludge etc. (Ahmad and Idris 2014, Méndez *et al.* 2005). AC precursors are mostly organic, easily available and inexpensive, and also can be stored for longer duration, and this makes the production of AC easy and inexpensive (Dabrowski *et al.* 2005).

The method of preparing AC from its precursors involves two steps: carbonization and activation (Ahmad and Idris 2014, Méndez *et al.* 2005). The first stage, carbonization is to increase the carbon content. During this carbonization stage, the precursors are dried and heated at temperature over 400°C in an anoxic environment, mainly to separate the bi-products (e.g. tars or other hydrocarbons) and remove any generated gases. The following step, activation is the process of addition of pores inside the carbons, and can be done either physically or chemically (Ahmad and Idris 2014). In physical activation, the carbonized materials are exposed to an oxidizing agent (steam or CO₂) at an elevated temperature (600 to 1000°C) (Valix *et al.* 2004). The oxidizing agent burns off the pore blocking structures created during the carbonization step

and therefore, develop a porous, three-dimensional graphite lattice structure. The degree of carbon burn-off depends on the gasification resulting from increased temperature and intensity of the oxidizing atmosphere. The type and size of the pores developed during activation is a function of the carbonization and gasification time, temperature and influence of the reactive gas (Ahmad and Idris 2014, Bansal and Goyal 2005). Longer exposure times result in larger pore sizes. For reactivation in CO₂, higher burn-off from elevated temperature results in more microporosity, whereas steam reactivation leads to wider pore size distribution and increased mesoporosity (Zhang *et al.* 2004). In chemical activation, carbonization of the raw material and activation is done simultaneously at lower temperatures (400 – 900°C). After impregnating with a strongly reacting agent such as KOH, NaOH, ZnCl₂, H₃PO₄, K₂CO₃, ammonia, or H₂O₂ etc., the precursor material is heated in an inert atmosphere (Ahmadpour and Do 1997, Wang and Kaskel 2012). Temperature, chemical agent, and impregnation ratio affect the properties of the activated material. Chemical activation helps to develop a desired pore size distribution more easily and efficiently compared to physical activation (Ahmadpour and Do 1997).

2.3.1 Types of AC

Different types of activated carbon are available with different physical properties such as pore size distributions, surface characteristics, and shapes (e.g., pelletized, granular, powdered, spherical or beads, etc.). Figure 2-3 shows different forms and shapes of commercially available AC. Based on the precursor material, activation method and conditions (e.g. temperature and oxygen), and post-treatment reactions, AC has different porous structure and surface functional groups. The most common forms of AC are the powdered and granular forms.



Figure 2-3. Different forms of activated carbon (a) powdered (b) granular (c) beaded (d) pelleted (Bansal and Goyal 2005)

Powdered activated carbon (PAC) is traditionally made in particular form as powder or fine granule of less than 1.0 mm in size with an average diameter between 0.15 and 0.25 mm. Thus, it presents a large surface-to-volume ratio with a small diffusion distance. PAC is made up of crushed or ground carbon particles, 95 to 100% of which will pass through a designated sieve. According to ASTM classification, particle sizes corresponding to an 80-mesh sieve (0.177 mm) and smaller are referred as PAC (Bansal and Goyal 2005, Kwiatkowski 2012). PAC provides very effective adsorption due to its small particles, however, with slower settling and removal process, for the same reasons.

Granular activated carbon (GAC) has a relatively larger particle size compared to PAC and thus, possesses a smaller external surface per unit volume. Diffusion of the adsorbate is thus an important concern. GAC is therefore preferred for gas and vapour phase adsorptions as their rates of diffusion are faster than PAC. Granulated carbons are also used for water treatment, deodorization and component separation in flow system (Bhatnagar 2013) and showed good performance in removing large number of organic compounds (Dabrowski *et al.* 2005). GAC is designated by sizes such as 8×20, 20×40, or 8×30 for liquid phase applications and 4×6, 4×8 or 4×10 for vapor phase applications (Bhatnagar 2013, Kwiatkowski 2012).

Recently, some novel types of AC such as beaded activated carbon (BAC), activated carbon fiber cloth (ACFC), extruded activated carbon (EAC), impregnated and polymer coated carbon are gaining attention because of their unique properties (Kwiatkowski 2012, Tascón 2012). BAC is prepared in spherical shape and has high void filling capability, flow-ability, high strength and wear resistance and low ash content (Marsh and Rodríguez-Reinoso 2006). ACFC is ash-free, and unlike BAC and PAC, it has continuous fiber structure providing it with higher electrical conductivity compared to other forms of AC (Niknaddaf *et al.* 2016). Extruded activated carbon (EAC) is combination of powdered activated carbon with a binder, fused together and extruded into a cylindrical shaped activated carbon block, and has low pressure drop, high mechanical strength and low ash content. Impregnated carbons are porous carbons containing several inorganic impregnates, such as iodine and silver or cations such as Al, Mn, Zn, Fe, Li, and Ca etc. Polymer coated carbons are porous carbon coated with a biocompatible polymer in order to give a smooth and permeable coat without blocking the pores, and these adsorbents are particularly useful in the field of medical treatment (Marsh and Rodríguez-Reinoso 2006).

2.3.2 Activated Carbon Fiber Cloth

Activated carbon fiber cloth (ACFC) is a novel form of AC which is ash-free and has high purity (Le Cloirec 2012). Compared to other commercial adsorbents such as GAC, alumina, silica and zeolites, ACFC exhibits large surface area, high micropore volume and surface reactivity, and therefore exhibits high adsorption capacity and faster adsorption kinetics (Hashisho *et al.* 2009, Ramos *et al.* 2010, Yao *et al.* 2009). ACFC has showed good performance as an alternative to conventional GAC in selective capture of VOCs (Le Cloirec 2012, Luo *et al.* 2006, Subrenat and Le Cloirec 2004). Some important properties of ACFC are discussed below:

2.3.2.1 Surface area and porosity: ACFC has a very high specific surface area (BET surface) ranging from 900 to 2,300 m²/g (Le Cloirec 2012). ACFC is mainly microporous with a micropore volume from 0.40 to 0.90 m³/g, which shows a microporosity of more than 90% of the total porosity. Some experimental results show that, the internal micropores of ACFC are directly connected to its external surface area, which provides a compact structure reducing the mass and heat transfer limitations and pressure drop through ACFC (Luo *et al.* 2006, Subrenat and Le Cloirec 2004). This provides faster adsorption/desorption of adsorbates through ACFC and decreases fire potential inside the adsorption bed.

2.3.2.2 Chemical properties: ACFC's structure is microcrystalline with an orientation of graphitic layers less ordered than in graphite (Ramos *et al.* 2010). Elemental analysis on ACFC showed high purity carbonaceous content with more than 99% carbon and hydrogen trace amount of oxygen, nitrogen and other acidic or basic surface functional group. This high purity of ACFC makes it a promising adsorbent in air and water treatment and purification applications (Le Cloirec 2012).

2.3.2.3 Electrical and thermal properties: The most unique property of ACFC compared to other adsorbents is its high electrical conductivity. Because of its crystalline structure (graphene), ACFC exhibits low resistance when an electrical current is passed through it, and is heated up. Therefore, ACFC can be regenerated by applying an electrical current and heating it up by Joule's heating (Johnsen *et al.* 2014, Son *et al.* 2016). ACFC has successfully captured industrial solvents and recovered them using electrothermal regeneration. ACFC also performed well in capturing VOCs at indoor level, which typically has low VOC concentration (Yao *et al.* 2009). VOCs with highly fluctuating concentrations were adsorbed by ACFC and successfully transformed into more well-defined concentrations with select gas velocities, which enabled the organic vapour to be further processed by biofilters or oxidizers (Emamipour *et al.* 2007a, Nabatilan *et al.* 2010).

2.3.2.4 ACFC precursors: ACFC can be prepared from several synthetic raw material precursors including pitch, asfran, PAN, rayon (viscose), cellulose etc. (Kawashima *et al.* 2000, Subrenat and Le Cloirec 2004). The surface functional groups and pore size distribution depends on the precursor material. The ACFC tested in this research was made from novoloid (phenolic) precursor produced by American Kynol. The preparation steps involve producing the novoloid fibers from novolak resin by melt spinning process, where the fiber polymer is heated and melt into a form suitable for extrusion. After that, the melt-spun fiber is cured with an acidic solution of formaldehyde and acid-catalyzed cross-linking of melt-spun novolak resin is done to form a fully cross-linked, three-dimensional, amorphous network polymer structure of novoloid fibers. Finally, one-step carbonisation and activation is done to form novoloid-based ACFC (Niknaddaf 2015). Figure 2-4 shows ACFC from macro to micro scale. The structural properties of ACFC mainly depend on the residence time in the production oven. These structural properties have a

strong influence on the external mass transfer rate and head loss in the adsorber modules, therefore the proper ACFC type should be chosen based on its application.

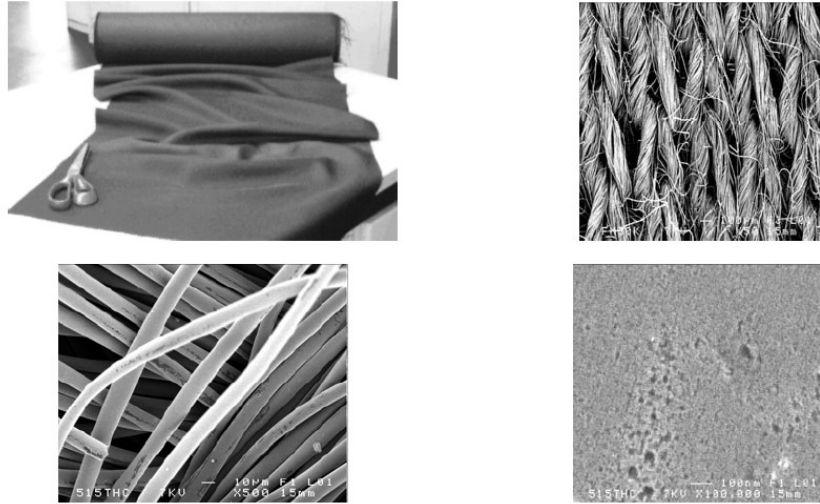


Figure 2-4. ACFC from macro to micro scale (Le Cloirec 2012)

2.4 Desorption/Regeneration

Desorption is the opposite of adsorption process, in which the adsorbates are released from the surface and pores of the adsorbents, also known as regeneration of adsorbent. The main purpose of desorbing the adsorbates and regenerating the adsorbents is to restore the adsorption capacity of adsorbents and also recovering the adsorbates for destruction or reuse (Salvador *et al.* 2015). Adsorption and desorption of VOCs on activated carbon has been an effective pre-treatment process that concentrates the VOCs to facilitate and improve the efficiency of incineration or recovery methods (Ledesma *et al.* 2014, Salvador *et al.* 2015)

2.4.1 Methods of Regeneration

Regeneration can be classified based on the type of regeneration mechanism and the type of regeneration agents used. There are different pathways through which regeneration may proceed. In some AC regeneration methods, the adsorption equilibrium is shifted toward desorption by applying heat (Ledesma *et al.* 2014), decreasing pressure or applying vacuum (Ruthven *et al.* 1994), varying pH of the system (Leng and Pinto 1996), or changing the medium surrounding the AC to a fluid that efficiently extracts the adsorbate (McLaughlin 1995). Other desorption mechanism, such as gasification involves removing the adsorbates by converting it into more easily removable products through chemical reactions or degradation processes.

Regeneration of AC adsorbents may also involve the use of different regeneration agents such as inert chemical species (inert gases like N₂) (Ruhl 2000), oxidizing agents (O₂, CO₂, ozone) (Álvarez *et al.* 2004), chemical reagents (Ince and Apikyan 2000), solvents (organic solvents, supercritical solvents) (McLaughlin 1995), electrical current (Niknaddaf *et al.* 2016), microwaves (Hashisho *et al.* 2008), microorganisms (Scholz and Martin 1998), catalysts (Sheintuch and Matatov-Meytal 1999), ultraviolet light etc. (Ince and Apikyan 2000).

Therefore, some AC regeneration methods use the same regeneration agent but different regeneration mechanisms (i.e., regeneration with supercritical CO₂ and gasification with CO₂ utilize the same regeneration agent but different mechanisms for regenerating the ACs) and vice versa (i.e., temperature swing adsorption (TSA), steaming and electrothermal swing adsorption (ESA) all use thermal regeneration mechanism, but different regeneration agents). Figure 2-5 shows the general classification of regeneration based on both the regeneration mechanism and the regeneration agents used for desorption of the adsorbates.

		Type of Regeneration Mechanism				
		Extraction	pH changes	Reaction/ Degradation	Thermal desorption	Vacuum
Type of Regeneration Agent	Hot gases	THERMAL REGENERATION			VACUUM REGENERATION	
	Physical waves					
	Electrical currents	CHEMICAL REGENERATION				
	Chemical Reagents					
	Supercritical Fluids					
	Microorganisms	MICROBIOLOGICAL REGENERATION				
				VACUUM REGENERATION		

Figure 2-5. Classification of methods used for regenerating activated carbon adsorbents (Salvador *et al.* 2015)

In pressure swing regeneration (PSR) or vacuum regeneration, adsorbates are desorbed by reducing the total pressure of an adsorbent bed and by applying vacuum. Though PSR is a fast process, it is limited by mass transfer and fluidization limitations, therefore smaller beds are recommended for this method. Moreover, this is a lossy process since the gas trapped in adsorbent's pores and voids are lost during blowdown and purging (Ruthven *et al.* 1994, Shonnard and Hiew 2000).

Thermal Regeneration is the process of heating the saturated AC to provide the amount of energy necessary to remove the retained adsorbate. In this method, sufficient amount of thermal energy is provided to break the adsorbent–adsorbate interactions across all the adsorption sites without degrading the adsorbates (Ledesma *et al.* 2014). Based on the source of the heat applied, thermal regeneration can be classified into temperature swing regeneration (TSR), electrical swing regeneration (ESR) and microwave regeneration.

In temperature swing regeneration (TSR), the adsorbent bed temperature is increased by using hot gas or heating jackets, coils, furnaces etc. (Suzuki *et al.* 1978). Steam or hot inert gases

(e.g. N₂, He, Ar) are used in TSR to heat the adsorbent and purge the desorbed pollutants simultaneously. For successfully desorbing the adsorbates, the maximum desorption temperature should overcome the heat of desorption, which is larger than the adsorbate vaporization enthalpy (Popescu *et al.* 2003). TSR was found to be more effective than solvent extraction for compounds with good thermal stability (Ramírez *et al.* 2010). TSR is usually slower process than PSR, and also limited by thermal inertia and lower heat capacity of adsorbents. Moreover, though use of steam in TSR lowers the regeneration temperature, but often water is retained on the surface of the adsorbent during desorption. Therefore, the remaining moisture on the adsorbents after regeneration need to be separated to avoid any competition between the condensed water and the pollutant in the following adsorption cycle which can decrease the adsorption capacity of AC (Schork and Fair 1988).

Electrical swing regeneration (ESR) is developed to overcome the limitations of TSR. In ESR, a low voltage electrical current is used as regeneration agent and that electrical current is directly changed into thermal energy due to the resistance of AC (Lordgooei *et al.* 1996). Therefore, in ESR, AC adsorbents are heated from inside instead of an external energy source. Inert purge gas like N₂, CO₂ or He are used to purge the adsorbates and regenerate the AC (An and Feng 2010). Since in ESR the adsorbates are desorbed by the heat generated by the Joule effect, this method largely depends on the resistivity of the carbonaceous adsorbents. GAC or PAC is not efficiently regenerated by ESR because these adsorbents' particles are not in continuous contact with each other, which makes their resistivity too high and requires very high power or voltage to pass electricity through these ACs. The highest potential candidate to be regenerated by this method is ACFC, since it has continuous fiber structure, which provides it with optimum electrical resistivity and therefore allows energy efficient and high temperature

regeneration (Niknaddaf *et al.* 2016). ESA is a more efficient regeneration method than the other TSR techniques mainly due to its higher heating rate and lower carrier gas consumption (An and Feng 2010, Mallouk *et al.* 2010). Since the thermal energy is directly delivered to the inside of the adsorbent, faster heating rate is achieved (Burchell *et al.* 1997). Table 2-1 shows a comparison between TSR and ESR of AC in terms of desorption efficiency, purge gas flow rate, regeneration time and temperature for desorbing different VOC adsorbates.

Table 2-1. Comparison between TSR and ESR for regeneration of activated carbon

Method	Adsorbent	Adsorbate & inlet conc. ¹ (ppm)	Desorption temp. (°C)	Purge gas & flow rate	Desorption time (min)	Efficiency (%)	Reference
TSR	GAC	Toluene, 190	180	N ₂	120	~85	(Torrents <i>et al.</i> 1997)
	GAC	Chlorobenzene, 300	180	N ₂	120	~85	(Torrents <i>et al.</i> 1997)
	GAC	Toluene, 373	300	He	60	98	(Kim <i>et al.</i> 2006)
	GAC	Methyl-ethylketone, 290	300	He	60	99	(Kim <i>et al.</i> 2006)
ESR	ACFC	Ethanol, 256	150	N ₂ , 2.4 mol/hr	30	~100	(Subrenat <i>et al.</i> 2001)
	GAC	Benzene, 133	--	N ₂ , 0.03 dm ³ /min	150	76	(Li <i>et al.</i> 2012)
	ACFC	Methyl-ethylketone, N/A	151	Air, 10 dm ³ /min	140	~95	(Emamipour <i>et al.</i> 2007b)
	monolith	Toluene, 146	139	N ₂ , 2.4 dm ³ /min	80	90	(Yu <i>et al.</i> 2007)

ESR is not limited neither by the heat capacity nor the heat or mass transfer rates of carrier gas. Besides, there is no need for separating the condensed water or drying the adsorbent bed, which is required in steam regeneration. Unlike hot gas regeneration, adsorbent heating rate in ESR is independent of carrier gas flow rate, decreasing the consumption of carrier gas

consumption. This allows obtaining higher concentration of desorbed adsorbates and successful adsorbate recovery from ESR (Ramirez *et al.* 2011, Sullivan *et al.* 2004).

Recently, microwave heating has emerged as an alternative AC regeneration technique which provides high regeneration efficiencies with lower energy consumption (Cherbański *et al.* 2011, Hashisho *et al.* 2005). Microwave desorption was applied as a rapid regeneration method to desorb organic compounds like phenol from AC without destructing the porous structure of the adsorbent (Ania *et al.* 2004). However, microwave regeneration largely depends on the properties of adsorbents and adsorbates (Reuss *et al.* 2002).

2.4.2 Factors Affecting Desorption Behaviour of Activated Carbon

The desorption of VOCs from AC is affected by the form, nature of pores, surface functional groups (Jahandar Lashaki *et al.* 2016a) and surface reactivity of the adsorbents (Boulinguez and Le Cloirec 2010, Yapsaklı *et al.* 2009). PAC has higher diffusivity and showed faster desorption kinetics, but higher tendency of irreversible adsorption (Akta and Çeçen 2006). Lower catalytic activity, uniformity in pore structure and adsorption site distribution in AC lead to better desorption of adsorbates (Rudling and Björkholm 1987). Mesoporous adsorbents show low temperature desorption while higher temperature is required to desorb adsorbates from microporous adsorbents (Boulinguez and Le Cloirec 2010).

Moreover, the desorption isotherm and overall adsorption reversibility also depends on the adsorbates' concentration, as well as different physical and chemical properties of the adsorbates (Fletcher *et al.* 2006, Suzuki *et al.* 1978). Different operational conditions such as desorption temperature (Lashaki *et al.* 2012b, Wang *et al.* 2012), carrier gas flow rate and its oxygen

content (Jahandar Lashaki *et al.* 2016b), heating rate (Fayaz *et al.* 2015) etc. may affect the desorption of VOCs from AC.

2.5 Irreversible Adsorption

Irreversible adsorption is the unwanted accumulation of adsorbates on the adsorbents' surface or pores after desorption of adsorbates (Jahandar Lashaki *et al.* 2016b). This phenomenon is also known as heel formation. Irreversible adsorption can be visible as a hysteresis loop in an adsorption-desorption isotherm (Okazaki 1996). Irreversibly adsorbed adsorbates on carbon are very hard to remove with a selected regeneration technique (Lashaki *et al.* 2012b). Heel formation is a challenge in using activated carbon for VOC adsorption because heel decreases the adsorbent's capacity and lifespan, which largely increase the operation and maintenance costs. Although many of the previous research on AC adsorption provide information on irreversible adsorption of VOCs from aqueous solutions, but similar studies in gas phase are limited. Both the aqueous phase and gas phase irreversible adsorption have been reviewed due to similarity in adsorption fundamentals among both the phases.

2.5.1 Mechanisms of Irreversible Adsorption

Irreversible adsorption can result from mainly three types of scenarios. a) chemisorption or chemical bonding between species, which leads to strong interactions between adsorbent and adsorbate, b) oligomerization or oxidative coupling of adsorbate molecules inside the narrow pores of AC, 3) decomposition of adsorbates during desorption resulting in coke formation inside the pores of AC adsorbent. The different phenomena of irreversible adsorption are described in detail below:

Chemisorption is due to chemical bonding (e.g. covalent bond) between the adsorbents and adsorbates (Aktaş and Çeçen 2007, Khan and Kr. Ghoshal 2000). Therefore, chemisorption produces very high heat of adsorption (up to 400 kJ/mol), approaching the energy of chemical bonds. Gaseous or liquid adsorbates interact with the carbon's surface or with the surface functional group forming chemical bonds. Unlike physisorption, chemisorption does not rely on carbon's accessible pore volumes, rather bonds are formed between the active sites and adsorbates, therefore only monolayer is formed during chemisorption (Langmuir 1916). To break this kind of chemical bonds, high temperature or huge pressure reduction is often required which increases the operational cost of the system. Example of chemisorption includes removal of trace contaminants such as mercury removal via surface functionalized ACs (Liu *et al.* 1998) and chlorine removal (Tobias and Soffer 1985). Loss of adsorption sites due to irreversible chemisorbed species significantly reduces the adsorbent's lifetime in successive adsorption desorption cycles.

Oxidative coupling or oligomerization is the polymerization of organic adsorbates in presence of oxygen (Brenner 1993, Suidan 1991). Oligomerization enhances reaction between the adsorbates and AC, causing formation of higher molecular weight/boiling point compounds that are difficult to desorb due to their large size. Several studies have reported that irreversible adsorption occurred for aqueous phenolic compounds due to oxidative coupling (Brenner 1993, Vidic *et al.* 1997). In oxidative coupling, a phenol molecule loses one hydrogen atom and is converted into a phenoxy radical that oligomerize with other phenoxy radicals. The oligomerization reaction can take place even at room temperature inside the carbon pores which works as an oxidation catalyst (Vidic *et al.* 1997).

Decomposition of organic adsorbates may occur during high temperature (above 300°C) regeneration of AC (Brandt and Donahue 2009). Adsorbate decomposition results in formation of coke (carbonaceous species) inside the pores of AC, which blocks the micropores and subsequently decreases the adsorption capacity of AC (Ania *et al.* 2004, Niknaddaf *et al.* 2016). Decomposition of adsorbates are mainly attributed to different regeneration conditions (temperature, heating rate etc.) as well as the properties of the adsorbates (Wang *et al.* 2012). Previous study on adsorbate decomposition in high temperature thermal regeneration shows that, the adsorbed phenols decomposed into coke and remained inside the AC pores even at temperatures as high as 800°C during thermogravimetric analysis (Suzuki *et al.* 1978). Steam regeneration at temperatures > 600°C can create oxidizing environment and remove some of the carbon deposits from the adsorbents (Liu *et al.* 1987), but this adds to the system operational cost. Moreover, during cyclic adsorption/desorption, coke formation causes significant reduction in the adsorption performance and lifetime of carbonaceous adsorbents (Niknaddaf *et al.* 2016).

2.5.2 Effects of Adsorption Conditions on Irreversible Adsorption

Irreversible adsorption is affected by various adsorption conditions including presence of dissolved oxygen (DO) during adsorption, adsorption temperatures and duration of adsorption.

AC's adsorption capacity for aqueous phase is increased by DO, which enhances oxidative coupling, but consequently irreversible adsorption also increases. Regeneration efficiency of adsorbent during solvent extraction decreased due to oligomerization of phenols under oxic conditions (Vidic *et al.* 1997).

Adsorption temperature also affects irreversible adsorption, since high temperature enhances polymerization and chemisorption, which caused irreversible adsorption (Nakhla *et al.*

1994). Effect of adsorption temperature on irreversible adsorption of gas phase VOCs were investigated and results show that a 10 to 15°C increase in temperature from room temperature (25°C) caused 30% increase of irreversible adsorption on BAC caused by chemisorption (Lashaki *et al.* 2012b). The duration of adsorption is important since increased irreversible adsorption has been reported in aqueous phase for longer adsorption period (Grant and King 1990). Gas phase irreversible adsorption was investigated for multi-component VOC adsorbate stream (Wang *et al.* 2012). Smaller and lower boiling point compounds were adsorbed quickly, whereas longer adsorption time passing breakthrough promoted adsorption of heavier and higher boiling point compounds (Wang *et al.* 2012). As heavier compounds tend to accumulate more on the AC surface, irreversible adsorption increases with increase in adsorption time (Wang *et al.* 2012).

2.5.3 Effects of Regeneration Conditions on Irreversible Adsorption

Several regeneration conditions including regeneration environment, regeneration temperature and heating rate, and desorption purge gas flow rate affect irreversible adsorption. For aqueous phase phenol desorption from AC, high temperature regeneration in oxidizing environment (CO₂) achieved > 90% efficiency (with 15% carbon burn off), whereas regeneration in an inert environment (N₂) could only recover < 50% of the initial adsorption capacity of the spent AC (Álvarez *et al.* 2004).

In conductive heating regeneration of BAC loaded with mixture of VOC adsorbates, increasing regeneration temperature from 288 to 400°C facilitated VOC desorption from narrow micropores and therefore decreased heel formation by 61% (Lashaki *et al.* 2012b). But in case of electrothermal regeneration of ACFC loaded with trimethylbenzene (TMB), higher heel was observed in samples regenerated at 400 °C than samples regenerated at 288°C (Niknaddaf *et al.*

2016). Enhancement of endothermic decomposition of TMB due to high temperature exposure caused higher heel formation on microporous ACFC (Niknaddaf *et al.* 2016).

Effects of regeneration heating rate on irreversible adsorption of VOCs typically emitted from automotive painting operations was investigated (Fayaz *et al.* 2015b) for two BACs with different microporosity. For higher regeneration temperature (400°C), higher heating rate increased heel build up by 92% in mainly microporous (88% microporosity) BAC and by 169% in partially microporous (46% microporosity) BAC. In contrary, lower regeneration temperature (288°C) showed no significant effect on heel build up, since there was < 16% and < 10% increase for the mainly microporous and partially microporous BACs, respectively (Fayaz *et al.* 2015b). Therefore, high regeneration temperature and high heating rate both can contribute to adsorbate decomposition, which leads to coke formation inside the carbon pores resulting in irreversible adsorption.

Regeneration purge gas constituent and flow rate can affect irreversible adsorption. (Jahandar Lashaki *et al.* 2016b) investigated the effect of desorption purge gas oxygen content on irreversible adsorption of mixtures of organic compounds on BAC. Results show 35% increase in heel formation when oxygen content increased from 5 ppm to 10,000 ppm in desorption purge gas, which is mainly attributed to the chemisorption of the VOCs.

Low purge gas flow may cause high adsorbate concentration inside carbon pores, particularly for highly microporous carbons such as ACFC. Exposure of high concentration adsorbates into high regeneration temperature may cause adsorbate decomposition and therefore coke formation (Niknaddaf *et al.* 2016).

2.5.4 Effects of Adsorbent Properties on Irreversible Adsorption

Adsorbents' pore size distributions and surface functional groups (SFGs) are the major contributors affecting reversibility of adsorption (Li *et al.* 2011). Adsorbents' narrow pore size distribution hindered oligomerization of phenolic compounds and therefore decreased irreversible adsorption (Yan and Sorial 2011). Contradictions were also found where adsorbents' narrow pore size increased irreversible adsorption by enhancing adsorption energy (Wang *et al.* 2009). Five types of commercially available BAC with similar elemental composition but different PSDs (30 to 88% microporous) were investigated for irreversible adsorption of organic vapours (Lashaki *et al.* 2016). Linear correlation was observed between the amount of heel and micropore volume of BAC, which confirmed the high energy micropores contributing more to heel formation.

The impact of surface functional groups on the irreversible adsorption of aqueous phase phenolic compounds was investigated in previous studies (Vidic *et al.* 1997). AC containing carboxylic groups exhibited lower tendency of forming oligomers (Terzyk 2007). In contrast, oligomerization can be enhanced by saturated SFGs such as methyl, ethyl, methoxy etc. (Yonge *et al.* 1985). For gas phase adsorption, effect of surface oxygen groups was investigated for heel formation in cyclic adsorption/regeneration of VOCs on BAC (Jahandar Lashaki *et al.* 2016a). The tested BACs were chemically tailored in three different ways, two were oxygen deficient (treated with heat and hydrogen respectively) and another was oxygen-rich (treated with nitric acid). Compared to heat-treated BAC, both hydrogen and acid treated samples showed higher heel. Oxygen functionalised BAC promoted chemisorption of adsorbates whereas physisorption was the main heel formation mechanism for oxygen-deficient BACs.

2.5.5 Effects of Adsorbate Properties on Irreversible Adsorption

Several properties of an organic adsorbate including molecular weight, kinetic diameter, boiling point, functional groups and thermal stability influence its irreversible adsorption on carbon adsorbents. Phenols have clearly showed irreversible adsorption in aqueous phase (Suzuki *et al.* 1978). Adsorbates' critical oxidation potential (COP), that is the amount of energy required to add or remove electron to or from an element or compound, largely controls the potential of oxidative coupling on AC and consequent heel formation. Therefore, adsorbates with electron donating group (methyl, ethyl etc.) reduce COP and increase irreversible adsorption. In contrast, electron withdrawing groups (e.g. nitro, chloro etc.) can increase the COP and hinder dehydrogenation of adsorbates, which minimizes irreversible adsorption (Grant and King 1990). Aqueous phase adsorption of both electron donating and electron attracting compounds on AC were compared and results showed irreversible adsorption in presence of electron-donating groups (e.g. -NH₂ and -OH), while electron-attracting groups (e.g. -NO₂) adsorbed reversibly (Tamon *et al.* 1990). In gas phase adsorption, higher molecular weight and higher boiling point compounds tend to form higher heel on BAC (Wang *et al.* 2012) To best knowledge of the author, effect of VOC adsorbate properties has not yet investigated for electrothermal regeneration of microporous adsorbent ACFC.

CHAPTER 3. MATERIALS AND METHODS

This chapter provides the detail of the materials i. e. the adsorbents and adsorbates used, the experimental setup and the methods used to fulfill the objectives of this research work.

3.1 Materials

3.1.1 Adsorbent

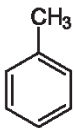
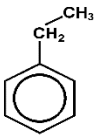
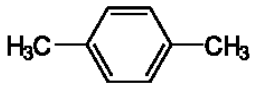
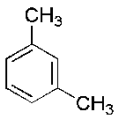
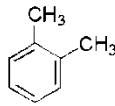
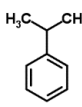
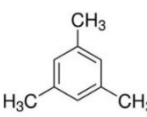
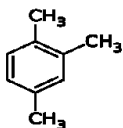
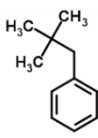
The adsorbent used in this research was activated carbon fiber cloth prepared from phenol-formaldehyde resin precursor, supplied by Nippon Kynol Company. ACC-5092-15 (ACFC15 with nominal surface area of 1500 m²/g) was used as adsorbent in all experiments. Prior to use, all ACFCs underwent 2 h of heat treatment at 400°C with a purge gas flow of 1 SLPM N₂, to remove any adsorbed water vapour and VOCs from the precursor. These treated samples are labelled as “heat treated ACFC” and characterized by Brunauer–Emmett–Teller (BET) surface area of 1503 m²/g, total pore volume of 0.59 cm³/g and micropore volume of 0.55 cm³/g, and average pore diameter of 7.0 Å. The detail procedure of measuring the BET surface area and the pore volume and micropore volume are provided in the Methods section.

3.1.2 Adsorbates

The adsorbates were selected from compounds commonly present in automotive paint solvents, and based on their expected tendency for heel formation. Larger kinetic diameter and high boiling point adsorbates with benzene ring are associated with heel formation (Wang *et al.* 2012), therefore alkylbenzenes with relatively high boiling point (>100°C) and large kinetic diameter (>5 Å) were chosen as adsorbates. Since previous study (Niknaddaf *et al.* 2016) on heel formation on ACFC during electrothermal regeneration showed that adsorbate decomposition at

high temperature results in heel formation on ACFCs, therefore the thermal stability of the adsorbates is another important property that affect heel formation during electrothermal regeneration of ACFCs. Thermal stability of the adsorbates was estimated from the conversion rates (weight percentages) of the tested adsorbates during pyrolysis at 595°C (Švob *et al.* 1974). The ACFC was tested with nine different alkylbenzenes as adsorbates: toluene (99.8%, Fisher Scientific) ethylbenzene (>95%, Fisher Scientific), p-xylene (>95%, Fisher Scientific), m-xylene (>95%, Fisher Scientific), o-xylene (>95%, Fisher Scientific), isopropylbenzene (98%, Sigma Aldrich) 1,3,5 trimethylbenzene (TMB) (99%, Acros Organics), 1,2,4 TMB (98%, Fisher Scientific) and neopentylbenzene (85%, ChemSampCo). Different properties of the tested adsorbates are provided in Table 3-1.

Table 3-1. Properties of the tested adsorbates

Compounds	Structure	Boiling point (°C)	Kinetic diameter (Å)	Vapor pressure at 25°C (mm Hg)	Conversion (weight %) ^e
toluene		110	5.9 ^a	28.6	0.6
ethylbenzene		136	6.2 ^b	10.0	20.7
p-xylene		138	5.9 ^a	8.8	0.8
m-xylene		139	6.8 ^a	8.3	0.7
o-xylene		144	6.8 ^a	6.6	1.3
isopropylbenzene (cumene)		152	6.8 ^a	4.5	41.7
1,3,5 TMB		164	7.5 ^c	2.5	0.7
1,2,4 TMB		171	6.8 ^c	2.1	0.9
neopentylbenzene		184	>7.5 ^d	1.0	~90.0

^a(Lashaki *et al.* 2012a); ^b(Zeynali. 2011); ^c(Eley 1996); ^d(Gédéon *et al.* 2008); ^e(Švob *et al.* 1974)

3.2 Methods

3.2.1 Adsorption and Regeneration Experiments

In this study, 5 cycles of adsorption/regeneration tests were done using the experimental setup shown in Figure 3-1 which is similar to the one used by (Niknaddaf *et al.* 2016). The major parts of this setup are: adsorption/regeneration enclosure containing an ACFC cartridge, adsorbate generation system, gas measurement system, heat application module, and data acquisition and control system (DAC). Details of these parts are described below.

The adsorption/regeneration enclosure consists of a quartz enclosure with inner diameter of 7.3 cm and length of 40 cm, and incorporates an ACFC cartridge. The ACFC cartridge was prepared with approximately 3.5 g of ACFC (21 cm long and 10 cm wide) wrapped to form an annular 3-layer hollow cylinder of 1.65 cm inner diameter (Figure 3.2). The edges of the hollow cylinder were made to overlap with the edges of two stainless steel electrode tubes having 1.65 cm outer diameter. Hose clamps were used to safely attach the ACFC to the two tubes, and to connect the cartridge to the power source. The prepared cartridge was mounted inside the quartz enclosure. The upper electrode tube was open allowing the gas stream to enter the cartridge while the lower tube was closed to force the gas to pass through the ACFC cartridge.

The adsorbate generation system utilized a syringe pump (New Era Inc., NE-300) for injecting liquid organic compounds into a dry air stream maintained at 10 SLPM (standard conditions are 25°C and 1 atm) with the help of a mass flow controller (Alicat Scientific). In all experiments, the inlet adsorbate concentration was maintained at 500 ppmv.

For the gas measurement system, a flame ionization detector (FID, Baseline-Mocon Inc., series 9000) was used to continuously measure VOC concentration at the reactor's outlet during

adsorption (2 min sampling frequency). The FID was calibrated before each adsorption test using the same gas generation system and with a bypass line.

The heat application module was used for adsorbent regeneration and includes a silicon-controlled rectifier (SCR) (1032A-v12-20-0/10v-IL-20-amp maximum with a 0-10-volt control signal) to apply voltage across the ACFC cartridge. One type-K ungrounded thermocouple (Omega) with an outer diameter of 1.6 mm was used to measure the temperature at the center of the ACFC cartridge during adsorption and regeneration.

The data acquisition and control system (DAC) has a data logger (National Instruments, Compact DAQ) with analog input/output modules. A LabVIEW program (National Instruments) recorded the enclosure's outlet concentration, cartridge temperature and the power applied by the SCR. A proportional-integral derivative control algorithm controlled the power applied to heat the cartridge so that the measured temperature matches the set point temperature during regeneration.

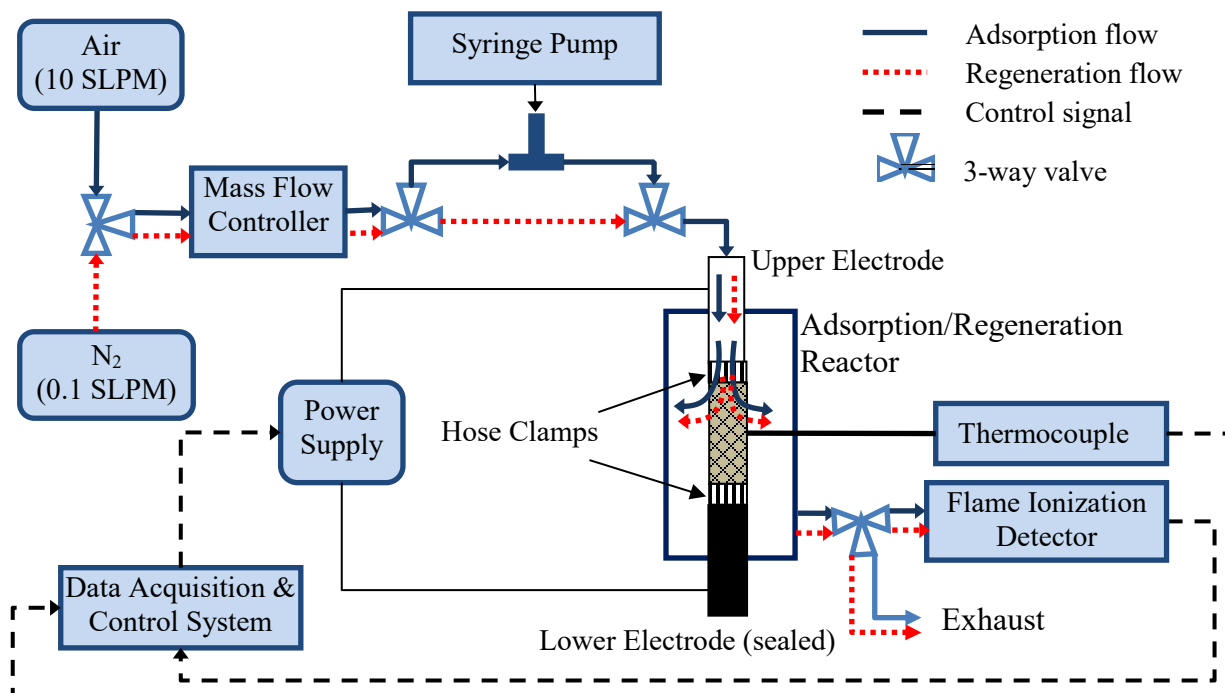


Figure 3-1. Schematic of the experimental setup of the adsorption/regeneration experiments (Niknaddaf *et al.* 2016)



Figure 3-2. ACFC cartridge used for adsorption/regeneration experiments

After calibrating the FID, the gas stream containing VOC adsorbate was directed to the enclosure to start adsorption. The outlet VOC concentration measurement began immediately after adsorption started, generating an adsorption breakthrough curve. Adsorption was performed at room temperature (22-23°C) and continued until the ACFC cartridge was completely saturated (approximately 2.5 hrs) and FID indicated steady state outlet concentration. The ACFC cartridge

was weighed before and after adsorption and the adsorption capacity was measured in the following way:

$$\begin{aligned} & \text{Amount adsorbed (wt\%)} \\ &= \frac{\text{Cartridge weight after adsorption} - \text{Cartridge weight before adsorption}}{\text{Weight of heat treated ACFC}} \times 100 \end{aligned}$$

The adsorption capacity loss of ACFC from the 1st cycle to the 5th cycle was calculated as follows:

$$\begin{aligned} & \text{Capacity loss(\%)} \\ &= \frac{\text{Amount adsorbed after 1}^{\text{st}} \text{ cycle} - \text{Amount adsorbed after 5}^{\text{th}} \text{ cycle}}{\text{Amount adsorbed after 1}^{\text{st}} \text{ cycle}} \times 100 \end{aligned}$$

Before starting regeneration, the saturated ACFC cartridge was purged with 1 SLPM of high purity (99.998%) nitrogen (Praxair) for 5 min to purge oxygen out of the enclosure. Based on the volume calculation of the quartz enclosure, 5 min purging with 1 SLPM N₂ can effectively remove the oxygen from the enclosure. The regeneration temperature and heating rate were chosen based on a previous study on the effects of regeneration condition on heel formation on ACFC (Niknaddaf 2015). (Niknaddaf 2015) showed that high heating temperature (400°C) and higher heating rate (70°C/min) resulted in the highest heel, therefore to study the worst case scenario and to amplify the heel formation, a regeneration temperature of 400°C and heating rate of 70°C/min were chosen in this study. Regeneration was conducted for 100 min, with simultaneous purge with 0.1 SLPM nitrogen. During desorption, the concentration of effluent adsorbates was measured using a FID at a sampling frequency of 30 s. The concentration of the adsorbates during desorption can rise beyond their saturation concentration which causes condensation inside and at the outlet of the quartz enclosure, and also in the FID tubing. To

avoid this problem, a heating tape was wrapped around the wall of the quartz enclosure and dilution with air was applied at the outlet of the enclosure. Adsorbates with higher vapour pressure exhibited higher concentration during desorption, therefore required higher dilution. Therefore 60-80-fold dilution with air was applied, based on the vapour pressure of the compounds. After completing the regeneration, the ACFC cartridge was cooled down to room temperature (25°) while the 0.1 SLPM purging with nitrogen continued till the end of cooling. The ACFC cartridge was then taken out of the enclosure, and weighed. The difference between weights before adsorption and after regeneration was used to calculate the amount of heel build up for that cycle. The 1st cycle heel buildup was calculated as follows:

$$\begin{aligned} & \textit{Heel buildup after 1st cycle (wt\%)} \\ & = \frac{\text{Weight after 1}^{st} \text{ regeneration cycle} - \text{Weight before 1}^{st} \text{ adsorption cycle}}{\text{Weight of heat treated ACFC}} \times 100 \end{aligned}$$

The cumulative heel buildup after five consecutive adsorption/regeneration cycles was calculated as follow:

$$\begin{aligned} & \textit{Cumulative Heel buildup (wt\%)} \\ & = \frac{\text{Weight after 5}^{th} \text{ regeneration cycle} - \text{Weight before 1}^{st} \text{ adsorption cycle}}{\text{Weight of heat treated ACFC}} \times 100 \end{aligned}$$

3.2.2 Characterization Tests

Several characterization tests were conducted on the heat-treated and regenerated ACFCs to determine the properties of the ACFCs before and after the 5-cycle adsorption/regeneration experiments.

3.2.2.1 *Thermogravimetric analysis*: thermogravimetric analysis (TGA) (TGA/DSC 1, Mettler Toledo) and derivative thermogravimetric analyses (DTG) was used to assess the temperature stability of heat treated and regenerated ACFC samples. In each run, samples were heated from 25°C to 100°C at a heating rate of 10°C/min, after that samples were isothermally heated at 100°C for 15 min, then a temperature was ramp up from 100°C to 900°C at 5°C/min heating rate. Throughout the test, a nitrogen flow of 50 mL/min was used to purge the desorbed species.

3.2.2.2 *Micropore surface analysis*: ACFC samples were analyzed using a micropore surface analyzer (Autosorb iQ2MP, Quantachrome). Nitrogen was used as probe molecule at relative pressure ranging from 10^{-7} to 1 at 77K. To remove water vapour and volatiles from the pores, ACFCs were cut into small pieces (2 mm × 2 mm), and 30 – 50 mg sample was added to a 6-mm cell, and de-gassed at 120°C for 5 hours before analysis. BET surface area (m^2/g) and micropore volume (cm^3/g) were obtained over the relative pressure ranges of 0.01 to 0.07 and 0.2 to 0.4, respectively. V-t model was used to determine micropore volume. Total pore volume was measured at a relative pressure of 0.975. Pore size distributions (PSDs) were obtained from the isotherm of nitrogen adsorption using the quenched solid density functional theory (QSDFT) for slit pores (Olivier 1998).

CHAPTER 4. RESULTS AND DISCUSSIONS

Adsorption and regeneration experiments on ACFCs were conducted in 5 cycles for different adsorbates to find out the effects of adsorbate properties on heel formation and adsorption capacity loss. The regenerated ACFC samples were also characterized by thermogravimetric analysis and micropore surface analysis. The obtained results are discussed below.

4.1 Breakthrough Curves

Figure 4-1 show the adsorption breakthrough curves for five consecutive adsorption cycles on ACFC loaded with nine different alkylbenzenes adsorbates. The reduction in breakthrough time for each cycle, and the cumulative heel formation are presented in Table 4-1. The breakthrough time, represented by $t_{1\%}$, refers to the time when the outlet concentration equals 1% of the inlet concentration. Toluene has the smallest reduction in breakthrough time in each cycle, mainly due to lower heel formation and less capacity loss compared to other adsorbates. Breakthrough time decreased more for p-xylene (20% higher reduction with respect to toluene in 5th cycle) which is expected since p-xylene resulted in 40% higher cumulative heel and 19% higher capacity loss over 5 consecutive cycles compared to toluene. For m-xylene, o-xylene and 1,2,4 TMB, similar trend in breakthrough time reduction was observed, and immediate breakthrough occurred for all three compounds after 4th cycle. Having similar heel formation and capacity loss for the three compounds might be the reason behind similar breakthrough time reduction for these adsorbates.

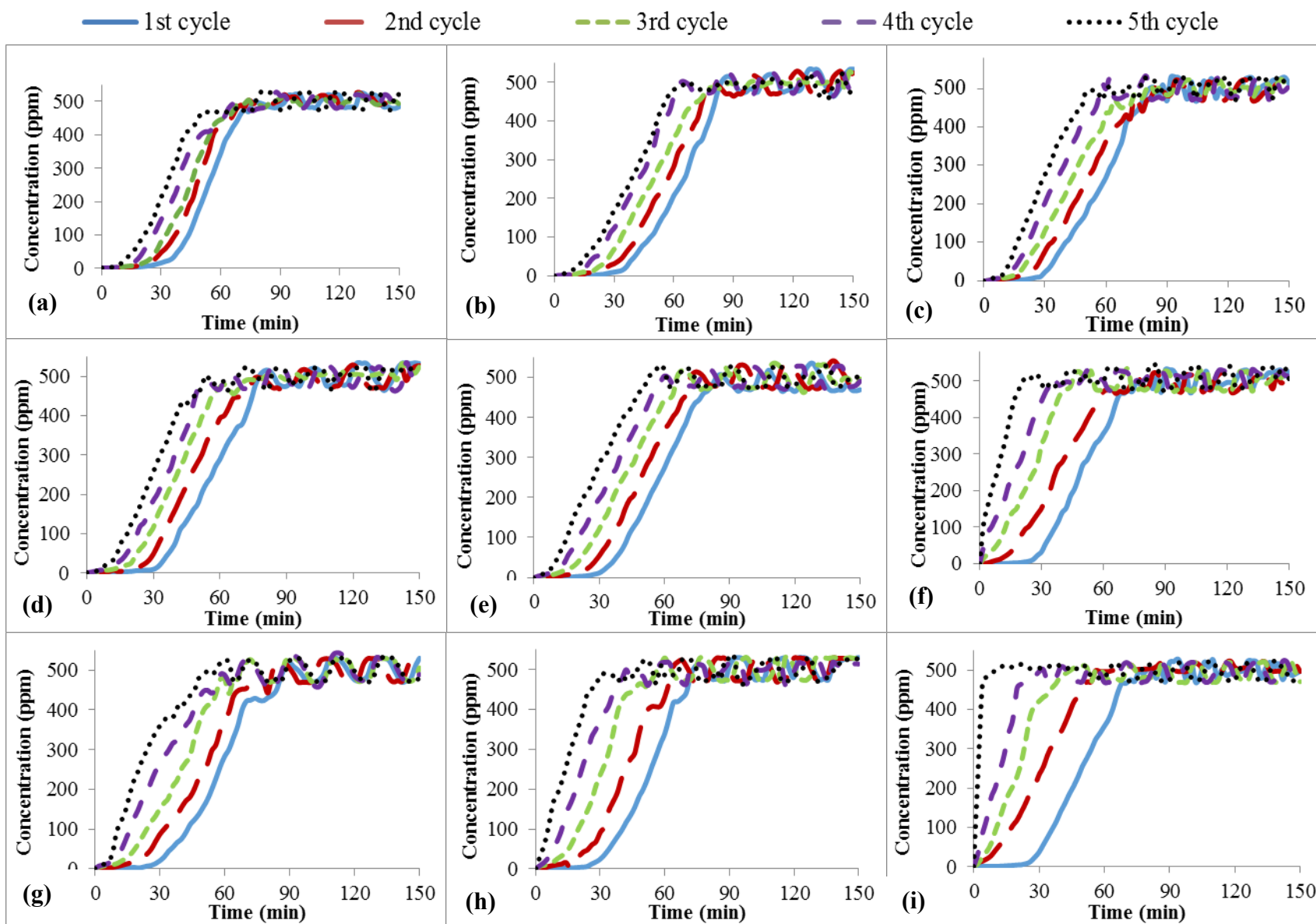


Figure 4-1. Breakthrough curves for adsorption of (a) toluene, (b) p-xylene, (c) m-xylene, (d) o-xylene, (e) 1,2,4 TMB, (f) 1,3,5 TMB,

(g) ethylbenzene, (h) isopropylbenzene and (i) neopentylbenzene.

Table 4-1. Reduction in 1% breakthrough time, cumulative heel and capacity loss of ACFC for 5 cycle adsorption/desorption of different adsorbates (Values are reported as mean \pm standard deviation of two experimental runs)

Compounds	Kinetic diameter (Å)	Reduction in breakthrough time (%)				5 cycle cumulative heel (%)	Capacity loss (%)
		2nd cycle	3rd cycle	4th cycle	5th cycle		
toluene	5.9	36 \pm 0	45 \pm 0	55 \pm 1	70 \pm 0	8.9 \pm 0.2	25.2 \pm 0.4
p-xylene	5.9	42 \pm 0	54 \pm 1	66 \pm 0	84 \pm 0	12.5 \pm 0.1	30.1 \pm 0.5
m-xylene	6.8	48 \pm 1	64 \pm 1	79 \pm 0	IBT	12.6 \pm 0.1	35.2 \pm 0.6
o-xylene	6.8	48 \pm 0	66 \pm 1	80 \pm 2	IBT	12.6 \pm 0.1	35.5 \pm 0.2
1,2,4 TMB	6.8	51 \pm 1	71 \pm 1	86 \pm 2	IBT	12.7 \pm 0.0	37.9 \pm 0.8
1,3,5 TMB	7.5	81 \pm 2	IBT	IBT	IBT	12.8 \pm 0.1	60.2 \pm 0.2
ethylbenzene	6.2	59 \pm 1	78 \pm 1	IBT	IBT	15.0 \pm 0.2	42.5 \pm 0.2
isopropylbenzene	6.8	75 \pm 2	98 \pm 3	IBT	IBT	16.0 \pm 0.2	53.4 \pm 0.2
neopentylbenzene	>7.5	98	IBT	IBT	IBT	17.2 \pm 0.3	80.0 \pm 0.2

*IBT: Immediate Breakthrough

Although 1,3,5 TMB had similar heel formation to 1,2,4 TMB, it showed about 58% higher reduction in 2nd cycle breakthrough time with respect to 1,2,4 TMB, and breakthrough occurred immediately after 2nd cycle for 1,3,5 TMB. The bulkier molecules of 1,3,5 TMB (7.5 Å) compared to 1,2,4 TMB (6.8 Å) might have partially blocked more pores of ACFCs (Niknaddaf *et al.* 2016), leading to higher capacity loss and breakthrough time reduction for 1,3,5 TMB compared to 1,2,4 TMB. Breakthrough reduction of ethylbenzene and isopropylbenzene followed similar trend in heel formation and capacity loss to toluene, xylenes and TMBs. Neopentylbenzene caused the highest heel formation and capacity loss, therefore breakthrough time decreased significantly (98%) in the 2nd cycle, and immediate breakthrough occurred in following cycles. Therefore, it is found that the heel formation varied for different adsorbates due to their varying properties.

4.2 Cumulative Heel Buildup on ACFC Samples during 5-Cycle Adsorption and Regeneration Experiments

Measurements of mass balance cumulative heel of ACFC samples after 5 cycle adsorption/desorption of different adsorbates are compared in Figure 4-2. The detailed mass balance results of all 5 cycle tests are provided in Appendices (from Appendix B to Appendix J). All tested adsorbates were alkylbenzenes having different levels of thermal stability. The conversion percentages of different alkylbenzenes from pyrolysis at 595°C (Švob *et al.* 1974) have been used as an indication of the thermal stability of the adsorbates. The conversion values (in percentage) has been included in parenthesis beside each compound's name in Figure 4-2.

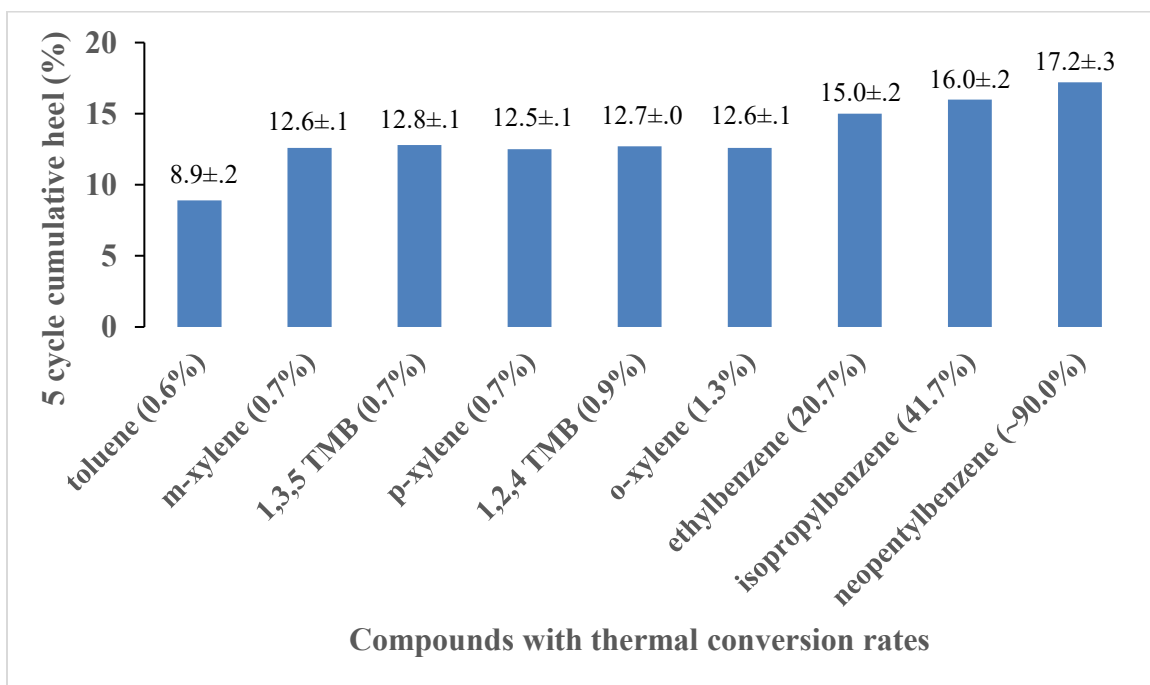


Figure 4-2. Cumulative heel on ACFC samples loaded with different alkylbenzene adsorbates. Values in parentheses indicate thermal conversion rates (as % weight) from literature

Figure 4-2 shows that cumulative heel varied from 8.9% to 17.2% for different alkylbenzene adsorbates. The lowest cumulative heel (8.9%) was observed for toluene, which is

the most thermally stable compound with lowest conversion rate. Cumulative heel formation increased from 8.9% for toluene to about 12.6% for xylenes and TMBs. Although the conversion rates of these five compounds are comparable to that of toluene, the heel was higher than toluene possibly due to toluene's lower boiling point (110°C) compared to the three xylenes (138-144°C) and TMBs (165-171°C), which caused faster desorption of toluene at a lower desorption temperature. The average pore diameter of the tested ACFC is 7.0 Å, therefore toluene's smaller kinetic diameter (5.9 Å) compared to other tested compounds might have reduced the diffusion resistance during desorption, leading to less heel formation. Ethylbenzene and p-xylene have comparable kinetic diameters (6.2 Å and 5.9 Å respectively), and boiling points (136°C and 138°C respectively), yet ethylbenzene showed 21% higher heel than p-xylene. This is because of ethylbenzene's very high conversion rate (20.7%) in pyrolysis compared to p-xylene which has conversion rates in the order of 1.0%. The low thermal stability of ethylbenzene might have caused adsorbate decomposition during high temperature (400°C) regeneration of microporous ACFC. Previous studies also confirmed that adsorbate decomposition causes irreversible adsorption by forming coke which blocks the adsorbate micropores (Ania *et al.* 2004, Niknaddaf *et al.* 2016). Coke (also known as char) is formed as a bi-product of the pyrolysis or decomposition of hydrocarbons in the absence of oxygen (Basu 2013, Guisnet and Magnoux 2001). Char consists mainly of carbon and is highly stable at high temperature of about 800°C (Banerjee *et al.* 1986, Guisnet and Magnoux 2001). The thermogravimetric analysis provided in Section 4.3 will provide further information on the nature of the heel and will identify if material decomposition as the main heel formation mechanism in this study. Isopropylbenzene's conversion rate is twice of that of ethylbenzene; however, it showed only 6% higher heel than ethylbenzene. This is because, the thermal decomposition of organic compounds usually forms

smaller molecules, but the resulting fragments may further interact with each other and produce larger compounds than the original one (Moldoveanu 2010). Therefore, the conversion rate includes both formation of larger and smaller molecules than the adsorbate molecule, and only the larger and high molecular weight compounds produced from the thermal degradation of the adsorbates formed heel on ACFC. For similar reason, neopentylbenzene with 116% higher conversion rate than isopropylbenzene caused only 6% higher heel than isopropylbenzene. Therefore, it is observed that the heel caused by different adsorbates is affected by the thermal stability of the compounds.

4.3 Thermo-Gravimetric Analysis

Thermogravimetric analysis and derivative thermogravimetric analysis were done by exposing the heat treated and regenerated ACFC samples loaded with different adsorbates to temperature up to 900°C. The temperature stability of the heel formed during the 5-cycle tests was evaluated and is shown in the TGA and DTG results in Figure 4-3 and Figure 4-4 respectively. Though the ACFC samples were regenerated at 400°C, no mass loss occurred before the temperature reached 520°C for any of the regenerated samples. Moreover, for the adsorbates showing highest heel formation (e.g. isopropylbenzene and neopentylbenzene, with 16% and 17.2% heel respectively), no significant weight loss was observed at temperature as high as 600°C.

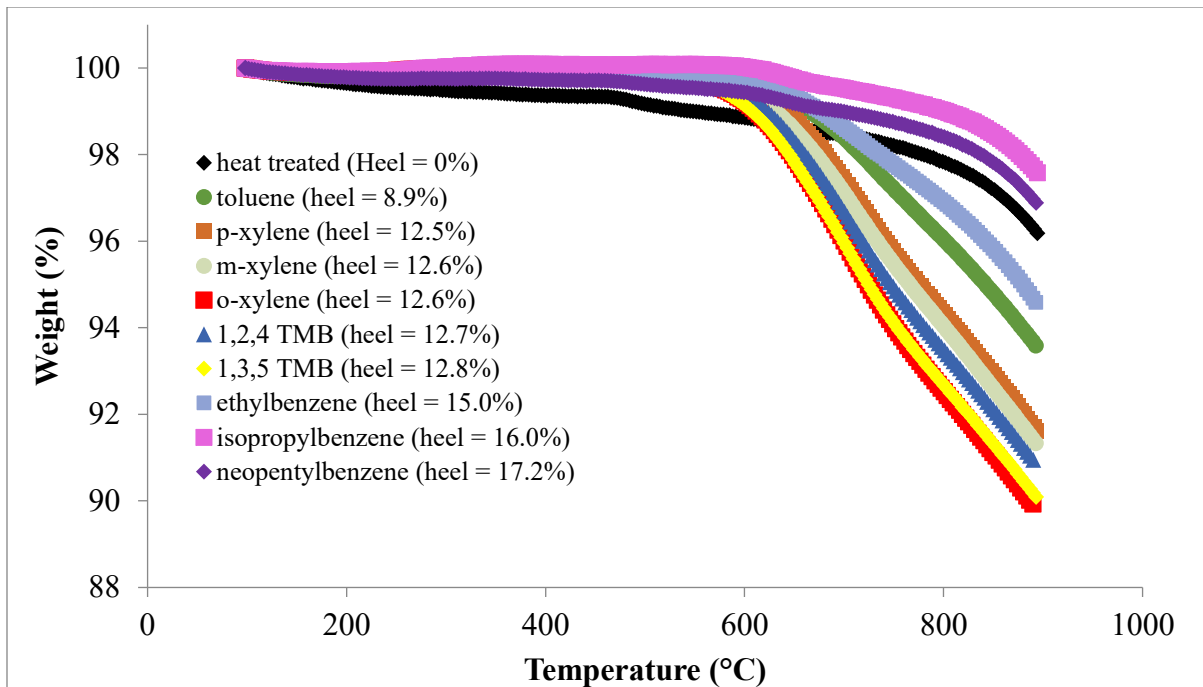


Figure 4-3. TGA results of heat treated and regenerated ACFCs loaded with different adsorbates

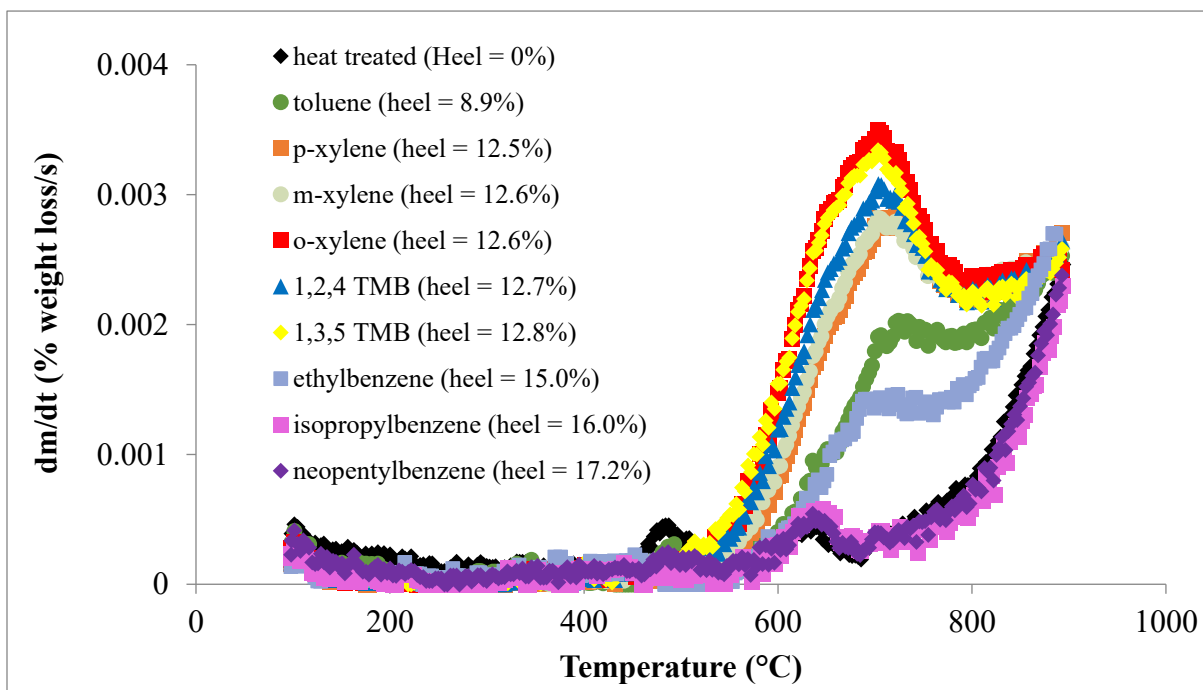


Figure 4-4. DTG results of heat treated and regenerated ACFCs loaded with different adsorbates

Even mass loss for isopropylbenzene and neopentylbenzene observed after this high temperature (600°C) was lower than that for the heat treated ACFC, and was mainly attributed to the adsorbent burn off. This indicates that the irreversibly adsorbed species on the regenerated ACFCs were highly stable and cannot be removed even at very high temperature. Since coke deposited from the pyrolysis of aromatic compounds proved to be highly stable at high temperature (Fuentes and Bartholomew 1997), a major portion of the heel formed on the regenerated ACFCs might be coke. The products of pyrolysis depend on the structure of the initial compound and the mechanism of decomposition (Moldoveanu 2010). The thermal degradation of alkylbenzenes follows a free radical mechanism (Švob *et al.* 1974) and the products of initial decomposition can undergo further reaction under the influence of heat (Moldoveanu 2010). Decomposition of alkylbenzene depends on various factors including the type of alkyl radicals attached to the benzene rings (Guisnet and Magnoux 2001, Towfighi *et al.* 2002). During thermal decomposition of alkylbenzenes, the longer the alkyl chain of the compounds, the more they are prone to decomposition that forms free radicals. β -hydrogens in free radicals are more prone to dehydrogenation than α -hydrogens (Figure 4-5) and dehydrogenation may leave carbon residue with very low hydrogen content during pyrolysis (Guisnet and Magnoux 2001, Jambor and Hájeková 2015, Van Speybroeck *et al.* 2007). This justifies that the tested adsorbates with longer alkyl chains (ethylbenzene, isopropylbenzene and neopentylbenzene) showed about 20% to 35% higher heel than other adsorbates with shorter branches (three xylenes and two TMBs). Though the cumulative heel for ethylbenzene (15.0%) was higher than toluene (8.9%), xylenes (12.5%) and TMBs (12.7%), ethylbenzene showed lower peak in DTG analysis, confirming that the heel is due to coke formation on ACFC. Though slightly higher DTG peaks were observed for the three xylenes and two TMBs, the maximum

heel recovery for these compounds were less than 40% at temperature of 900°C. If the heel was formed by strong physisorption or chemisorption, single or multiple mass loss peak would have appeared earlier at temperature lower than 900°C, and larger recovery of heel would have been possible (Jahandar Lashaki *et al.* 2016a, Jahandar Lashaki *et al.* 2016b).

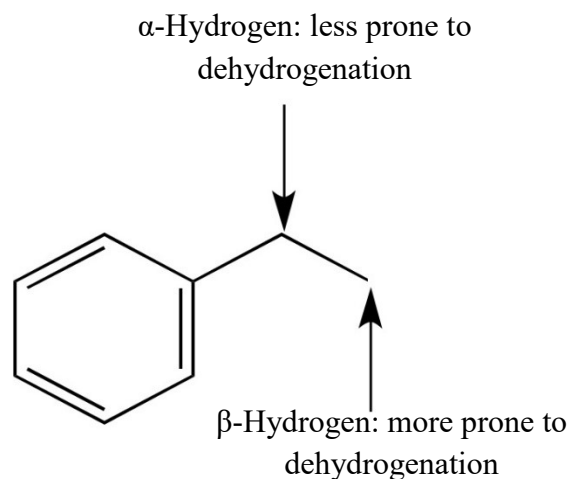


Figure 4-5. Positions and dehydrogenation tendency of α and β -hydrogen in alkylbenzenes
[modified from (Švob *et al.* 1974)]

The magnitude of the peaks in DTG curve depends on the different constituents of the non-desorbed products and its intermediate and bi-products. For adsorbate transformation at temperature above 350°C, the non-desorbed products mainly consist of highly polyaromatic compounds with varying temperature stability (Guisnet and Magnoux 2001), therefore, the amount of these non-desorbed polyaromatics that come off the carbon at high temperature during TGA varies depending on the product type. Therefore, the peaks for different adsorbates varied in magnitude in DTG results.

4.4 Desorption Profile and Applied Power during Regeneration Cycles

Since thermogravimetric analysis suggested coke formation as the main mechanism of irreversible adsorption, further investigation was done to find out what conditions favoured adsorbates coking on ACFCs. Previous studies showed that coke formation on adsorbent is mainly affected by the desorption temperature (Niknaddaf *et al.* 2016), desorption concentration of the reacting species (Jambor and Hájeková 2015, Moldoveanu 2010), and its residence time inside the adsorbent pores (Moldoveanu 2010). Both gas phase homogenous or gas-solid phase heterogeneous reactions enhance the coke formation process, therefore adsorbates' higher concentration and residence time increase the rate and extent of coke formation. The measured outlet concentration of the reactor during desorption and the proportion of adsorbate remaining inside the adsorbent pores provide good indication on the adsorbate concentration and residence time during desorption. Therefore, the desorption concentration of all tested adsorbates during 1st regeneration cycle was measured as an indicator of concentration inside the ACFC pores. Figure 4-6 shows the temperature and desorption profiles for the entire desorption period of 2 hrs, including the 5-min purging with nitrogen prior to heating. Figure 4-7 presents the same plots for the initial 30 min of regeneration for clarity. The area below the desorption profile was integrated to calculate the fraction of residual adsorbate exposed to high temperature (400°C) during regeneration and presented in Table 4-2. These values help in understanding how exposure of high concentration of adsorbates to high temperature contribute towards heel formation on ACFC. The average applied power during regeneration in 5 cycles for desorption of each adsorbate are presented in the last column of Table 4-2, confirming good consistency among applied power in 5-cycle tests for all adsorbates. This rules out the possibility that desorption

concentrations and heel results are related to bias in power application or temperature measurement.

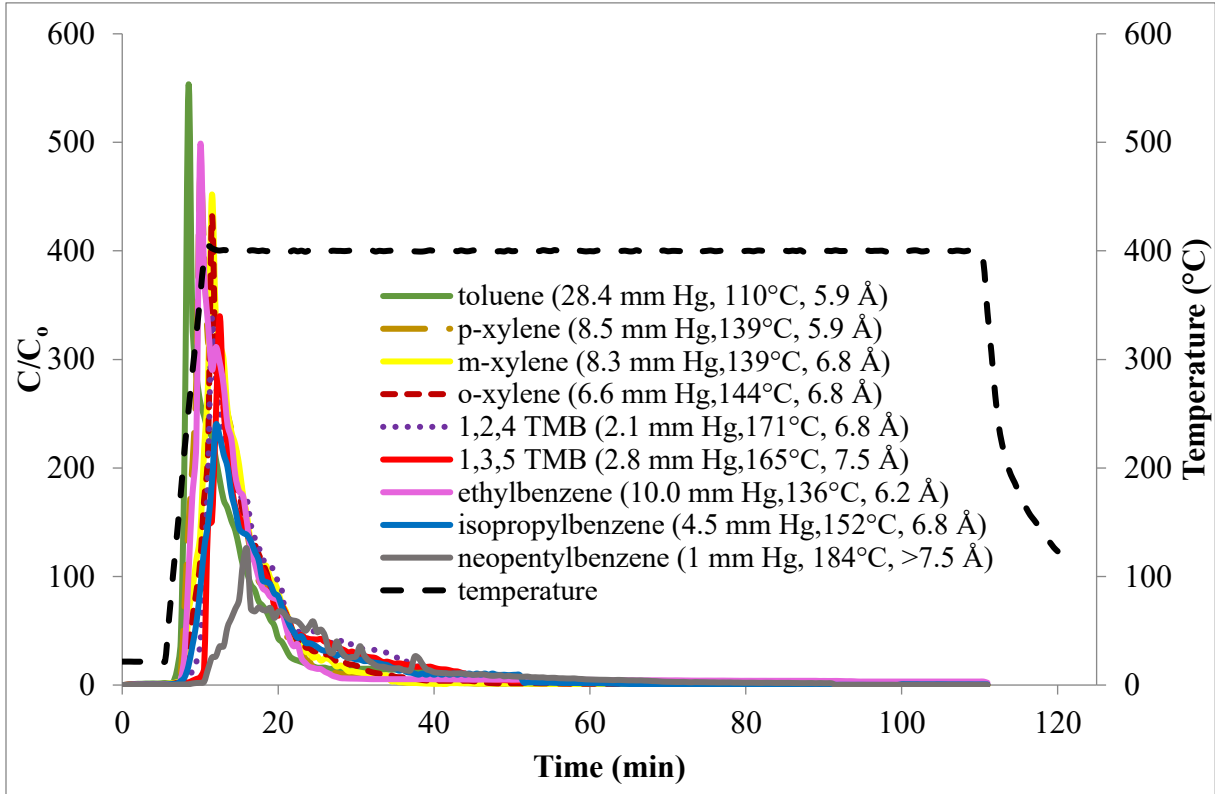


Figure 4-6. Desorption profiles for the 1st regeneration cycle of ACFC loaded with different adsorbates

In figure 3-7, the temperature profile shows that the ACFCs were at room temperature (about 22°C) during the initial 5 min of purging with 1 SLPM nitrogen. After that, heating started and the adsorbates' outlet concentration increased with temperature to a maximum value (C_{max}) at a specific temperature. Toluene came out first among all adsorbates, since it has the lowest boiling point (110°C) and smallest kinetic diameter (5.9 Å). Due to its high vapour pressure (28.4 mm Hg), toluene's desorbed concentration peak went up very fast and sharply reached the highest value ($C_{max}/C_o = 552$) at 252°C. Toluene's high vapour pressure also caused rapid decrease in concentration, therefore only 55.5% of the desorbed toluene remained as

residual inside ACFC pore when temperature reached 400°C. So, toluene showed the only 3.2% heel after 1st cycle desorption. The average power applied in each cycle desorption of toluene was consistent (varying between 180 to 190 W) (Appendix B, Figure B-2), therefore applied power and regeneration temperature were consistent across the 5 cycles, and the heel formation mechanism is expected to be similar across the 5 cycles, resulting in a cumulative heel of 8.9%.

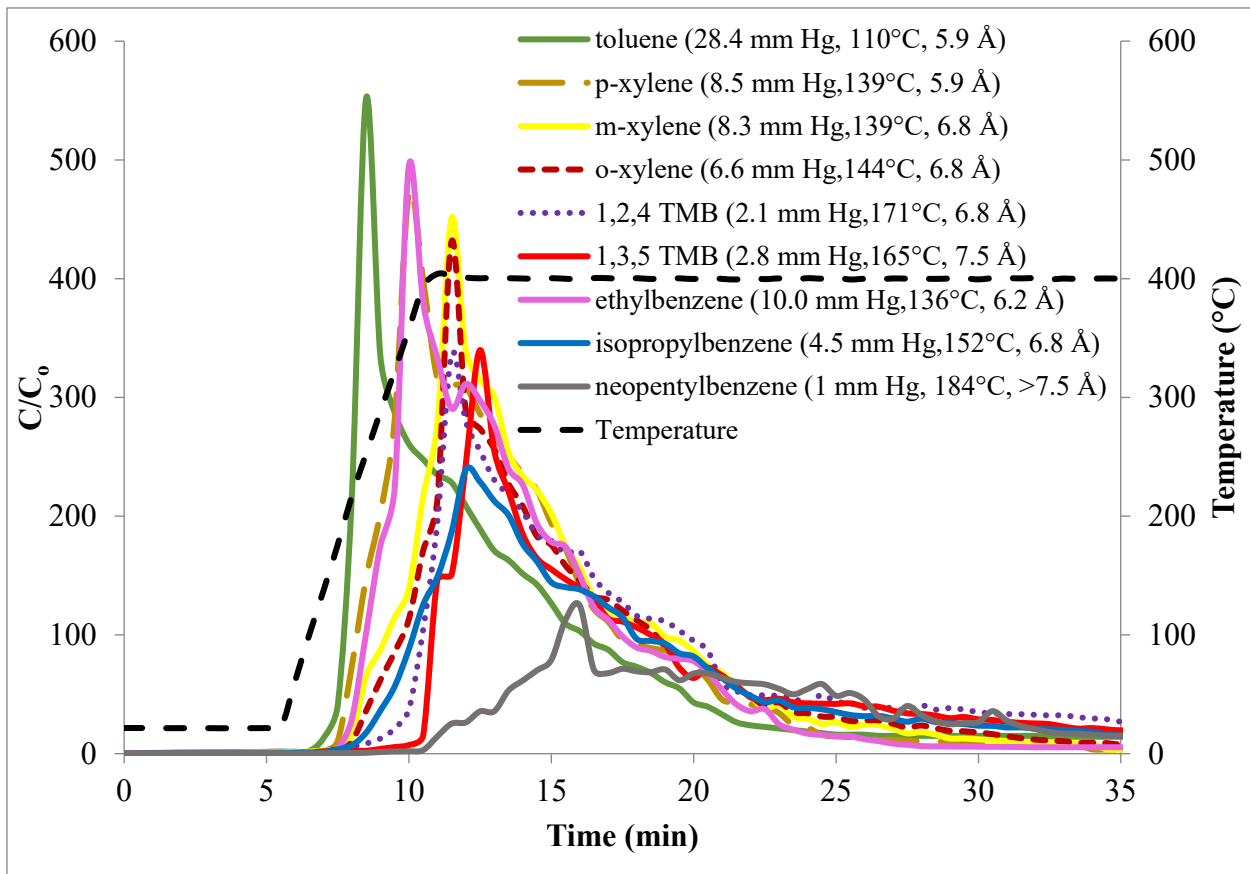


Figure 4-7. Desorption profiles for the initial 30 min of the 1st regeneration cycle of ACFC loaded with different adsorbates

After toluene, p-xylene and ethylbenzene came out almost at same time and reached maximum concentration (C_{\max}/C_o) of 472 and 495 respectively at around 360°C, since they have similar boiling point, vapour pressure and kinetic diameter. Fraction of p-xylene and

ethylbenzene exposed to 400°C were 70% and 66% respectively, but ethylbenzene showed 15% higher heel in 1st cycle than p-xylene (Table 4-2), due to 20 times higher conversion rate, which caused more decomposition and coke formation for ethylbenzene. Not all the decomposed products of ethylbenzene turned into coke; only the ones with higher molecular weight and bigger molecular size turned into non-desorbed species. Similar trend is observed for m-xylene and o-xylene, since their comparable physical properties caused similar exposure of concentrated desorption stream to high temperature, causing similar heel formation. 1,2,4 TMB has a kinetic diameter (6.8 Å) similar to m-xylene and o-xylene, but due to its higher boiling point (171°C), it started desorbing at higher temperature, and reached a maximum concentration ($C_{\max}/C_o=336$) after the temperature reached 400°C, therefore residual 1,2,4 TMB exposure to 400°C was about 12% higher than m-xylene and o-xylene, which caused 9% higher heel in 1st cycle, but due to slightly higher (7%) capacity loss (Appendix F. Table F-1), heel accumulation in consecutive cycles decreased for 1,2,4 TMB and it ended up with similar 5 cycle cumulative heel as the three xylenes. Figure 4-7 also shows that 1,3,5 TMB, due to its larger kinetic diameter (7.5 Å) compared to 1,2,4 TMB, desorbed at a slower rate and therefore reached the maximum concentration ($C_{\max}/C_o=340$) later than 1,2,4 TMB causing 9% higher residual adsorbate exposure to 400°C and 13% higher 1st cycle heel. However, very high capacity loss (60.2%) (Appendix G) decreased cyclic heel accumulation, resulting in similar cumulative heel for both TMBs. For isopropylbenzene, 78% of residual adsorbate was exposed to 400°C, which is quite similar to m-xylene and o-xylene, since these compounds have similar kinetic diameter and comparable boiling points. However, because of 40 times higher conversion rate than xylenes, isopropylbenzene went through significant decomposition, reducing its maximum concentration ($C_{\max}/C_o=239$). Considerable thermal degradation of isopropylbenzene resulted in 36% higher 1st

cycle heel and 27% higher cumulative heel after 5 cycles (Table 4-2) than the three xylenes and two TMBs. Neopentylbenzene has the highest boiling point (184°C) and the largest kinetic diameter ($>7.5 \text{ \AA}$), among the tested adsorbates, therefore it started desorbing significantly late (Figure 4-7). In addition, its lowest vapour pressure (1 mm Hg) and highest conversion rate ($\sim 90\%$) decreased its maximum concentration ($C_{\text{max}}/C_0=124$). Since most of its desorption occurred after the temperature reached 400°C, therefore about 98% of residual neopentylbenzene was exposed to 400°C, which caused the highest 1st cycle heel (10.9%) (Table 4-2), but significantly higher capacity loss (80%) lowered the heel addition in each consecutive cycle, showing a 5-cycle cumulative heel of 17.2%.

Table 4-2. Exposure of residual adsorbates to 400°C, 1st cycle and 5 cycle cumulative heel, 5 cycle capacity loss and 5 cycle average power applied during regeneration of ACFCs loaded with different adsorbates. (Values are reported as mean ± standard deviation of two experimental runs)

Compound	Residual adsorbates (%)	Conversion (%) (Švob <i>et al.</i> 1974)	1st cycle heel (%)	Cumulative heel (%)	Capacity loss (%)	Average Power (W)
toluene (28.4 mm Hg, 110°C, 5.9 Å)	55.5±0.1	0.6	3.2±0.1	8.9±0.2	25.2±0.4	177.1
p-xylene (8.5 mm Hg, 139°C, 5.9 Å)	70.1±1.7	0.8	6.2±0.2	12.5±0.1	30.1±0.5	182.3
m-xylene (8.3 mm Hg, 139°C, 6.8 Å)	75.1±2.8	0.7	6.7±0.2	12.6±0.1	35.2±0.6	181.5
o-xylene (6.6 mm Hg, 144°C, 6.8 Å)	76.1±2.1	1.3	6.8 ± 0.1	12.6±0.1	35.5±0.2	174.3
1,2,4 TMB (2.1 mm Hg, 171°C, 6.8 Å)	82.5±1.4	0.9	7.4±0.2	12.7±0.0	37.9±0.8	180.4
1,3,5 TMB (2.8 mm Hg, 165°C, 7.5 Å)	90.1±0.3	0.7	8.1±0.2	12.8±0.1	60.2±1.5	185.2
ethylbenzene (10.0 mm Hg, 136°C, 6.2 Å)	65.5±2.5	20.7	7.3±0.3	15.0±0.2	42.5±0.4	180.3
isopropylbenzene (4.5 mm Hg, 152°C, 6.8 Å)	78.1±0.9	41.7	9.1±0.2	16.0±0.2	53.4±0.7	186.7
neopentylbenzene (1.0 mm Hg, 184°C, >7.5 Å)	97.5±0.2	~90.0	10.9±0.4	17.2±0.3	80.0±2.0	186.4

4.5 Micropore Surface Analysis

Micropore surface analysis provides information on physical properties (BET surface area, total pore and micropore volume) of the heat treated and regenerated ACFCs. The results are provided in Table 4-3, along with adsorbates' kinetic diameter, heel formation and capacity loss data, for clear interpretation of results.

Table 4-3. BET surface area, pore volume and micropore volume of heat treated and regenerated ACFCs loaded with different adsorbates

Compounds	Cumulative heel (wt%)	Kinetic diameter (Å)	Adsorption capacity loss (wt%)	BET surface area (m ² /g)	Total pore volume (cm ³ /g)	Micropore volume (cm ³ /g)
Heat treated ACFC15				1503±22	0.59±0.0	0.55±0.0
Toluene	8.9±0.2	5.9	25.2±0.4	1043±20	0.47±0.2	0.38±0.2
p-xylene	12.5±0.1	5.9	30.1±0.5	1039±19	0.43±0.1	0.38±0.0
m-xylene	12.6±0.1	6.8	35.2±0.6	990±10	0.40±0.1	0.35±0.1
o-xylene	12.6±0.1	6.8	35.4±0.2	990±15	0.40±0.1	0.36±0.2
1,2,4 TMB	12.7±0.0	6.8	37.9±0.8	991±25	0.40±0.2	0.35±0.1
1,3,5 TMB	12.8±0.1	7.5	60.2±1.5	995±10	0.40±0.1	0.36±0.1
ethylbenzene	15.0±0.2	6.0	42.5±0.4	975±12	0.37±0.2	0.33±0.1
isopropylbenzene	16.0±0.2	6.8	53.4±0.7	960±15	0.35±0.1	0.34±0.2
neopentylbenzene	17.2±0.3	>7.5	80.0±2.0	912±21	0.34±0.2	0.32±0.0

The results show that after five cycles of adsorption/regeneration with different adsorbates, the BET surface area, micropore volume, and total pore volume of all regenerated ACFC samples decreased. These results are in good agreement with previous reports that heel formation results in partially or fully blocked adsorbent pores (Ania *et al.* 2005, Caliskan *et al.* 2012) .

There has been a decrease of 30% to 40% in surface area, 20% to 42% in pore volume and 28% to 40% in micropore volume from toluene (with lowest heel of 8.9%) to neopentylbenzene (with highest heel of 17.2%) loaded ACFCs. The regenerated ACFC loaded with toluene had highest BET surface area (1043 m²/g), pore volume (0.47 cm³/g) and micropore volume (0.38 cm³/g), since toluene caused the lowest heel (8.9%). P-xylene had 40% higher heel than toluene, therefore regenerated ACFC loaded with p-xylene showed 9% higher reduction in pore volume than the regenerated ACFC loaded with toluene. The surface area and pore volume obtained for ACFC samples loaded with m-xylene, o-xylene, 1,2,4 TMB and 1,3,5 TMB were quite similar because of similar heel formation. The surface area and pore volume results for 1,3,5 TMB also prove that the significant capacity loss (60.2%) caused by 1,3,5 TMB is mainly due to the partial pore blockage by its bulkier molecules (7.5 Å). The average pore width of ACFC15 is 7.0 Å (Niknaddaf *et al.* 2016), therefore its adsorption capacity for N₂ molecules was much higher than it showed for 1,3,5 TMB. This indicates that the partial occlusion inhibits the accessibility of ACFC pores to bulkier adsorbates, but allows access for smaller molecules such as N₂. The reduction in surface area and pore volume for ethylbenzene and isopropylbenzene were mainly attributed to their higher cumulative heel. Again, ethylbenzene showed 18% higher heel but 32% less capacity loss than 1,3,5 TMB since ethylbenzene's molecules (6.2 Å) were smaller than the average pore width of ACFC15 (7.0 Å) and therefore caused less partial pore blockage. For the same reason neopentylbenzene with the largest kinetic diameter (>7.5 Å) among all tested adsorbates, showed highest capacity loss (80%). Compared to isopropylbenzene, neopentylbenzene exhibited 6% higher heel and 5%, 3% and 6% lower surface area, pore volume and micropore volume respectively, however, it had a significantly higher capacity loss (80%) than isopropylbenzene (53.4%). This is mainly due to neopentylbenzene's large kinetic diameter

which facilitated extensive partial pore blockage in ACFC. These results illustrate how the adsorbate's kinetic diameter affect its accessibility of the adsorbent pores, therefore bigger molecules cause higher and faster capacity loss compared to smaller molecules. Similar findings were also reported in a previous study, where ACFCs regenerated following adsorption of 1,2,4 TMB depicted large loss in adsorption capacity for 1,2,4 TMB, but maintained good adsorption capacity for acetone which is smaller than 1,2,4 TMB (Niknaddaf *et al.* 2016).

CHAPTER 5. CONCLUSIONS AND RECOMMENDATIONS

5.1 Conclusions

The effects of adsorbate properties (boiling point, kinetic diameter and thermal stability) on heel build up and adsorption capacity loss of ACFC15 were investigated in this research. For this purpose, nine different alkylbenzenes were tested as adsorbates in 5-cycle adsorption/regeneration experiments. Regeneration experiments were conducted using resistive heating at a regeneration temperature of 400°C, with a heating rate of 70°C /min and in 0.1 SLPM N₂ flow. Characterization tests were also completed using thermogravimetric analysis and micropore surface analysis. Desorption profile for all the adsorbates were obtained in the 1st regeneration cycle. Major findings from this research are provided below:

- Heel formation for different compounds varied between 8.9% to 17.2%, and capacity loss ranged from 25.2% to 80.0%. The breakthrough curves showed the cyclic adsorption performance of different adsorbates and the effects of heel formation on capacity loss of ACFC.
- Adsorbates with lower thermal stability (higher conversion value during pyrolysis) showed higher heel buildup and vice versa. This is mainly due to adsorbate decomposition resulting from exposure of residual adsorbate to high regeneration temperature of 400°C, leading to coke formation.
- TGA results showed less than 40% heel recovery at temperature as high as 900°C, confirming that the heel mainly consists of highly stable coke formation from thermal decomposition of adsorbates.

- The 1st cycle desorption profiles of the tested adsorbates showed that adsorbates with higher boiling points and larger kinetic diameters had higher adsorbate decomposition and heel formation in that cycle due to exposure of residual adsorbates to the high regeneration temperature. However, the 5-cycle cumulative heel depends on the amount of adsorbed compounds during each consecutive cycle and a decrease in the amount adsorbed reduced the amount of heel formed during that cycle.
- Micropore surface analysis showed heel formation reduced BET surface area and pore volume in regenerated ACFC compared to heat treated ACFC. The kinetic diameter of the adsorbates affected the pore blockage of ACFC during regeneration and the bulkier compounds showed significant loss in their adsorption capacity mainly due to the inaccessibility of blocked ACFC pores.

It can generally be concluded that, heel formation on ACFC samples caused by different alkylbenzenes was mainly due to thermal decomposition of the adsorbates resulting from their exposure to high temperature during desorption. Therefore, thermal stability of the adsorbates is a highly important property that needs to be considered during high temperature regeneration of activated carbon in cyclic VOC adsorption/desorption. In addition, the boiling point and kinetic diameter of the adsorbates also need to be considered since these properties determine how much of the residual adsorbate is exposed to high temperature. This research helps explaining how different adsorbate properties contribute to irreversible adsorption on ACFC and will ultimately help increasing the lifetime of activated carbon adsorbents, and consequently result in lowering the operation and maintenance cost of the abatement system.

5.2 Recommendations

This research has investigated the effects of three main adsorbate properties (i.e. boiling point, kinetic diameter and thermal stability) on heel formation on ACFC during electrothermal regeneration. For further understanding of the heel formation mechanism affected by the adsorbates' properties, additional investigation should be conducted on the following topics:

- Effects of the adsorbates' functional group should be investigated. The general understanding from the literature is that adsorbates from different functional groups may interact differently with ACFC and also will go through different level of thermal degradation; therefore, the heel formation mechanism might change for adsorbates from different functional groups.
- Multi-component adsorption should to be investigated. Based on related information in the literature, it is expected that, in case of adsorbates mixture, there is a high chance that the adsorbates might react with each other and therefore involve different heel formation mechanism.

REFERENCES

- Ahmad, A.A., and Idris, A. 2014. Preparation and characterization of activated carbons derived from bio-solid: a review. *Desalination & Water Treatment*, **52**(25-27): 4848-4862.
- Ahmadpour, A., and Do, D.D. 1997. The preparation of activated carbon from macadamia nutshell by chemical activation. *Carbon*, **35**(12): 1723-1732.
- Akta, Ö, and Çeçen, F. 2006. Effect of type of carbon activation on adsorption and its reversibility. *Journal of Chemical Technology & Biotechnology*, **81**(1): 94-101.
- Aktaş, Ö, and Çeçen, F. 2007. Bioregeneration of activated carbon: A review. *International Biodeterioration & Biodegradation*, **59**(4): 257-272.
- Álvarez, P.M., Beltrán, F.J., Gómez-Serrano, V., Jaramillo, J., and Rodríguez, E.M. 2004. Comparison between thermal and ozone regenerations of spent activated carbon exhausted with phenol. *Water Research*, **38**(8): 2155-2165.
- An, H., and Feng, B. 2010. Desorption of CO₂ from activated carbon fibre–phenolic resin composite by electrothermal effect. *International Journal of Greenhouse Gas Control*, **4**(1): 57-63.
- Ania, C.O., Menéndez, J.A., Parra, J.B., and Pis, J.J. 2004. Microwave-induced regeneration of activated carbons polluted with phenol. a comparison with conventional thermal regeneration. *Carbon*, **42**(7): 1377.
- Ania, C.O., Parra, J.B., Menéndez, J.A., and Pis, J.J. 2005. Effect of microwave and conventional regeneration on the microporous and mesoporous network and on the adsorptive capacity of activated carbons. *Microporous and Mesoporous Materials*, **85**(1–2): 7-15.
- Atkinson, R. 2000. Atmospheric chemistry of VOCs and NO_x. *Atmospheric Environment*, **34**(12–14): 2063-2101.

- Banerjee, D.K., Laidler, K.J., Nandi, B.N., and Patmore, D.J. 1986. Kinetic studies of coke formation in hydrocarbon fractions of heavy crudes. *Fuel*, **65**(4): 480-484.
- Bansal, R.C. and Goyal, M. 2005. *Activated carbon adsorption*. Taylor & Francis, Boca Raton.
- Bari, M.A., Kindzierski, W.B., and Spink, D. 2016. Twelve-year trends in ambient concentrations of volatile organic compounds in a community of the Alberta Oil Sands Region, Canada. *Environment International*, **91**: 40-50.
- Basu, P. 2013. *Biomass gasification, pyrolysis and torrefaction*. Academic Press, Amsterdam.
- Berenjian, A., Chan, N., and Hoda, J.M. 2012. Volatile organic compounds removal methods: a review. *American Journal of Biochemistry and Biotechnology*,(4): 220.
- Bhatnagar, A. 2013. *Application of adsorbents for water pollution control*. Bentham Science Publishers, Oak Park.
- Boulinguez, B., and Le Cloirec, P. 2010. Adsorption on activated carbons of five selected volatile organic compounds present in biogas: comparison of granular and fiber cloth materials. *Energy and Fuels*, **24**(5): 4756-4765.
- Brandt, J.C. and Donahue, W.S. 2009. *Pyrolysis : types, processes, and industrial sources and products*. Nova Science Publishers, Inc, New York.
- Brenner, R. 1993. Oxidative coupling of phenols on activated carbon. Impact on adsorption equilibrium. *Environmental Science and Technology*, **27**(10): 2079.
- Brunauer, S., Emmett, P.H., and Teller, E. 1938. Adsorption of gases in multimolecular layers. *Journal of the American Chemical Society*, **60**(2): 309-319.
- Burchell, T.D., Judkins, R.R., Rogers, M.R., and Williams, A.M. 1997. A novel process and material for the separation of carbon dioxide and hydrogen sulfide gas mixtures. *Carbon*, **35**(9): 1279-1294.

- Caliskan, E., Bermúdez, J.M., Parra, J.B., Menéndez, J.A., Mahramanlioğlu, M., and Ania, C.O. 2012. Low temperature regeneration of activated carbons using microwaves: Revising conventional wisdom. *Journal of Environmental Management*, **102**: 134-140.
- Canada. 2004. Silicon dioxide and silica gel. Pest Management Regulatory Agency, Ottawa.
- Che, M. and Védrine, J.C. 2012. Characterization of solid materials and heterogeneous catalysts. Wiley-VCH ;Chichester, Weinheim.
- Cherbański, R., Komorowska-Durka, M., Stefanidis, G.D., and Stankiewicz, A.I. 2011. Microwave swing regeneration vs temperature swing regeneration-comparison of desorption kinetics. *Industrial & Engineering Chemistry Research*, **50**(14): 8632-8644.
- Chung-Hwei Su, Sheng-Hung Wu, Sun-Ju Shen, Gong-Yih Shiue, Yih-Weng Wang, and Chi-Min Shu 2009. Thermal characteristics and regeneration analyses of adsorbents by differential scanning calorimetry and scanning electron microscope. *Journal of Thermal Analysis & Calorimetry*, **96**(3): 765-769.
- Cooper, C.D. and Alley, F.C. 2011. Air pollution control : a design approach. Waveland Press, Long Grove, Ill.
- Dabrowski, A., Podkoscielny, P., Hubicki, Z., and Barczak, M. 2005. Adsorption of phenolic compounds by activated carbon—a critical review. *Chemosphere*, **58**(8): 1049-1070.
- Davankov, V.A. and Tsyurupa, M. 2011. Hypercrosslinked polymeric networks and adsorbing materials. Elsevier, Amsterdam ;Oxford.
- Davis, M.E. 2002. Ordered porous materials for emerging applications. *Nature*, **417**(6891): 813.
- Deosarkar, S.P., and Pangarkar, V.G. 2004. Adsorptive separation and recovery of organics from PHBA and SA plant effluents. *Separation & Purification Technology*, **38**(3): 241-254.
- Do, D.D. 1998. Adsorption analysis. Imperial College Press, London.

- Dou, J., Qin, W., Ding, A., Xie, E., Zheng, L., and Ding, W. 2015. Engineering application of activated alumina adsorption dams for emergency treatment of arsenic-contaminated rivers. *Environmental Technology*, **36**(21): 2755-2762.
- Eley, D.D. 1996. *Advances in Catalysis*. Academic Press, USA.
- Emamipour, H., Hashisho, Z., Cevallos, D., Rood, M.J., Thurston, D.L., Hay, K.J., Kim, B.J., and Sullivan, P.D. 2007a. Steady-state and dynamic desorption of organic vapor from activated carbon with electrothermal swing adsorption. *Environmental Science & Technology*, **41**(14): 5063-5069.
- Emamipour, H., Hashisho, Z., Cevallos, D., Rood, M.J., Thurston, D.L., Hay, K.J., Kim, B.J., and Sullivan, P.D. 2007b. Steady-state and dynamic desorption of organic vapor from activated carbon with electrothermal swing adsorption. *Environmental Science & Technology*, **41**(14): 5063-5069.
- Environment and Climate Change Canada. Volatile organic compound (VOC) concentration limits for automotive refinishing products regulations, Last updated on May 05, 2015, Accessed on June 16, 2016, available at <http://www.ec.gc.ca/cov-voc/default.asp?lang=En&n=71378DBB-1>.
- Environment and Climate Change Canada. 2016. Canadian environmental sustainability indicators: air pollutant emissions., Gatineau, QC, Canada, <http://www.ec.gc.ca/indicateurs-indicators/default.asp?lang=en&n=E79F4C12-1>.
- Fayaz, M., Niknaddaf, S., Jahandar Lashaki, M., Shariaty, P., Hashisho, Z., Phillips, J.H., Anderson, J.E. and Nichols, M. 2015b. The effect of regeneration temperature and heating rate on heel build-up during microwave regeneration. *In* Proceedings of the American Institute of Chemical Engineers' Annual Meeting, Salt Lake City, UT, 2015.
- Fayaz, M., Shariaty, P., Atkinson, J.D., Hashisho, Z., Phillips, J.H., Anderson, J.E., and Nichols, M. 2015. Using microwave heating to improve the desorption efficiency of high

- molecular weight VOC from beaded activated carbon. *Environmental Science & Technology*, **49**(7): 4536-4542.
- Fiedler, N., Laumbach, R., Kelly-McNeil, K., Liou, P., Fan, Z., Zhang, J., Ottenweller, J., Ohman-Strickland, P., and Kipen, H. 2005. Health effects of a mixture of indoor air volatile organics, their ozone oxidation products, and stress. *Environmental Health Perspectives*, **113**(11): 1542-1548.
- Flanigen, E.M., Sand, L.B. and American Chemical Society. 1971. *Molecular sieve zeolites*. American Chemical Society, Washington.
- Fletcher, A.J., Yüzak, Y., and Thomas, K.M. 2006. Adsorption and desorption kinetics for hydrophilic and hydrophobic vapors on activated carbon. *Carbon*, **44**(5): 989-1004.
- Foo, K.Y., and Hameed, B.H. 2010. Insights into the modeling of adsorption isotherm systems. *Chemical Engineering Journal*, **156**(1): 2-10.
- Fuentes, G.A. and Bartholomew, C.H. 1997. *Catalyst Deactivation 1997*. Elsevier Science.
- Garcia, A.A. 1991. Strategies for the recovery of chemicals from fermentation: a review of the use of polymeric adsorbents. *Biotechnology Progress*, **7**(1): 33-42.
- Gédéon, A., Massiani, P. and Babonneau, F. 2008. *Zeolites and related materials*. Elsevier, Amsterdam ;London.
- Grant, T.M., and King, C.J. 1990. Mechanism of irreversible adsorption of phenolic compounds by activated carbons. *Industrial & Engineering Chemistry Research*, **29**(2): 264-271.
- Guisnet, M., and Magnoux, P. 2001. Organic chemistry of coke formation. *Applied Catalysis A: General*, **212**(1-2): 83-96.
- Gupta, V.K., and Verma, N. 2002. Removal of volatile organic compounds by cryogenic condensation followed by adsorption. *Chemical Engineering Science*, **57**(14): 2679-2696.

- Hashisho, Z., Rood, M., and Botich, L. 2005. Microwave-swing adsorption to capture and recover vapors from air streams with activated carbon fiber cloth. *Environmental Science & Technology*, **39**(17): 6851-6859.
- Hashisho, Z., Emamipour, H., Rood, M.J., Hay, K.J., Kim, B.J., and Thurston, D. 2008. Concomitant adsorption and desorption of organic vapor in dry and humid air streams using microwave and direct electrothermal swing adsorption. *Environmental Science & Technology*, **42**(24): 9317-9322.
- Hashisho, Z., Rood, M.J., Barot, S., and Bernhard, J. 2009. Role of functional groups on the microwave attenuation and electric resistivity of activated carbon fiber cloth. *Carbon*, **47**(7): 1814-1823.
- Hradil, J. 2008. Adsorption properties of polymer adsorbents. *In Recent Advances in Adsorption Processes for Environmental Protection and Security. Edited by J.P. Mota and S. Lyubchik. Springer Netherlands, Dordrecht. pp. 65-74.*
- Ince, N.H., and Apikyan, I.G. 2000. Combination of activated carbon adsorption with light-enhanced chemical oxidation via hydrogen peroxide. *Water Research*, **34**(17): 4169-4176.
- Jahandar Lashaki, M., Atkinson, J.D., Hashisho, Z., Phillips, J.H., Anderson, J.E., and Nichols, M. 2016a. The role of beaded activated carbon's surface oxygen groups on irreversible adsorption of organic vapors. *Journal of Hazardous Materials*, **317**: 284-294.
- Jahandar Lashaki, M., Atkinson, J.D., Hashisho, Z., Phillips, J.H., Anderson, J.E., Nichols, M., and Misovski, T. 2016b. Effect of desorption purge gas oxygen impurity on irreversible adsorption of organic vapors. *Carbon*, **99**: 310-317.
- Jambor, B., and Hájeková, E. 2015. Formation of Coke Deposits and Coke Inhibition Methods during Steam Cracking. *Petroleum & Coal*, **57**(2): 143-153.

- Johnsen, D.L., Zhang, Z., Emamipour, H., Yan, Z., and Rood, M.J. 2014. Effect of isobutane adsorption on the electrical resistivity of activated carbon fiber cloth with select physical and chemical properties. *Carbon*, **76**: 435-445.
- Juan Carratalá-Abril, Maria Angeles Lillo-Ródenas, Angel Linares-Solano, and Diego Cazorla-Amorós 2009. Activated carbons for the removal of low-concentration gaseous toluene at the semipilot scale. *Industrial & Engineering Chemistry Research*, **48**(4): 2066-2075.
- Kampa, M., and Castanas, E. 2008. Human health effects of air pollution. *Environmental Pollution*, **151**(2): 362-367.
- Karatum, O., and Deshusses, M.A. 2016. A comparative study of dilute VOCs treatment in a non-thermal plasma reactor. *Chemical Engineering Journal*, **294**: 308-315.
- Kawashima, D., Aihara, T., Kobayashi, Y., Kyotani, T., and Tomita, A. 2000. Preparation of mesoporous carbon from organic polymer/silica nanocomposite. *Chemistry of Materials*, **12**: 3397-3401.
- Keller, J.U. and Staudt, R. 2005. *Gas adsorption equilibria*. Springer, New York.
- Kennes, C. and Veiga, M.C. 2013. *Air pollution prevention and control: bioreactors and bioenergy*. Wiley, Chichester, West Sussex.
- Kesraoui-Ouki, S., Cheeseman, C.R., and Perry, R. 1994. Natural zeolite utilisation in pollution control: A review of applications to metals' effluents. *Journal of Chemical Technology & Biotechnology*, **59**(2): 121-126.
- Khan, F.I., and Kr. Ghoshal, A. 2000. Removal of volatile organic compounds from polluted air. *Journal of Loss Prevention in the Process Industries*, **13**(6): 527-545.
- Kim, B.R. 2011. VOC emissions from automotive painting and their Control: a review. *Environmental Engineering Research*, **16**(1): 1-9.

- Kim, K., Kang, C., You, Y., Chung, M., Woo, M., Jeong, W., Park, N., and Ahn, H. 2006. Adsorption–desorption characteristics of VOCs over impregnated activated carbons. *Catalysis Today*, **111**(3–4): 223-228.
- Knaebel, K.S. 2016. Adsorbent selection, Dublin, Ohio, USA, <http://www.adsorption.com/wp-content/uploads/2016/04/AdsorbentSel1B.pdf>.
- Kunin, R. 1977. Polymeric adsorbents for treatment of waste effluents. *Polymer Engineering & Science*, **17**(1): 58-62.
- Kwiatkowski, J.F. 2012. Activated carbon. Nova Science Publishers, New York.
- Langmuir, I. 1916. The Constitution and fundamental properties of solids and liquids. part I. solids. *Journal of the American Chemical Society*, **38**(11): 2221-2295.
- Lapkin, A., Joyce, L., and Crittenden, B. 2004. Framework for evaluating the "greenness" of chemical processes: case studies for a novel VOC recovery technology. *Environmental Science & Technology*, **38**(21): 5815-5823.
- Lashaki, M., Jahandar, Fayaz, M., Niknaddaf, S., and Hashisho, Z. 2012a. Effect of the adsorbate kinetic diameter on the accuracy of the Dubinin–Radushkevich equation for modeling adsorption of organic vapors on activated carbon. *Journal of Hazardous Materials*, **241-242**: 154-163.
- Lashaki, M.J., Fayaz, M., Wang, H.(., Hashisho, Z., Philips, J.H., Anderson, J.E., and Nichols, M. 2012b. Effect of adsorption and regeneration temperature on irreversible adsorption of organic vapors on beaded activated carbon. *Environmental Science & Technology*, **46**(7): 4083-4090.
- Lashaki, M.J., Atkinson, J.D., Hashisho, Z., Phillips, J.H., Anderson, J.E., and Nichols, M. 2016. The role of beaded activated carbon's pore size distribution on heel formation during cyclic adsorption/desorption of organic vapors. *Journal of Hazardous Materials*, **315**: 42-51.

- Le Cloirec, P. 2012. Adsorption onto activated carbon fiber cloth and electrothermal desorption of volatile organic compound (VOCs): a specific review. *Chinese Journal of Chemical Engineering*, **20**(3): 461-468.
- Ledesma, B., Román, S., Álvarez-Murillo, A., Sabio, E., and González-García, C. 2014. Fundamental study on the thermal regeneration stages of exhausted activated carbons: kinetics. *Journal of Thermal Analysis & Calorimetry*, **115**(1): 537-543.
- Leng, C., and Pinto, N.G. 1996. An investigation of the mechanisms of chemical regeneration of activated carbon. *Industrial & Engineering Chemistry Research*, **35**(6): 2024-2031.
- Li, J., Lu, R., Dou, B., Ma, C., Hu, Q., Liang, Y., Wu, F., Qiao, S., and Hao, Z. 2012. Porous graphitized carbon for adsorptive removal of benzene and the electrothermal regeneration. *Environmental Science & Technology*, **46**(22): 12648-12654.
- Li, L., Liu, S., and Liu, J. 2011. Surface modification of coconut shell based activated carbon for the improvement of hydrophobic VOC removal. *Journal of Hazardous Materials*, **192**(2): 683-690.
- Liu, P.K.T., Felch, S.M., and Wagner, N.J. 1987. Thermal desorption behavior of aliphatic and aromatic hydrocarbons loaded on activated carbon. *Industrial & Engineering Chemistry Research*, **26**(8): 1540-1545.
- Liu, W., Vidić, R.D., and Brown, T.D. 1998. Optimization of sulfur impregnation protocol for fixed-bed application of activated carbon-based sorbents for gas-phase mercury removal. *Environmental Science & Technology*, **32**(4): 531-538.
- Lordgooei, M., Carmichael, K.R., Kelly, T.W., Rood, M.J., and Larson, S.M. 1996. Carbon-based materials activated carbon cloth adsorption-cryogenic system to recover toxic volatile organic compounds. *Gas Separation & Purification*, **10**(2): 123-130.
- Luo, L., Ramirez, D., Rood, M.J., Grevillot, G., Hay, K.J., and Thurston, D.L. 2006. Adsorption and electrothermal desorption of organic vapors using activated carbon adsorbents with novel morphologies. *Carbon*, **44**(13): 2715-2723.

- Mallouk, K.E., Johnsen, D.L., and Rood, M.J. 2010. Capture and recovery of isobutane by electrothermal swing adsorption with post-desorption liquefaction. *Environmental Science & Technology*, **44**(18): 7070-7075.
- Marsh, H. and Rodríguez-Reinoso, F. 2006. *Activated carbon*. Elsevier, Amsterdam ;London.
- McLaughlin, H. 1995. Regenerate activated carbon using organic solvents. *Chemical Engineering Progress*, **91**(7).
- Méndez, A., Gascó, G., Freitas, M.M.A., Siebielec, G., Stuczynski, T., and Figueiredo, J.L. 2005. Preparation of carbon-based adsorbents from pyrolysis and air activation of sewage sludges. *Chemical Engineering Journal*, **108**(1–2): 169-177.
- Moldoveanu, S. 2010. *Pyrolysis of organic molecules with applications to health and environmental issues*. Elsevier, Amsterdam.
- Nabatilan, M.M., Harhad, A., Wolenski, P.R., and Moe, W.M. 2010. Activated carbon load equalization of transient concentrations of gas-phase toluene: Effect of gas flow rate during pollutant non-loading intervals. *Chemical Engineering Journal*, **157**(2–3): 339-347.
- Nakhla, G., Abuzaid, N., and Farooq, S. 1994. Activated carbon adsorption of phenolics in oxic systems: effect of pH and temperature variations. *Water Environment Research*, **66**(6): 842-850.
- Niknaddaf, S. 2015. Heel buildup during electrothermal regeneration of Activated Carbon Fiber Cloth. MSc thesis, University of Alberta.
- Niknaddaf, S., Atkinson, J.D., Shariaty, P., Jahandar Lashaki, M., Hashisho, Z., Phillips, J.H., Anderson, J.E., and Nichols, M. 2016. Heel formation during volatile organic compound desorption from activated carbon fiber cloth. *Carbon*, **96**: 131-138.
- Okazaki, M. 1996. Desorption characteristics of aromatic compounds in aqueous solution on solid adsorbents.

- Olivier, J.P. 1998. Improving the models used for calculating the size distribution of micropore volume of activated carbons from adsorption data. *Carbon*, **36**(10): 1469-1472.
- Pan, B., Pan, B., Zhang, W., Lv, L., Zhang, Q., and Zheng, S. 2009. Development of polymeric and polymer-based hybrid adsorbents for pollutants removal from waters. *Chemical Engineering Journal*, **151**(1-3): 19-29.
- Pariselli, F., Sacco, M.G., Ponti, J., and Rembges, D. 2009. Effects of toluene and benzene air mixtures on human lung cells (A549). *Experimental and Toxicologic Pathology*, **61**(4): 381-386.
- Parmar, G.R., and Rao, N.N. 2009. Emerging control technologies for volatile organic compounds. *Critical Reviews in Environmental Science & Technology*, **39**(1): 41-78.
- Popescu, M., Joly, J.P., Carré, J., and Danatoiu, C. 2003. Dynamical adsorption and temperature-programmed desorption of VOCs (toluene, butyl acetate and butanol) on activated carbons. *Carbon*, **41**(4): 739.
- Radecki, P.P. and American Institute of Chemical Engineers. 1999. Emerging separation and separative reaction technologies for process waste reduction : adsorption and membrane systems. Center for Waste Reduction Technologies, American Institute of Chemical Engineers, New York.
- Ramírez, N., Cuadras, A., Rovira, E., Borrull, F., and Marcé, R.M. 2010. Comparative study of solvent extraction and thermal desorption methods for determining a wide range of volatile organic compounds in ambient air. *Talanta*, **82**(2): 719-727.
- Ramirez, D., Emamipour, H., Vidal, E.X., Rood, M.J., and Hay, K.J. 2011. Capture and recovery of methyl ethyl Ketone with electrothermal-swing adsorption systems. *Journal of Environmental Engineering*, **137**(9): 826-832.
- Ramos, M.E., Bonelli, P.R., Cukierman, A.L., Ribeiro Carrott, M.M.L., and Carrott, P.J.M. 2010. Adsorption of volatile organic compounds onto activated carbon cloths derived

- from a novel regenerated cellulosic precursor. *Journal of Hazardous Materials*, **177**(1-3): 175-182.
- Ratnasamy, C., Wagner, J.P., Spivey, S., and Weston, E. 2012. Removal of sulfur compounds from natural gas for fuel cell applications using a sequential bed system. *Catalysis Today*, **198**(1): 233-238.
- Reuss, J., Bathen, D., and Schmidt-Traub, H. 2002. Desorption by microwaves: mechanisms of multicomponent mixtures. *Chemical Engineering and Technology*, **25**: 381-384.
- Riccardi, E., Jee-Ching Wang, and Liapis, A.I. 2014. Modeling the construction of polymeric adsorbent media: effects of counter-ions on ligand immobilization and pore structure. *Journal of Chemical Physics*, **140**(8): 084901-084901; 084901-9.
- Robinson, A.L., Donahue, N.M., Shrivastava, M.K., Weitkamp, E.A., Sage, A.M., Grieshop, A.P., Lane, T.E., Pierce, J.R., and Pandis, S.N. 2007. Rethinking organic aerosols: semivolatile emissions and photochemical aging. *Science*, **315**(5816): 1259-1262.
- Rouquerol, F. 2014. Adsorption by powders and porous solids. Academic Press, Amsterdam ;Boston.
- Rudling, J., and Björkholm, E. 1987. Irreversibility effects in liquid desorption of organic solvents from activated carbon. *Journal of Chromatography A*, **392**: 239-248.
- Ruhl, J. 2000. Reducing the pressures of VOC recovery. *Pollution Engineering*, **32**(1): 40.
- Ruthven, D.M., Farooq, S. and Knaebel, K.S. 1994. Pressure swing adsorption. VCH Publishers, New York, N.Y.
- Salvador, F., Martin-Sanchez, N., Sanchez-Hernandez, R., Sanchez-Montero, M., and Izquierdo, C. 2015. Regeneration of carbonaceous adsorbents. Part I: thermal regeneration. *Microporous & Mesoporous Materials*, **202**: 259-276.

- Scholz, M., and Martin, R.J. 1998. Control of bio-regenerated granular activated carbon by spreadsheet modelling. *Journal of Chemical Technology & Biotechnology*, **71**(3): 253-261.
- Schork, J.M., and Fair, J.R. 1988. Steaming of activated carbon beds. *Industrial & Engineering Chemistry Research*, **27**(8): 1545-1547.
- Sheintuch, M., and Matatov-Meytal, Y.I. 1999. Comparison of catalytic processes with other regeneration methods of activated carbon. *Catalysis Today*, **53**(1): 73-80.
- Shonnard, D.R., and Hiew, D.S. 2000. Comparative environmental assessments of VOC recovery and recycle design alternatives for a gaseous waste stream. *Environmental Science and Technology*, **34**: 5222-5228.
- Slejko, F.L. 1985. *Adsorption technology : a step-by-step approach to process evaluation and application*. M. Dekker, New York.
- Son, H.K., Sivakumar, S., Rood, M.J., and Kim, B.J. 2016. Electrothermal adsorption and desorption of volatile organic compounds on activated carbon fiber cloth. *Journal of Hazardous Materials*, **301**: 27-34.
- Strazhesko, D.N. and Barouch, A. 1973. *Adsorption and Adsorbents*. John Wiley & Sons Australia, Limited.
- Subrenat, A., Baléo, J.N., Le Cloirec, P., and Blanc, P.E. 2001. Electrical behaviour of activated carbon cloth heated by the joule effect: desorption application. *Carbon*, **39**(5): 707-716.
- Subrenat, A., and Le Cloirec, P. 2004. Adsorption onto activated carbon cloths and electrothermal regeneration: its potential industrial applications. *Journal of Environmental Engineering*, **130**(3): 249-257.
- Suffet, I.H. and McGuire, M.J. 1980. *Activated carbon adsorption of organics from the aqueous phase*. Ann Arbor Science, Ann Arbor, Mich.

- Suidan, M. 1991. Role of dissolved oxygen on the adsorptive capacity of activated carbon for synthetic and natural organic matter. *Environ. Sci. Technol.*, **25**(9): 1612-1618.
- Sullivan, P.D., Rood, M.J., Grevillot, G., Wander, J.D., and Hay, K.J. 2004. Activated carbon fiber cloth electrothermal swing adsorption system. *Environmental Science & Technology*, **38**(18): 4865-4877.
- Suzuki, M., Misic, D.M., Koyama, O., and Kawazoe, K. 1978. Study of thermal regeneration of spent activated carbons: thermogravimetric measurement of various single component organics loaded on activated carbons. *Chemical Engineering Science*, **33**(3): 271-279.
- Švob, V., Deur-Šiftar, Đ, and Cramers, C.A. 1974. Mechanisms of the thermal degradation of alkylbenzenes. *Journal of Chromatography A*, **91**: 659-675.
- Tamon, H., Saito, T., Kishimura, M., Okazaki, M., and Toei, R. 1990. Solvent regeneration of spent activated carbon in wastewater treatment. *Journal of Chemical Engineering of Japan*, **23**(4): 426-432.
- Tascón, J.M.D. 2012. *Novel carbon adsorbents*. Elsevier, Amsterdam ; Waltham, MA.
- Terzyk, A.P. 2007. The impact of carbon surface chemical composition on the adsorption of phenol determined at the real oxic and anoxic conditions. *Applied Surface Science*, **253**(13): 5752-5755.
- Tobias, H., and Soffer, A. 1985. Chemisorption of halogen on carbon—II thermal reversibility of Cl₂, HCl and H₂ chemisorption. *Carbon*, **23**(3): 291-299.
- Torrents, A., Damera, R., and Hao, O.J. 1997. Low-temperature thermal desorption of aromatic compounds from activated carbon. *Journal of Hazardous Materials*, **54**(3): 141-153.
- Towfighi, J., Sadrameli, M., and Niaei, A. 2002. Coke Formation Mechanisms and Coke Inhibiting Methods in Pyrolysis Furnaces. *Journal of Chemical Engineering of Japan*, **35**(10): 923-937.

- Tzabar, N., and ter Brake, H. J. M. 2016. Adsorption isotherms and sips models of nitrogen, methane, ethane, and propane on commercial activated carbons and polyvinylidene chloride. *Adsorption*, **22**: 901.
- US Environmental Protection Agency. 2016. Technical Overview of Volatile Organic Compounds, <https://www.epa.gov/indoor-air-quality-iaq/technical-overview-volatile-organic-compounds#EPA>.
- USEPA. 1991. EPA handbook: control technologies for hazardous air pollutants, Washington, DC.
- Valix, M., Cheung, W.H., and McKay, G. 2004. Preparation of activated carbon using low temperature carbonisation and physical activation of high ash raw bagasse for acid dye adsorption. *Chemosphere*, **56**(5): 493-501.
- Van Speybroeck, V., Hemelsoet, K., Minner, B., Marin, G.B., and Waroquier, M. 2007. Modeling elementary reactions in coke formation from first principles. *Molecular Simulation*, **33**(9-10): 879-887.
- Vidic, R.D., Tessmer, C.H., and Uranowski, L.J. 1997. Impact of surface properties of activated carbons on oxidative coupling of phenolic compounds. *Carbon*, **35**(9): 1349-1360.
- Wang, H., Lashaki, M.J., Fayaz, M., Hashisho, Z., Philips, J.H., Anderson, J.E., and Nichols, M. 2012. Adsorption and desorption of mixtures of organic vapors on beaded activated carbon. *Environmental Science & Technology*, **46**(15): 8341-8350.
- Wang, J., and Kaskel, S. 2012. KOH activation of carbon-based materials for energy storage. *Journal of Materials Chemistry*, **22**(45): 23710-23725.
- Wang, Q., Liang, X., Zhang, R., Liu, C., Liu, X., Qiao, W., Zhan, L., and Ling, L. 2009. Preparation of polystyrene-based activated carbon spheres and their adsorption of dibenzothiophene. *New Carbon Materials*, **24**(1): 55-60.

- Wu, J. 2004. Modeling adsorption of organic compounds on activated carbon. PhD thesis, Umeå University, Sweden.
- Yan, L., and Sorial, G.A. 2011. Chemical activation of bituminous coal for hampering oligomerization of organic contaminants. *Journal of Hazardous Materials*, **197**: 311-319.
- Yao, M., Zhang, Q., Hand, D.W., Perram, D., and Taylor, R. 2009. Adsorption and regeneration on activated carbon fiber cloth for volatile organic compounds at indoor concentration levels. *Journal of the Air & Waste Management Association*, **59**(1): 31-36.
- Yapsaklı, K., Çeçen, F., Aktaş, Ö, and Can, Z.S. 2009. Impact of surface properties of granular activated carbon and preozonation on adsorption and desorption of natural organic matter. *Environmental Engineering Science*, **26**(3): 489-500.
- Yonge, D.R., Zhan, P.J., Poznanska, K., and Keinath, T.M. 1985. Single-solute irreversible adsorption on granular activated carbon. *Environmental Science & Technology*, **19**(8): 690.
- Yu, F.D., Luo, L., and Grevillot, G. 2007. Electrothermal swing adsorption of toluene on an activated carbon monolith: experiments and parametric theoretical study. *Chemical Engineering and Processing: Process Intensification*, **46**(1): 70-81.
- Zeynali., M.E. 2011. Evaluation of the effect of catalyst pore-size distribution on the effectiveness factor in ethylbenzene dehydrogenation by orthogonal collocation. *Defect and Diffusion Forum*, **316-317**: 155-169.
- Zhang, K., Zhang, D., and Zhang, K. 2016. Arsenic removal from water using a novel amorphous adsorbent developed from coal fly ash. *Water Science & Technology*, **73**(8): 1954-1962.
- Zhang, T., Walawender, W.P., Fan, L.T., Fan, M., Dugaard, D., and Brown, R.C. 2004. Preparation of activated carbon from forest and agricultural residues through CO₂ activation. *Chemical Engineering Journal*, **105**(1-2): 53-59.

Zhao, L., Huang, S., and Wei, Z. 2014. A demonstration of biofiltration for VOC removal in petrochemical industries. *Environmental Science: Processes & Impacts*, **16**(5): 1001-1007.

Zheng, Z., Yong, Q., Geoff, X.W., and Xuehai, F. 2013. Numerical description of coalbed methane desorption stages based on isothermal adsorption experiment. *Science China Earth Sciences*, **56**(6): 1029-1036.

Zhou, L. 2007. *Adsorption*. World Scientific, Singapore ;Hackensack, NJ.

APPENDICES

Appendix A: Environment Canada VOC concentration limit for automotive refinishing products

Table A-1. Concentration limits of VOCs imposed by Environment Canada for automotive refinishing products

Product category	VOC concentration limit (g/L)
Primer surface	250
Prime sealer	340
Pre-treatment wash primer	660
Adhesion promoter	840
Colour coating	420
Uniform finish coating	540
Truck-bed liner coating	310
Temporary protective coating	60
Underbody coating	430
Single-stage coating	420
Multi-colour coating	680
Clear coating	250
Other coatings	250
Surface cleaners	50

Appendix B: Detail of 5 cycle adsorption/desorption tests of toluene on ACFC

Table B-1. Mass balance of 5 cycle adsorption/desorption of toluene on ACFC

Weight of dry virgin ACFC: 3.5 g					
Cycle No.	Amount adsorbed (g)	% adsorption capacity g adsorbed/g adsorbent	% adsorption capacity cm ³ adsorbed/cm ³ adsorbent pore	Total heel (g)	% accumulated heel formation (g adsorbate remained/g adsorbent)
1	1.25	35.82	70.02	0.11	3.15
2	1.12	32.09	68.90	0.18	5.16
3	1.04	29.80	68.34	0.24	6.88
4	0.97	27.79	67.78	0.26	7.45
5	0.94	26.91	67.16	0.31	8.74

Table B-2. Mass balance of 5 cycle adsorption/desorption of toluene on ACFC – duplicated test

Weight of dry virgin ACFC: 3.5 g					
Cycle No.	Amount adsorbed (g)	% adsorption capacity g adsorbed/g adsorbent	% adsorption capacity cm ³ adsorbed/cm ³ adsorbent pore	Total heel (g)	% accumulated heel formation (g adsorbate remained/g adsorbent)
1	1.25	35.82	70.02	0.12	3.32
2	1.11	31.92	68.90	0.19	5.44
3	1.03	29.51	68.34	0.26	7.45
4	0.95	27.22	67.78	0.29	8.31
5	0.93	26.63	68.30	0.32	9.11

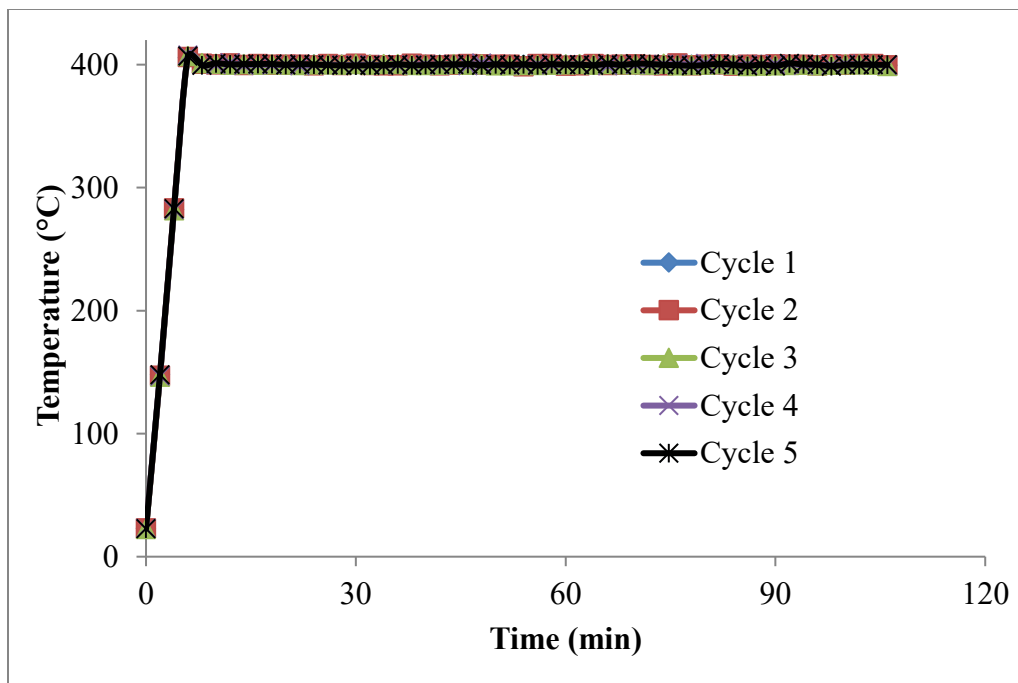


Figure B-1. Temperature profile during desorption of toluene from ACFC in 5 cycle adsorption/desorption tests

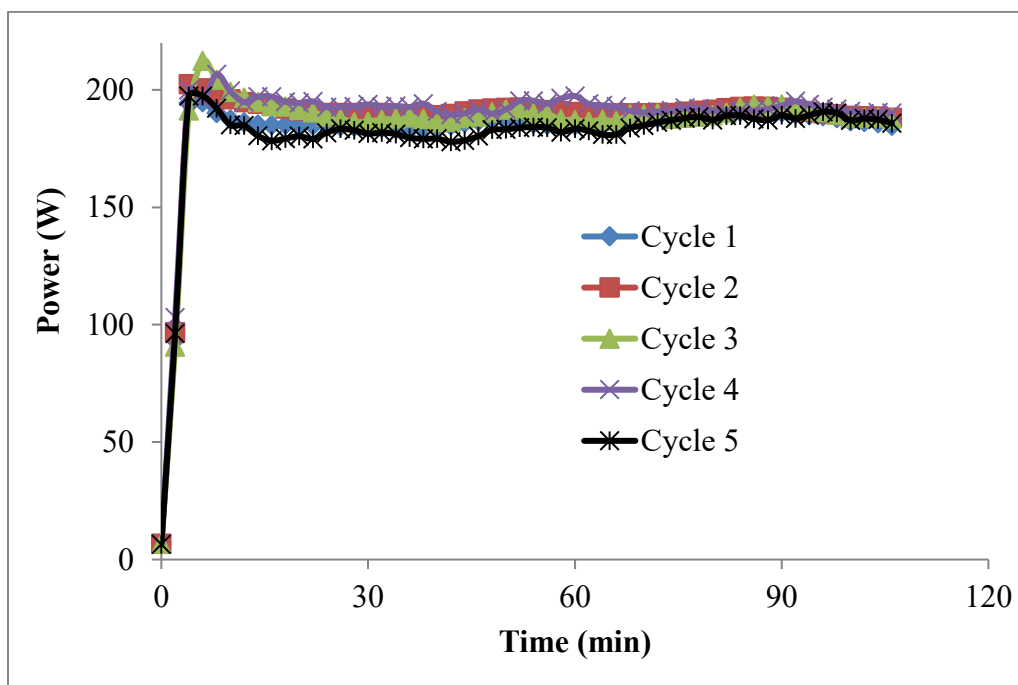


Figure B-2. Power profile during desorption of toluene from ACFC in 5 cycle adsorption/desorption tests

Appendix C: Detail of 5 cycle adsorption/desorption tests of p-xylene on ACFC

Table C-1. Mass balance of 5 cycle adsorption/desorption of p-xylene on ACFC

Weight of dry virgin ACFC: 3.5 g					
Cycle No.	Amount adsorbed (g)	% adsorption capacity g adsorbed/g adsorbent	% adsorption capacity cm ³ adsorbed/cm ³ adsorbent pore	Total heel (g)	% accumulated heel formation (g adsorbate remained/g adsorbent)
1	1.41	40.14	78.57	0.22	6.39
2	1.18	33.61	78.29	0.33	9.37
3	1.07	30.54	78.12	0.38	10.80
4	1.02	28.98	77.84	0.41	11.65
5	0.98	27.84	77.29	0.44	12.64

Table C-2. Mass balance of 5 cycle adsorption/desorption of p-xylene on ACFC – duplicated test

Weight of dry virgin ACFC: 3.5 g					
Cycle No.	Amount adsorbed (g)	% adsorption capacity g adsorbed/g adsorbent	% adsorption capacity cm ³ adsorbed/cm ³ adsorbent pore	Total heel (g)	% accumulated heel formation (g adsorbate remained/g adsorbent)
1	1.41	40.14	78.57	0.21	6.05
2	1.19	33.95	78.29	0.33	9.37
3	1.08	30.60	78.23	0.38	10.80
4	1.03	29.15	78.18	0.41	11.65
5	1.00	28.27	78.12	0.44	12.44

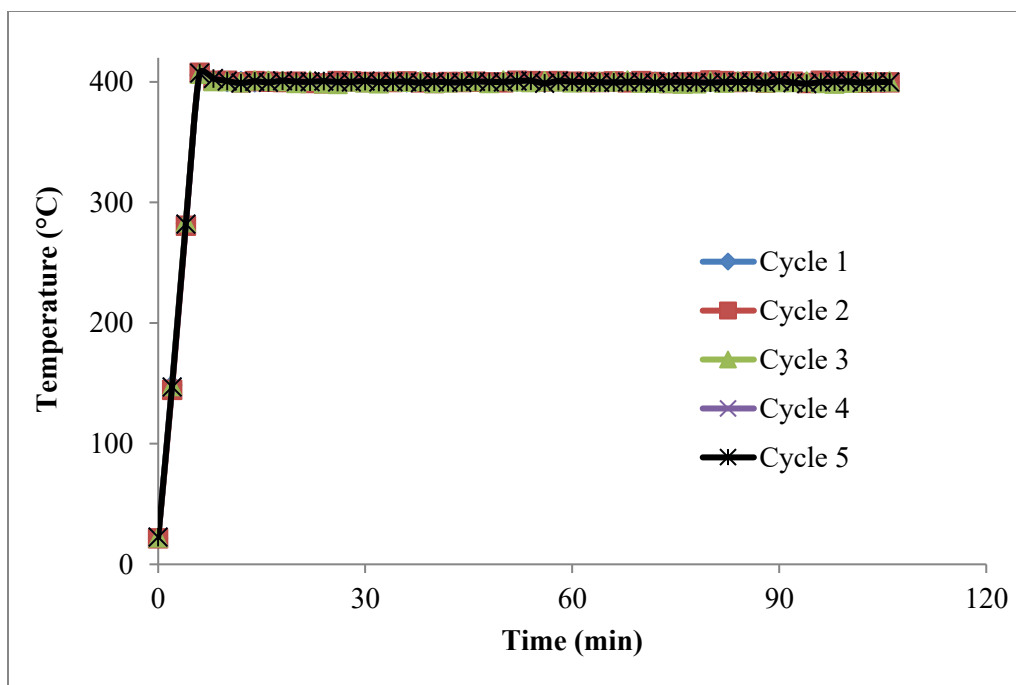


Figure C-1. Temperature profile during desorption of p-xylene from ACFC in 5 cycle adsorption/desorption tests

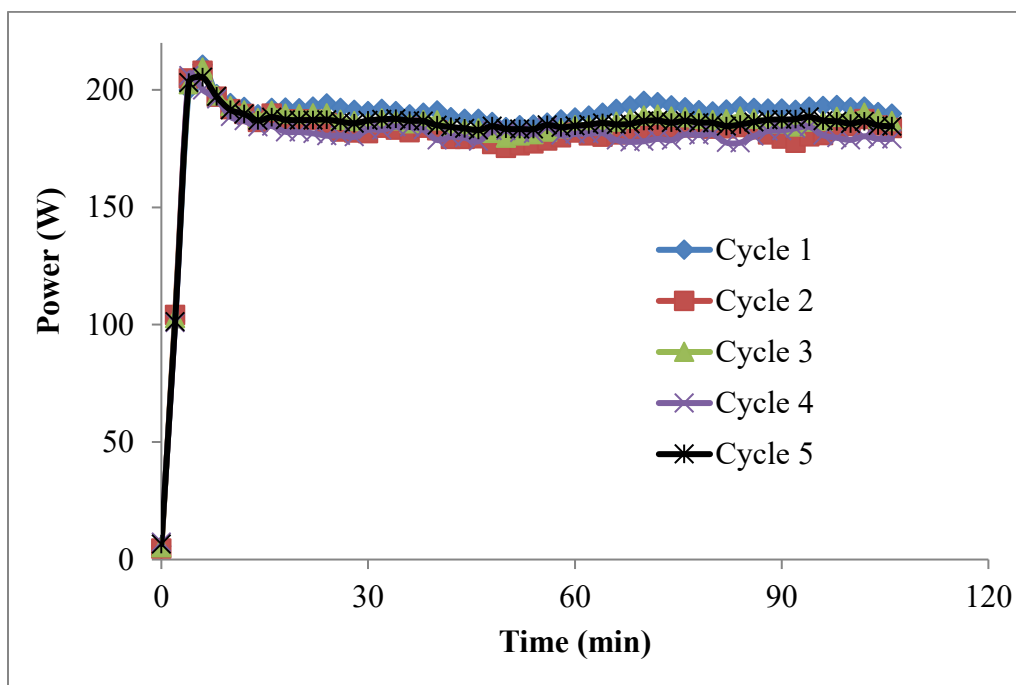


Figure C-2. Power profile during desorption of p-xylene from ACFC in 5 cycle adsorption/desorption tests

Appendix D: Detail of 5 cycle adsorption/desorption tests of m-xylene on ACFC

Table D-1. Mass balance of 5 cycle adsorption/desorption of m-xylene on ACFC

Weight of dry virgin ACFC: 3.5 g					
Cycle No.	Amount adsorbed (g)	% adsorption capacity (g adsorbed/g adsorbent)	% adsorption capacity (cm ³ adsorbed/cm ³ adsorbent pore)	Total heel (g)	% accumulated heel formation (g adsorbate remained/g adsorbent)
1	1.23	35.23	69.43	0.23	6.51
2	1.00	28.63	69.26	0.30	8.57
3	0.92	26.29	68.70	0.36	10.29
4	0.85	24.29	68.13	0.40	11.43
5	0.81	23.03	67.91	0.44	12.51

Table D-2. Mass balance of 5 cycle adsorption/desorption of m-xylene on ACFC – duplicated test

Weight of dry virgin ACFC: 3.5 g					
Cycle No.	Amount adsorbed (g)	% adsorption capacity (g adsorbed/g adsorbent)	% adsorption capacity (cm ³ adsorbed/cm ³ adsorbent pore)	Total heel (g)	% accumulated heel formation (g adsorbate remained/g adsorbent)
1	1.24	35.37	69.71	0.24	6.86
2	1.00	28.57	69.82	0.31	8.86
3	0.92	26.29	69.26	0.36	10.29
4	0.86	24.57	68.70	0.42	12.00
5	0.80	22.71	68.42	0.44	12.69

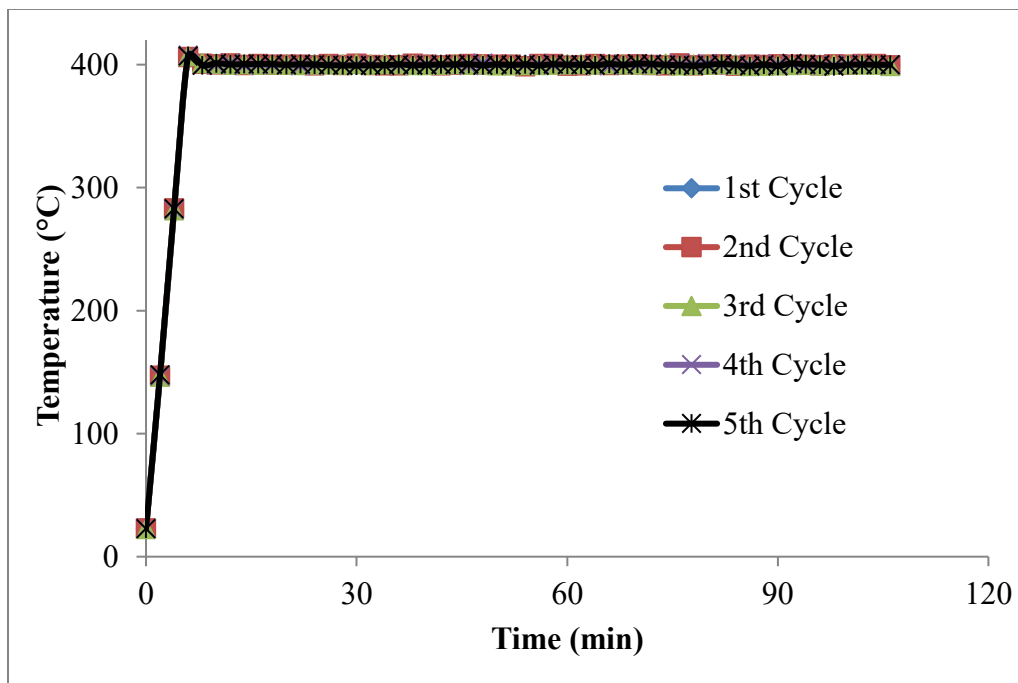


Figure D-1. Temperature profile during desorption of m-xylene from ACFC in 5 cycle adsorption/desorption tests

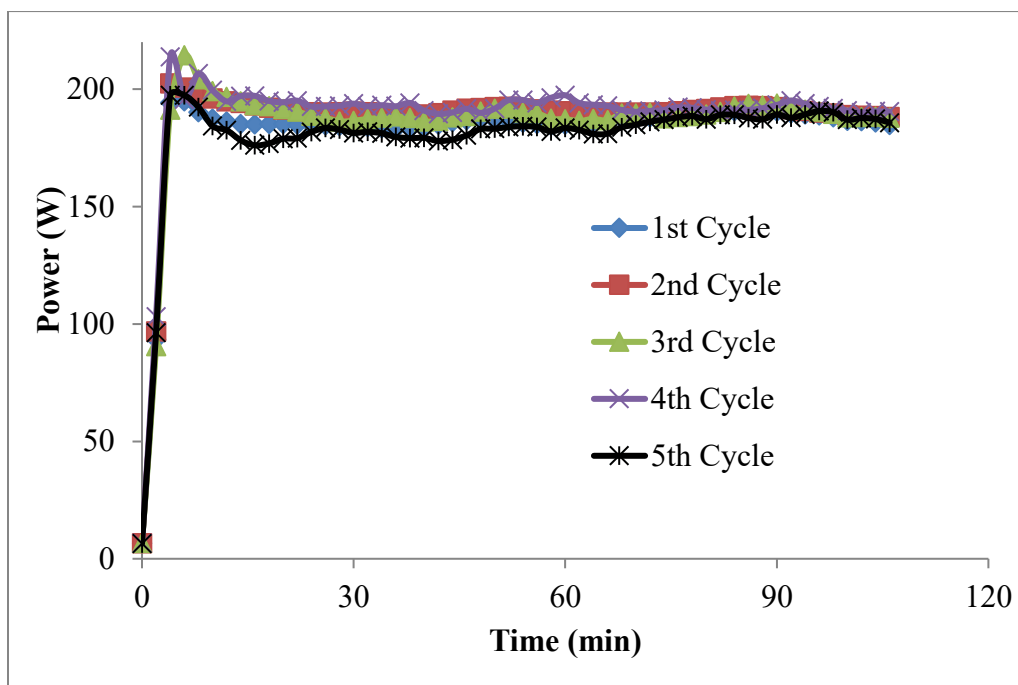


Figure D-2. Power profile during desorption of m-xylene from ACFC in 5 cycle adsorption/desorption tests

Appendix E: Detail of 5 cycle adsorption/desorption tests of o-xylene on ACFC

Table E-1. Mass balance of 5 cycle adsorption/desorption of o-xylene on ACFC

Weight of dry virgin ACFC: 3.50 g					
Cycle No.	Amount adsorbed (g)	% adsorption capacity (g adsorbed/g adsorbent)	% adsorption capacity (cm ³ adsorbed/cm ³ adsorbent pore)	Total heel (g)	% accumulated heel formation (g adsorbate remained/g adsorbent)
1	1.28	36.66	70.60	0.24	6.71
2	1.05	29.94	70.60	0.33	9.43
3	0.94	26.86	69.89	0.40	11.43
4	0.86	24.57	69.34	0.43	12.29
5	0.83	23.71	69.34	0.44	12.54

Table E-2. Mass balance of 5 cycle adsorption/desorption of o-xylene on ACFC – duplicated test

Weight of dry virgin ACFC: 3.50 g					
Cycle No.	Amount adsorbed (g)	% adsorption capacity (g adsorbed/g adsorbent)	% adsorption capacity (cm ³ adsorbed/cm ³ adsorbent pore)	Total heel (g)	% accumulated heel formation (g adsorbate remained/g adsorbent)
1	1.29	36.93	71.12	0.24	6.90
2	1.04	29.97	71.01	0.33	9.48
3	0.94	27.01	70.29	0.37	10.63
4	0.89	25.57	69.74	0.41	11.78
5	0.83	23.74	68.41	0.44	12.73

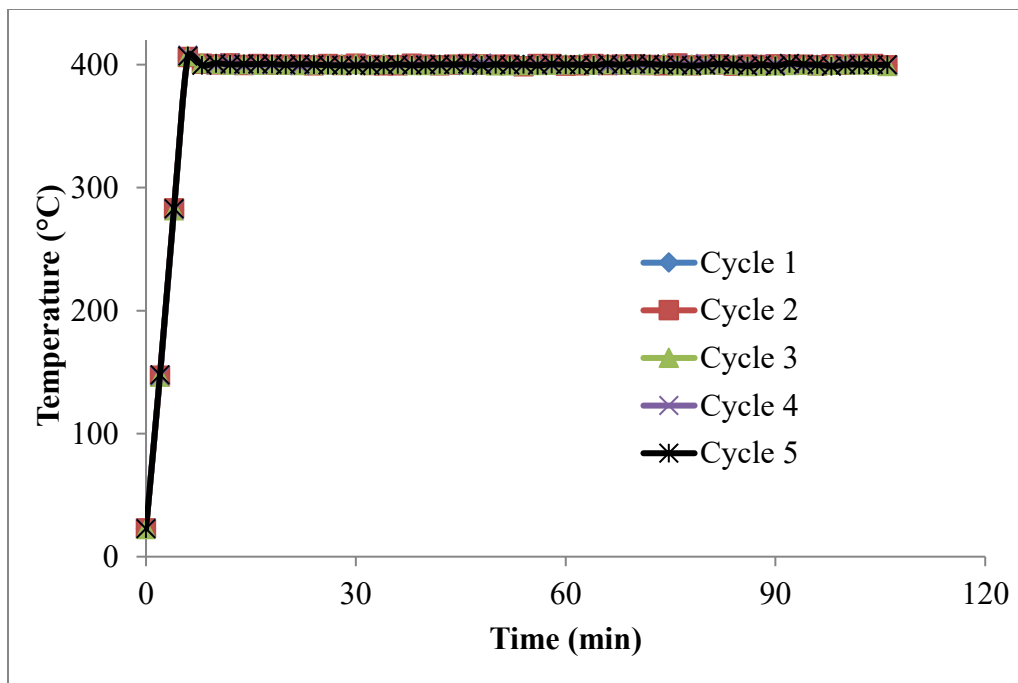


Figure E-1. Temperature profile during desorption of o-xylene from ACFC in 5 cycle adsorption/desorption tests

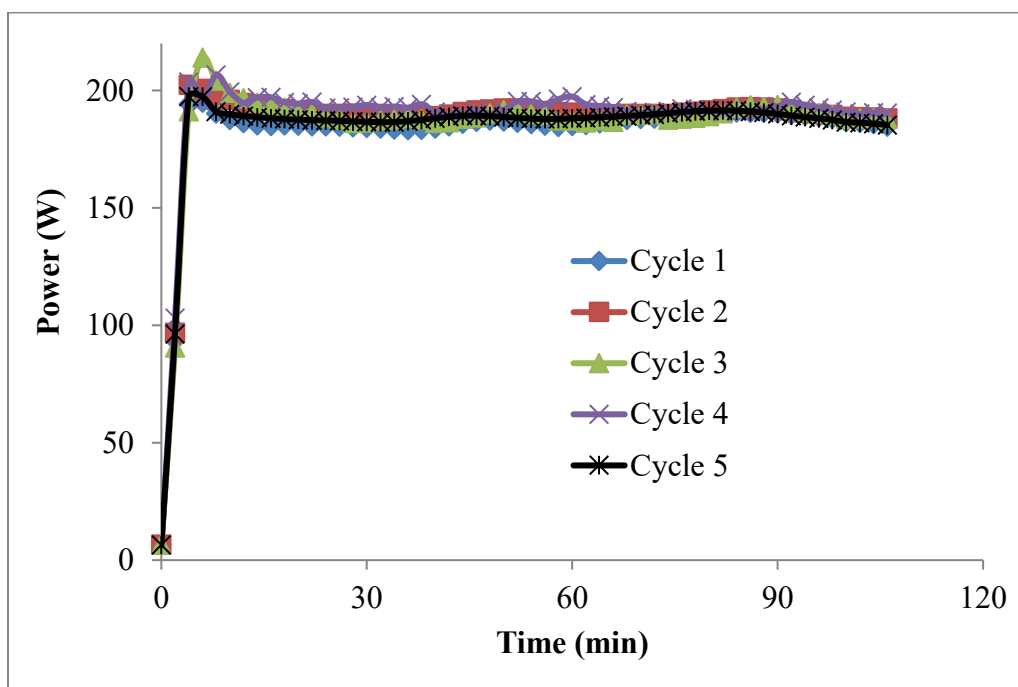


Figure E-2. Power profile during desorption of o-xylene from ACFC in 5 cycle adsorption/desorption tests

Appendix F: Detail of 5 cycle adsorption/desorption tests of 1,2,4 TMB on ACFC

Table F-1. Mass balance of 5 cycle adsorption/desorption of 1,2,4 TMB on ACFC

Weight of dry virgin ACFC: 3.50 g					
Cycle No.	Amount adsorbed (g)	% adsorption capacity (g adsorbed/g adsorbent)	% adsorption capacity (cm ³ adsorbed/cm ³ adsorbent pore)	Total heel (g)	% accumulated heel formation (g adsorbate remained/g adsorbent)
1	1.40	40.00	77.39	0.25	7.20
2	1.14	32.51	76.84	0.33	9.43
3	1.05	30.00	76.29	0.40	11.43
4	0.93	26.57	73.52	0.43	12.29
5	0.88	25.14	72.42	0.44	12.71

Table F-2. Mass balance of 5 cycle adsorption/desorption of 1,2,4 TMB on ACFC – duplicated test

Weight of dry virgin ACFC: 3.50 g					
Cycle No.	Amount adsorbed (g)	% adsorption capacity (g adsorbed/g adsorbent)	% adsorption capacity (cm ³ adsorbed/cm ³ adsorbent pore)	Total heel (g)	% accumulated heel formation (g adsorbate remained/g adsorbent)
1	1.40	40.00	77.39	0.27	7.63
2	1.12	32.09	76.84	0.33	9.43
3	1.05	30.00	76.29	0.40	11.43
4	0.93	26.57	73.52	0.43	12.29
5	0.86	24.51	71.20	0.44	12.71

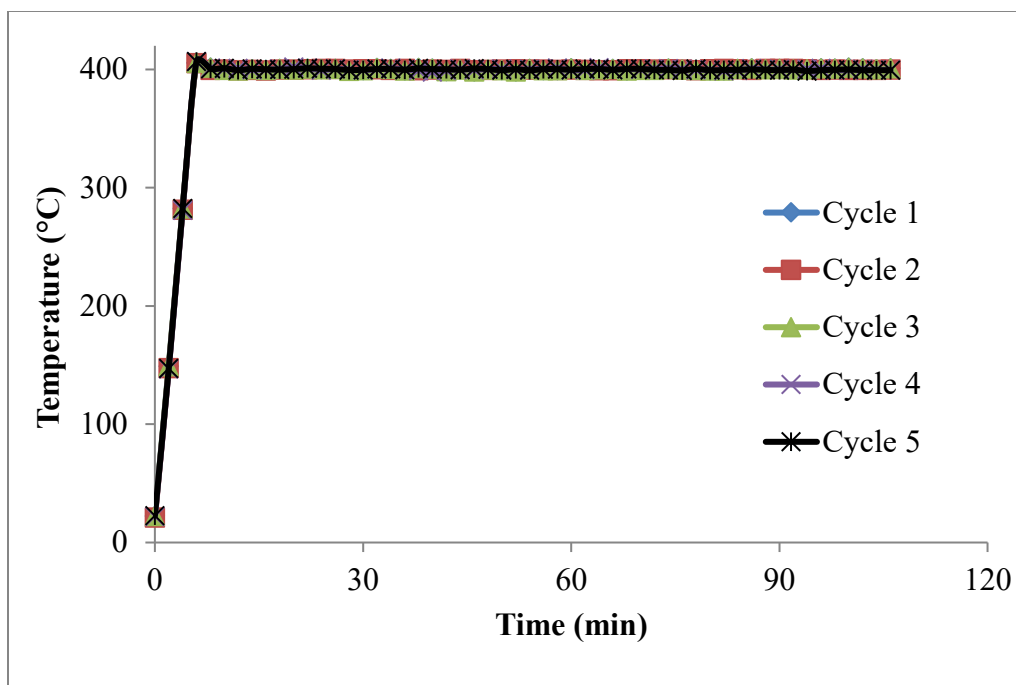


Figure F-1. Temperature profile during desorption of 1,2,4 TMB from ACFC in 5 cycle adsorption/desorption tests

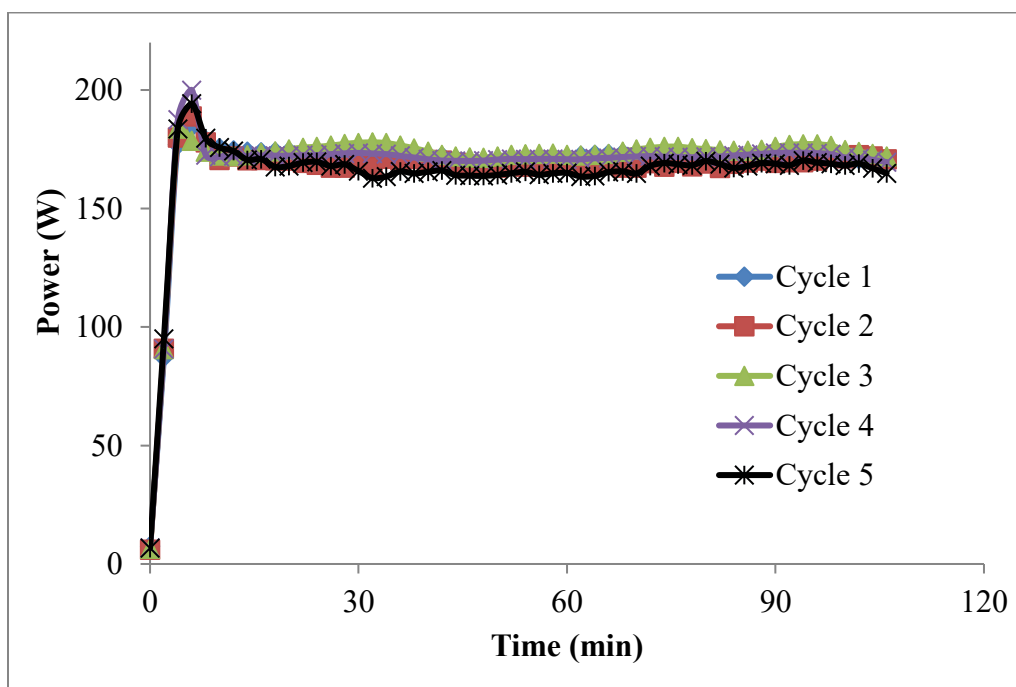


Figure F-2. Power profile during desorption of 1,2,4 TMB from ACFC in 5 cycle adsorption/desorption tests

Appendix G: Detail of 5 cycle adsorption/desorption tests of 1,3,5 TMB on ACFC

Table G-1. Mass balance of 5 cycle adsorption/desorption of 1,3,5 TMB on ACFC

Weight of dry virgin ACFC: 3.50 g					
Cycle No.	Amount adsorbed (g)	% adsorption capacity (g adsorbed/g adsorbent)	% adsorption capacity (cm ³ adsorbed/cm ³ adsorbent pore)	Total heel (g)	% accumulated heel formation (g adsorbate remained/g adsorbent)
1	1.31	37.43	73.17	0.28	7.94
2	1.03	29.49	73.17	0.37	10.57
3	0.87	24.86	69.26	0.41	11.71
4	0.69	19.71	61.44	0.44	12.57
5	0.54	15.46	54.79	0.45	12.74

Table G-2. Mass balance of 5 cycle adsorption/desorption of 1,3,5 TMB on ACFC – duplicated test

Weight of dry virgin ACFC: 3.50 g					
Cycle No.	Amount adsorbed (g)	% adsorption capacity (g adsorbed/g adsorbent)	% adsorption capacity (cm ³ adsorbed/cm ³ adsorbent pore)	Total heel (g)	% accumulated heel formation (g adsorbate remained/g adsorbent)
1	1.12	37.33	72.98	0.24	8.13
2	0.87	28.87	72.33	0.30	10.00
3	0.75	25.00	68.42	0.33	11.00
4	0.57	19.00	58.65	0.36	12.00
5	0.43	14.30	51.41	0.39	12.90

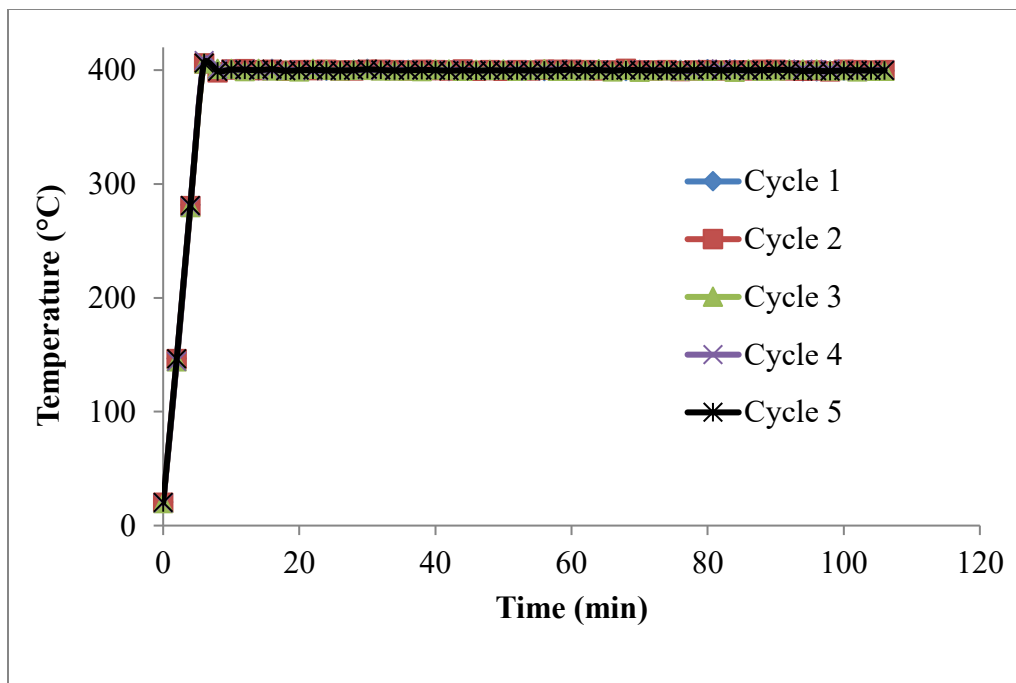


Figure G-1. Temperature profile during desorption of 1,2,4 TMB from ACFC in 5 cycle adsorption/desorption tests

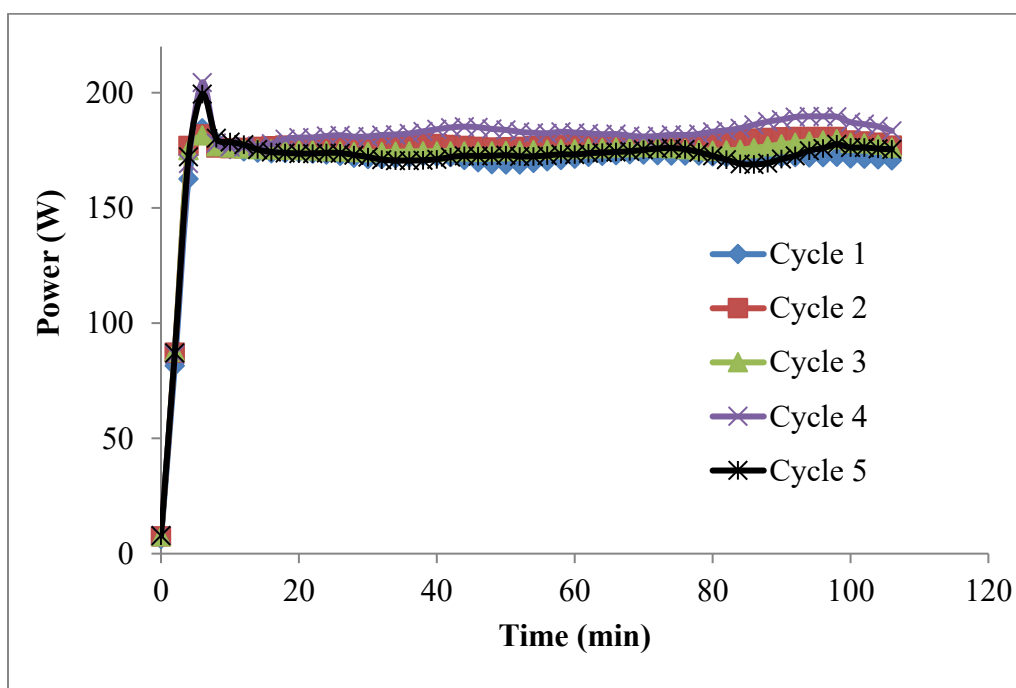


Figure G-2. Power profile during desorption of 1,2,4 TMB from ACFC in 5 cycle adsorption/desorption tests

Appendix H: Detail of 5 cycle adsorption/desorption tests of ethylbenzene on ACFC

Table H-1. Mass balance of 5 cycle adsorption/desorption of ethylbenzene on ACFC

Weight of dry virgin ACFC: 3.50 g					
Cycle No.	Amount adsorbed (g)	% adsorption capacity (g adsorbed/g adsorbent)	% adsorption capacity (cm ³ adsorbed/cm ³ adsorbent pore)	Total heel (g)	% accumulated heel formation (g adsorbate remained/g adsorbent)
1	1.31	37.29	72.97	0.25	7.03
2	1.05	30.11	72.70	0.38	10.86
3	0.90	25.71	71.58	0.46	13.14
4	0.80	22.86	70.46	0.49	14.00
5	0.75	21.57	69.62	0.52	14.80

Table H-2. Mass balance of 5 cycle adsorption/desorption of ethylbenzene on ACFC – duplicated test

Weight of dry virgin ACFC: 3.50 g					
Cycle No.	Amount adsorbed (g)	% adsorption capacity (g adsorbed/g adsorbent)	% adsorption capacity (cm ³ adsorbed/cm ³ adsorbent pore)	Total heel (g)	% accumulated heel formation (g adsorbate remained/g adsorbent)
1	1.29	36.56	71.56	0.27	7.59
2	1.01	28.78	71.17	0.37	10.51
3	0.89	25.28	70.06	0.43	12.22
4	0.82	23.30	69.50	0.50	14.20
5	0.73	20.87	68.64	0.53	15.11

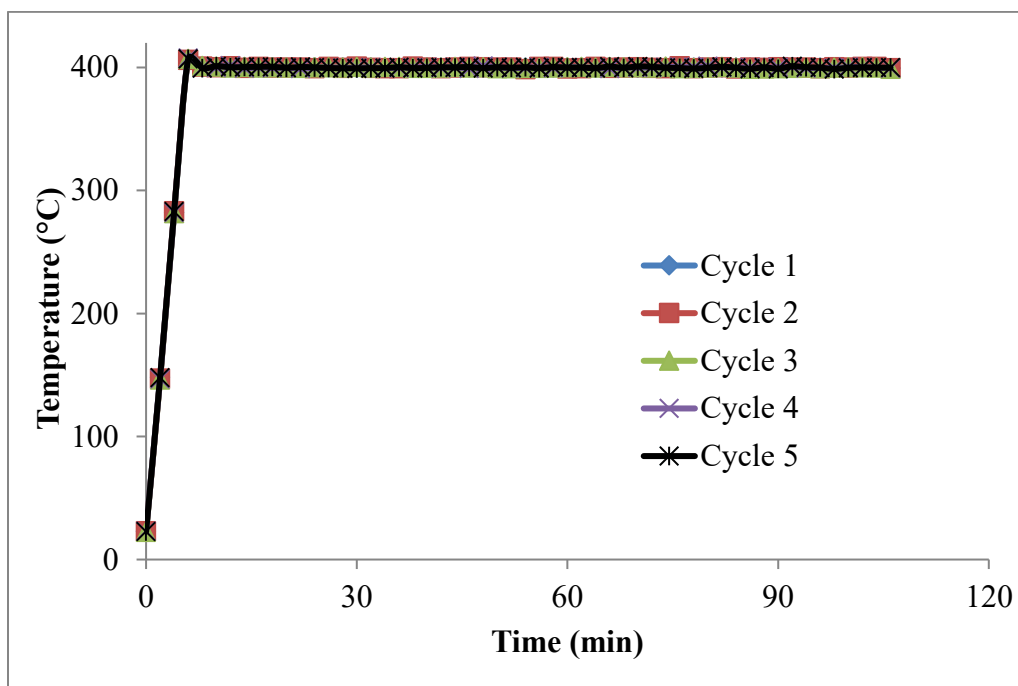


Figure H-1. Temperature profile during desorption of ethylbenzene from ACFC in 5 cycle adsorption/desorption tests

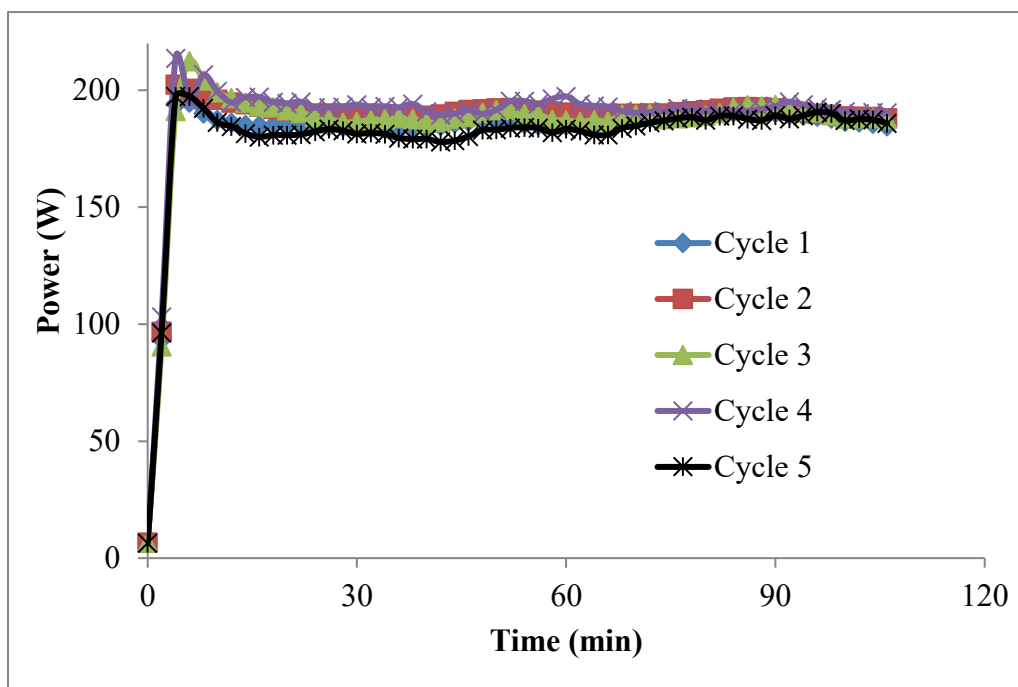


Figure H-2. Power profile during desorption of ethylbenzene from ACFC in 5 cycle adsorption/desorption tests

Appendix I: Detail of 5 cycle adsorption/desorption tests of isopropylbenzene on ACFC

Table I-1. Mass balance of 5 cycle adsorption/desorption of isopropylbenzene on ACFC

Weight of dry virgin ACFC: 3.50 g					
Cycle No.	Amount adsorbed (g)	% adsorption capacity (g adsorbed/g adsorbent)	% adsorption capacity (cm ³ adsorbed/cm ³ adsorbent pore)	Total heel (g)	% accumulated heel formation (g adsorbate remained/g adsorbent)
1	1.38	39.77	78.20	0.31	8.93
2	0.97	27.95	72.53	0.42	12.10
3	0.82	23.63	70.26	0.49	14.12
4	0.74	21.18	69.41	0.54	15.56
5	0.65	18.82	67.60	0.55	15.82

Table I-2. Mass balance of 5 cycle adsorption/desorption of isopropylbenzene on ACFC – duplicated test

Weight of dry virgin ACFC: 3.50 g					
Cycle No.	Amount adsorbed (g)	% adsorption capacity (g adsorbed/g adsorbent)	% adsorption capacity (cm ³ adsorbed/cm ³ adsorbent pore)	Total heel (g)	% accumulated heel formation (g adsorbate remained/g adsorbent)
1	1.38	39.77	78.20	0.32	9.31
2	0.96	27.58	72.53	0.42	12.10
3	0.82	23.63	70.26	0.49	14.12
4	0.74	21.18	69.41	0.54	15.56
5	0.63	18.24	66.47	0.56	16.22

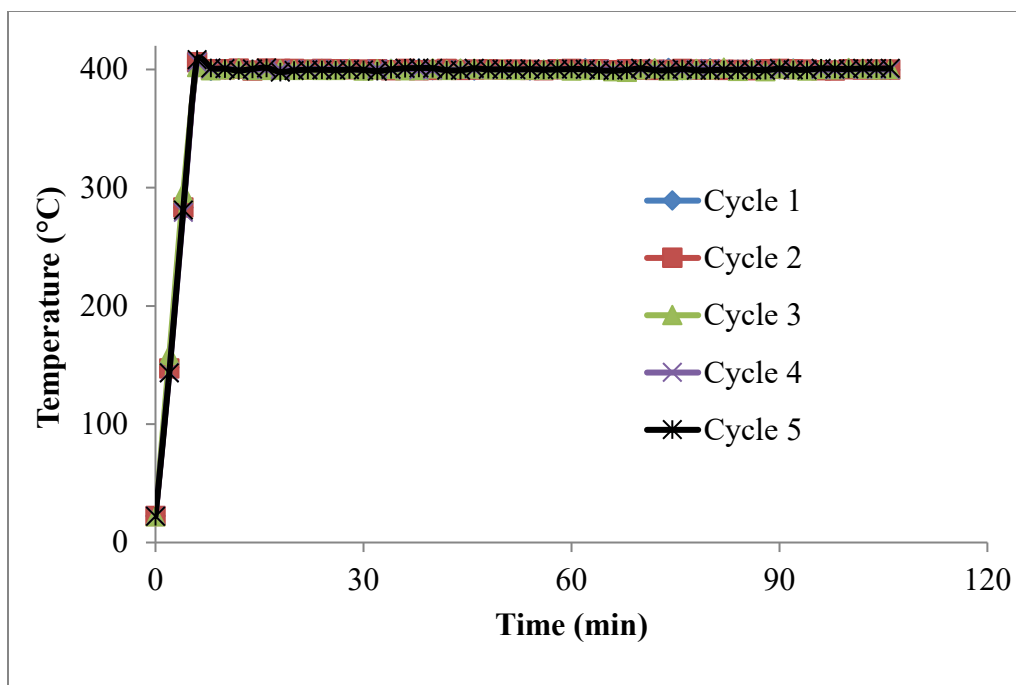


Figure I-1. Temperature profile during desorption of isopropylbenzene from ACFC in 5 cycle adsorption/desorption tests

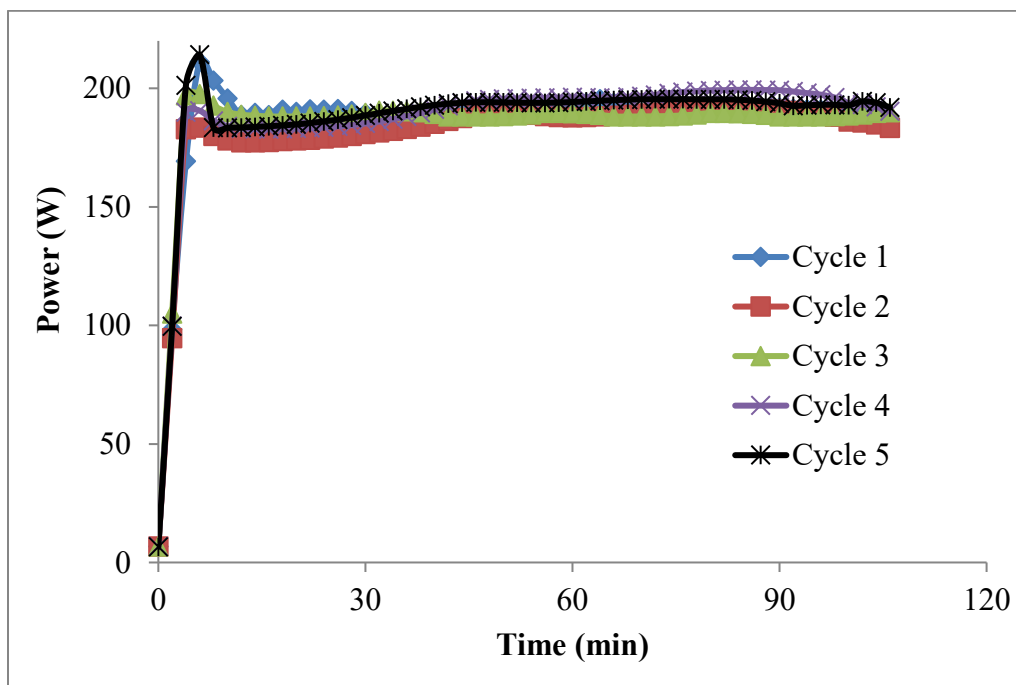


Figure I-2. Power profile during desorption of isopropylbenzene from ACFC in 5 cycle adsorption/desorption tests

Appendix J: Detail of 5 cycle adsorption/desorption tests of neopentylbenzene on ACFC

Table J-1. Mass balance of 5 cycle adsorption/desorption of neopentylbenzene on ACFC

Weight of dry virgin ACFC: 3.50 g					
Cycle No.	Amount adsorbed (g)	% adsorption capacity (g adsorbed/g adsorbent)	% adsorption capacity (cm ³ adsorbed/cm ³ adsorbent pore)	Total heel (g)	% accumulated heel formation (g adsorbate remained/g adsorbent)
1	1.25	35.71	68.79	0.37	10.51
2	0.73	20.91	60.53	0.46	13.14
3	0.54	15.43	55.03	0.55	15.71
4	0.40	11.43	52.28	0.56	16.00
5	0.28	7.86	45.95	0.59	16.91

Table J-2. Mass balance of 5 cycle adsorption/desorption of neopentylbenzene on ACFC – duplicated test

Weight of dry virgin ACFC: 3.50 g					
Cycle No.	Amount adsorbed (g)	% adsorption capacity (g adsorbed/g adsorbent)	% adsorption capacity (cm ³ adsorbed/cm ³ adsorbent pore)	Total heel (g)	% accumulated heel formation (g adsorbate remained/g adsorbent)
1	1.25	35.71	68.79	0.40	11.29
2	0.70	20.14	60.53	0.46	13.14
3	0.57	16.29	56.68	0.55	15.71
4	0.40	11.43	52.28	0.59	16.86
5	0.22	6.29	44.57	0.61	17.51

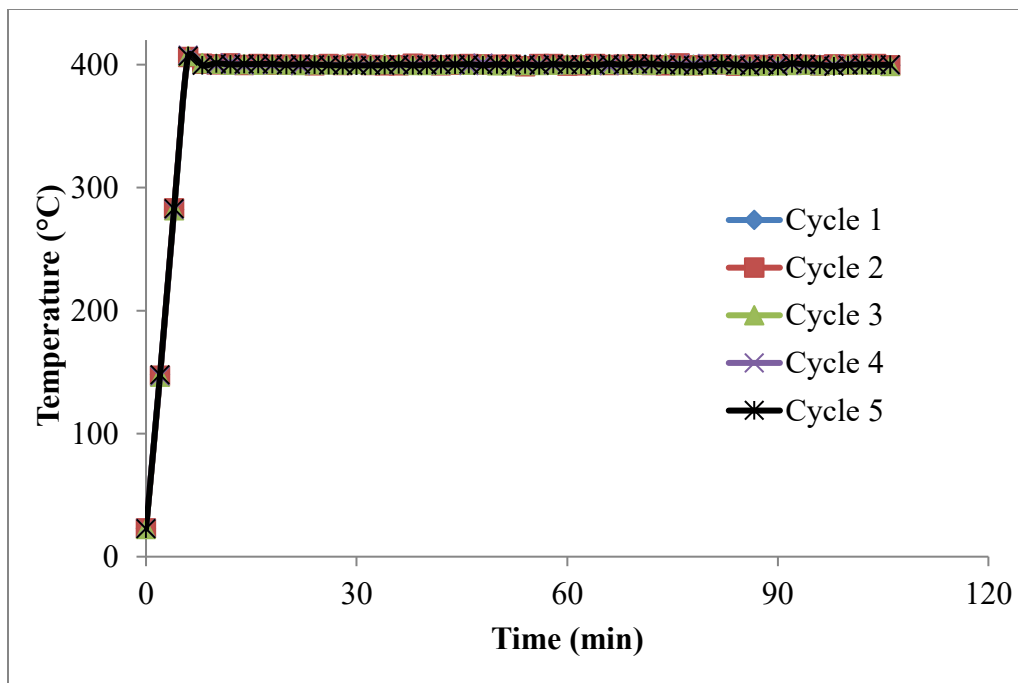


Figure J-1. Temperature profile during desorption of neopentylbenzene from ACFC in 5 cycle adsorption/desorption tests

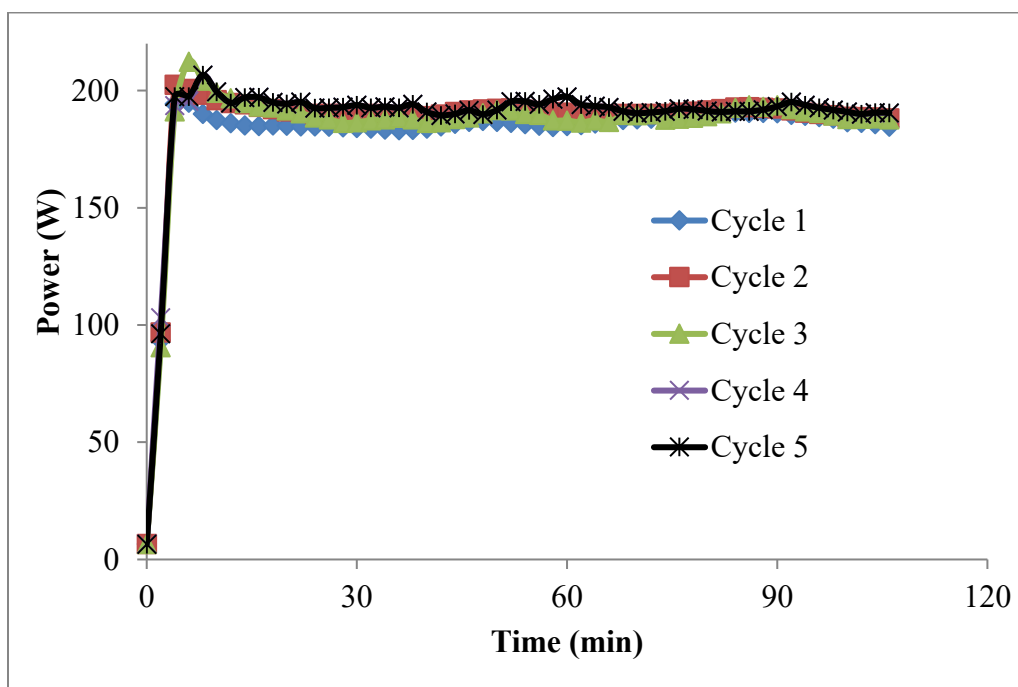


Figure J-2. Power profile during desorption of neopentylbenzene from ACFC in 5 cycle adsorption/desorption tests